

## Flameless combustion and its potential towards gas turbines

Perpignan, André A.V.; Gangoli Rao, Arvind; Roekaerts, Dirk J.E.M.

**DOI**

[10.1016/j.pecs.2018.06.002](https://doi.org/10.1016/j.pecs.2018.06.002)

**Publication date**

2018

**Document Version**

Final published version

**Published in**

Progress in Energy and Combustion Science

**Citation (APA)**

Perpignan, A. A. V., Gangoli Rao, A., & Roekaerts, D. J. E. M. (2018). Flameless combustion and its potential towards gas turbines. *Progress in Energy and Combustion Science*, 69, 28-62.  
<https://doi.org/10.1016/j.pecs.2018.06.002>

**Important note**

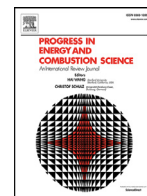
To cite this publication, please use the final published version (if applicable).  
Please check the document version above.

**Copyright**

Other than for strictly personal use, it is not permitted to download, forward or distribute the text or part of it, without the consent of the author(s) and/or copyright holder(s), unless the work is under an open content license such as Creative Commons.

**Takedown policy**

Please contact us and provide details if you believe this document breaches copyrights.  
We will remove access to the work immediately and investigate your claim.



# Flameless combustion and its potential towards gas turbines



André A.V. Perpignan<sup>a</sup>, Arvind Gangoli Rao<sup>a\*</sup>, Dirk J.E.M. Roekaerts<sup>b,c</sup>

<sup>a</sup> Faculty of Aerospace Engineering, Delft University of Technology, Kluyverweg 1, 2629 HS, Delft, The Netherlands

<sup>b</sup> Faculty of Mechanical, Maritime and Materials Engineering, Delft University of Technology, Leeghwaterstraat 39, 2628 CB, Delft, The Netherlands

<sup>c</sup> Department of Mechanical Engineering, Eindhoven University of Technology, P.O. Box 513, 5600 MB, Eindhoven, The Netherlands

## ARTICLE INFO

### Article History:

Received 2 August 2017

Accepted 25 June 2018

Available online xxx

### Keywords:

Flameless combustion

Gas turbines

Gas turbine combustion

Jet-in-Hot-Coflow

MILD combustion

## ABSTRACT

Since its discovery, the Flameless Combustion (FC) regime has been seen as a promising alternative combustion technique to reduce pollutant emissions of gas turbine engines. This combustion mode is often characterized by well-distributed reaction zones, which can potentially decrease temperature gradients, acoustic oscillations and, consequently NO<sub>x</sub> emission. However, the application of FC to gas turbines is still not a reality due to the inherent difficulties faced in attaining the regime while meeting all the engine requirements. Over the past years, investigations related to FC have been focused on understanding the fundamentals of this combustion regime, the regime boundaries, its computational modelling, and combustor design attempts. This article reviews the progress achieved so far, discusses the various definitions of the FC regime, and attempts to point the directions for future research. The review suggests that modelling of the FC regime is still not capable of predicting intermediate species and pollutant emissions. Comprehensive experimental databases with conditions relevant to gas turbine combustors are not available, and moreover, many of the current experiments do not necessarily represent the FC regime. By analysing the latest developments in computational modelling, the review points to the most promising approaches for the prediction of reaction zones and pollutant emissions in FC. The lessons learned from previous design attempts provide valuable insights into the design of a successful gas turbine engine operating under the FC regime. The review concludes with some examples where the gas turbine architecture has been exploited to advance the possibilities of FC in gas turbines.

© 2018 The Authors. Published by Elsevier Ltd. This is an open access article under the CC BY-NC-ND license. (<http://creativecommons.org/licenses/by-nc-nd/4.0/>)

## Contents

|  |    |
|--|----|
| 1. Introduction .....  | 2  |
| 2. Definition of flameless combustion .....                    | 3  |
| 3. Basic experimental investigations .....                     | 8  |
| 3.1. Axisymmetric burners in non-enclosed environment .....    | 8  |
| 3.2. Experiments in enclosed environment .....                 | 13 |
| 3.2.1. Axisymmetric environment .....                          | 14 |
| 3.2.2. Non-Axisymmetric environment .....                      | 16 |
| 3.3. Observations and recommendations .....                    | 17 |
| 4. Computational modelling .....                               | 17 |
| 4.1. Overview of modelling approaches .....                    | 18 |
| 4.2. Chemical kinetics .....                                   | 19 |
| 4.3. Direct numerical simulation .....                         | 20 |
| 4.4. Extension of tabulated chemistry .....                    | 21 |
| 4.5. RANS-based modelling .....                                | 22 |
| 4.5.1. Early studies .....                                     | 22 |
| 4.5.2. Application of EDC .....                                | 23 |
| 4.5.3. Application of statistical models (CMC, CSE, PDF) ..... | 23 |
| 4.6. LES-based modelling .....                                 | 24 |
| 4.7. Chemical reactor networks .....                           | 24 |
| 4.8. Modelling comparison of a DJHC flame .....                | 24 |

|  |    |
|--|----|
| 4.8.1. Velocity predictions.....                                   | 25 |
| 4.8.2. Temperature predictions .....                               | 25 |
| 4.9. Conclusions and future outlook for computational models ..... | 25 |
| 5. Conceptual designs for gas turbine FC combustors .....          | 27 |
| 6. Conclusions, open challenges and recommendations.....           | 33 |

## 1. Introduction

The manufacture of stone tools and manipulation of fire are the most important extrasomatic milestones in our early evolutionary trajectory. Hominids learned to make fire and use it for beneficial purposes more than a million years ago [1]. Thus, combustion technology is the second oldest technology of human kind. However, it was only in the 19th century, during the industrial revolution that combustion was looked into scientifically. The energy harness through the combustion process made the modern civilization possible.

Even though the advances in combustion sciences made in the 20th century were phenomenal with the progress in experimental techniques and numerical modelling, we still do not understand every aspect of combustion. The advances in combustion in the 21st century will be driven by fuel flexibility and emission reduction, due to increase in the “energy mix” and a strong drive to reduce emissions.

Gas turbines play an important role, both in the transport and energy sector. Thus in order to reduce global warming and to make our environment more sustainable, it is important that the emissions from gas turbines are reduced substantially.

Even though sustainable energy sources and storage systems are increasingly becoming more important, alternatives to combustion in aviation are still underdeveloped and will not become feasible solutions in commercial aircraft for the next decades due to the extremely low energy density of batteries [2].

The trends and goals in aviation engines are paradoxical in relation to NOx emissions. Turbine inlet temperatures (TIT) and overall pressure ratios (OPR) have been increasing over time in the pursuit of increasing thermal efficiency and thereby reducing the fuel consumption and CO<sub>2</sub> emissions [3]. While on the other hand, NOx emissions have to be reduced, in spite of their tendency to increase with both TIT and OPR. T.

The data displayed in Fig. 1 shows the trend of increasing OPR over time and the corresponding NOx emission index. In order to lower or maintain NOx emissions while increasing OPR and TIT, new combustion technologies have to be developed. According to the goals set by the Advisory Council for Aviation Research and Innovation in Europe (ACARE), the NOx emission levels in 2050 should be only 10% as compared to a baseline aircraft of year 2000 [5].

Pollutant emissions regulations for land-based gas turbines differ significantly in relation to that of aero engines because of their interaction with the systems operating at power plants and the larger variety in terms of power output, fuels and usage (mechanical drive or electricity). A summary of existing regulations in different countries was presented by Klein [6]. Regardless of the differences, the regulatory pressures on land-based gas turbines have also been a concern to designers and operators. Emission regulations for NOx and CO have been increasingly stringent, while greenhouse gases taxation and emission trading schemes have already been introduced in some countries.

Although the current trend in electricity generation is to shift towards sustainable and renewable energy conversion methods, land-based gas turbines are far from becoming obsolete. Gas turbines are pointed as one of the solutions to be employed along with wind or solar [7] energy systems to deal with the inherent

intermittency of these energy sources [8]. Energy storage in the form of fuels and the decoupling of the compression and expansion cycles of gas turbines with compressed air energy storage are regarded as feasible approaches in combined cycle power plants based on wind or solar energy [9].

Consequently, research and development have been focused on options that minimize the environmental impact of gas turbine combustion while retaining high efficiencies. Broadly, it may be achieved by using alternative fuels, improving current combustor designs, or adopting new combustion concepts. The latter is arguably the most complex alternative but has more potential for providing significant improvements.

A few approaches have been investigated and attempted as new combustion concepts for aeronautical gas turbines, such as the Trapped Vortex Combustor (TVC) and Lean Direct Injection (LDI). However, these concepts are not likely to be able to meet the ambitious ACARE and NASA emission reduction goals for aero engines as the pressure ratio and operating temperatures are being increased in the pursuit of increasing efficiency. Therefore alternative combustion concepts like Flameless Combustion (FC) have to be explored. A qualitative comparison of different types of combustors with FC is shown in Table 1, in which the advantages of FC are clear: the well-distributed reactions that characterise the FC regime often yield low temperature gradients, low NOx emissions, high stability and low acoustic oscillations. It is worth pointing out that the level of readiness for application of FC-based combustors is lower than that of the other types, therefore the characteristics stated in Table 1 are based on its potential.

Some of the advantageous characteristics are results of the decoupling between fluid dynamics and heat release under the FC regime [10]. The most attractive feature is the potential for low NOx emissions, which is a result of three factors that come into play under FC: i) homogenization of the reaction zones, ii) local reduction of the availability of the main reactants for NOx formation and iii) alteration of the NOx formation chemistry, with effects on pathways as NNH, N<sub>2</sub>O and prompt, as well as increased NOx reburning. The link between homogeneity and lower NOx is well-established [11–13], as thermal NOx formation is reduced if temperatures peaks decrease. The reduction of the reactants is because FC is attained with lower O<sub>2</sub> concentration, which in the context of gas turbines is often realised by flue-gas recirculation, which results in lower N<sub>2</sub> as well. The recirculation of combustion products is also responsible for changing the NOx chemistry, as further discussed in Section 4.2.

A similar situation is found for land-based gas turbines, as the goals for reduction are also challenging. Additionally, the intermittent and flexible operation required from gas turbines for their application along with renewable energy sources makes the scenario even more demanding, as broad operational range is required due to the fact engines would often have to constantly operate at part-load. One of the alternatives to achieve stable and efficient part-load operation is through exhaust gas recirculation (EGR). From the combustion point of view, EGR may be used to achieve FC conditions [14].

Therefore, the FC regime is an opportunity for both aeronautical and land-based gas turbines. Although FC is already successfully applied in industrial furnaces, the conditions required to attain the

## Nomenclature

### Acronyms

|        |  |
|--------|--|
| CARS   | coherent anti-Stokes Raman spectroscopy                    |
| CMC    | conditional momentum closure                               |
| CRN    | chemical reactor network                                   |
| CSE    | conditional source-term estimation                         |
| DA-FGM | flamelet generated manifolds using “diluted air” flamelets |
| DNS    | direct numerical simulation                                |
| EDC    | eddy dissipation concept                                   |
| EDC-LP | eddy dissipation concept with local parameters             |
| EDM    | eddy dissipation model                                     |
| FC     | flameless combustion                                       |
| FGM    | flamelet generated manifolds                               |
| FPVA   | flamelet/progress variable approach                        |
| HRR    | heat release rate  |
| ICAO   | international civil aviation organization                  |
| ISAT   | in situ adaptive tabulation                                |
| ITB    | inter-turbine burner                                       |
| JHC    | Jet-in-Hot-Coflow  |
| LDV    | laser Doppler velocimetry                                  |
| LES    | large-eddy simulation                                      |
| LIF    | laser-induced fluorescence                                 |
| LTO    | landing and take-off                                       |
| NG     | natural gas  |
| OPR    | overall pressure ratio                                     |
| PaSR   | partially stirred reactor                                  |
| PDI    | phase Doppler interferometry                               |
| PFR    | plug flow reactor  |
| PIV    | particle image velocimetry                                 |
| PLIF   | planar laser-induced fluorescence                          |
| PSR    | perfectly stirred reactor                                  |
| PVA    | principal variable analysis                                |
| RANS   | Reynolds-averaged Navier–Stokes                            |
| RQL    | Rich-Burn, Quick-Quench, Lean-Burn                         |
| TIT    | turbine inlet temperature                                  |

### Symbols

|          |                                    |
|----------|------------------------------------|
| $c_p$    | specific heat at constant pressure |
| $D$      | diameter                           |
| $Da$     | Damköhler number                   |
| $E$      | activation energy                  |
| $Ka$     | Karlovitz number                   |
| $l$      | length                             |
| $p$      | pressure                           |
| $Q$      | heat of combustion                 |
| $Re$     | Reynolds number                    |
| $S$      | flame speed                        |
| $T$      | temperature                        |
| $u'$     | velocity fluctuation               |
| $V$      | velocity                           |
| $W$      | molecular weight                   |
| $x$      | side length                        |
| $Y$      | mass fraction                      |
| $Z$      | mixture fraction                   |
| $\delta$ | flame thickness                    |
| $\Phi$   | global equivalence ratio           |
| $\chi$   | scalar dissipation rate            |

### Subscripts

|      |               |
|------|---------------|
| $F$  | fuel          |
| $in$ | reactants     |
| $L$  | laminar flame |

|      |                 |
|------|-----------------|
| $T$  | integral scale  |
| $tr$ | transport scale |

|                     |                 |
|---------------------|-----------------|
| <i>Superscripts</i> |                 |
| *                   | non-dimensional |

FC regime are not trivial to be obtained in a gas turbine. The requirement to preheat the reactants and to lower  $O_2$  concentrations present a significant challenge for the designers. Limitations in volume, which is translated into high heat density, as well as strict requirements in terms of pressure losses and operational range combined with lower overall equivalence ratios and residence times, impose challenging barriers to the design.

The present work intends to provide an overview of the current development concerning FC for gas turbine engines. The goal is to summarize the lessons learned from previous efforts and to identify the gaps to be filled by future research.

This paper first reviews the progress made so far towards understanding the fundamentals of the FC regime and discusses the different definitions of the regime and their consequences. Subsequently, the fundamental canonical research focused on the understanding of the phenomena involved are reviewed, followed by a comprehensive overview of the computational modelling efforts, and finally the design attempts are presented (Table 6).

## 2. Definition of flameless combustion

Since its first description, the FC regime received different designations. This fact is in part related to the absence of a formal and consensual definition of the boundaries of the regime or of the features that characterize it. Acronyms such as MILD (Moderate or Intense Low Oxygen Dilution), HiTAC (High Temperature Air Combustion), HiCOT (High Temperature Combustion Technology), and CDC (Colourless Distributed Combustion) refer to the FC regime or slightly different but overlapping concepts.

Cavaliere and de Joannon [15] tackled the issue of the different designations in their review paper. They pointed that HiCOT is a broader concept which comprises of combustion with reactants at relatively high temperatures. HiTAC was then defined by them as a subarea of HiCOT, in which only the air was heated up to high temperatures. The authors then defined Mild Combustion (not as the MILD acronym) as a subset of HiTAC, which could be identified by two parameters: temperature of reactants and temperature rise due to the release of combustion energy.

However, Cavaliere and de Joannon [15] acknowledged the possible differences between FC, CDC and Mild Combustion as a matter of terminology that could not be fully clarified. As the FC and CDC denominations are the result of aspects related to the emission of visible radiation during the combustion process, the authors pointed that their definition of Mild Combustion could overlap but not necessarily coincide with the FC regime, considering FC to be simply a combustion regime without emission of visible radiation.

The issue is more complex if one considers that FC is often attainable using recirculation of exhaust gases, without actual air preheating (HiTAC); or that having lower luminosity is not necessarily related to distributed reactions and lower emissions [16]. As will become clear throughout the present review, the FC regime requires a precise definition to guide the research on the subject.

Historically, the regime was first described by Wünnig and Wünnig [17] and was referred to as Flameless Oxidation (FLOX®). The study was in the context of industrial burners and furnaces. The authors described the main features and advantages of the regime, and the definition of the boundaries was based on the furnace

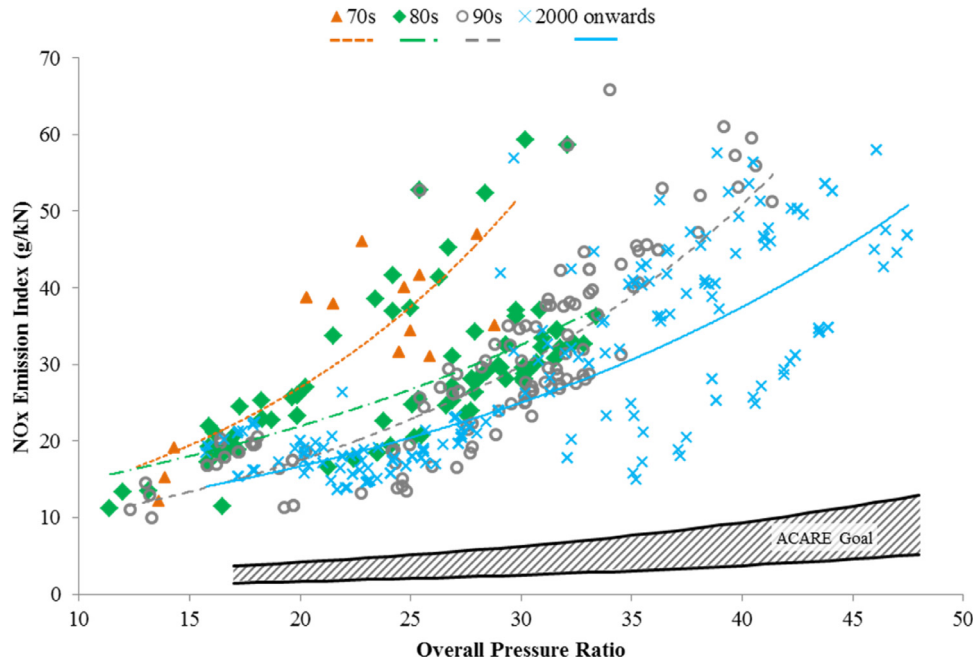


**Fig. 1.** Variation of overall pressure ratios and NOx emissions index for aero engines over time. Data from ICAO Aircraft Engine Emissions Databank [4]. Representation of the ACARE Goal for 2050 [5].

**Table 1**  
Qualitative comparison of different combustor types.

|                         | Combustor type |                       |          |                 |
|-------------------------|----------------|-----------------------|----------|-----------------|
|                         | Lean premixed  | Lean direct injection | RQL      | Flameless-based |
| Combustion efficiency   | High           | High                  | High     | High            |
| Combustion instability  | High           | Low                   | Low      | Low             |
| Fuel flexibility        | Moderate       | High                  | High     | Moderate        |
| Integration into engine | Moderate       | Moderate              | Easy     | Difficult       |
| Mechanical complexity   | Moderate       | High                  | Moderate | Moderate        |
| NOx emission            | Low            | Low                   | Moderate | Ultra-low       |
| Operating range         | Moderate       | High                  | High     | Low             |
| Soot emission           | Very Low       | Low                   | Moderate | Low             |
| Volume requirement      | Moderate       | Low                   | Low      | High            |

temperature and recirculation ratio. According to the authors, the regime could be attained if these parameters were above certain approximate values, which were obtained from their practical experience in industrial furnaces.

The recirculation of combustion products was a central parameter, defined by the recirculation ratio. The air was split into two streams, one injected along with the fuel (primary) and the other directly into the furnace (secondary). By varying the ratio between primary and secondary air, the furnace studied by Wünnig and Wünnig [17] changed its regime from normal to FLOX. It was observed that increasing the relative amount of secondary air allowed the reactants to mix with the combustion products prior to reacting with the fuel. In other words, the recirculation ratio increased with increasing secondary air.

Cavaliere and de Joannon [15] proposed the most used definition for the FC regime. Also referred to as a PSR-like definition [18], such definition imposes the reactant mixture to be above auto-ignition temperature at the inlet while the temperature rise due to energy release has to be lower than the same temperature. The authors defined auto-ignition temperature in the context of PSRs: the lowest reactor  $T_{in}$  in which any increment in temperature shifts the system

the higher branch of the S-shaped curve ( $T_{in}$  vs. final temperature, in this case). In systems relying on recirculation to preheat the reactants, as usually done for gas turbine combustors aimed to operate in the FC regime, such definition poses difficulties. Considering the reactants inlet temperature prior to the mixing with vitiated gases is not sufficient to describe the attainment of the regime, while considering the reactants and recirculated gases to be perfectly premixed prior to any reaction is also inaccurate.

Retaining the focus on the application to gas turbines, one of the most comprehensive definitions was that of Rao and Levy [19]. The proposed diagram, an improved version of which is shown in Fig. 2, highlights the roles of  $T_{in}$ , the  $O_2$  concentration, and the recirculation ratio. However, the depicted values are only representative and can vary significantly depending on the specific application. The diagram is useful to understand the difficulties in achieving FC in gas turbine combustors, as the values of recirculation ratio required to achieve lower  $O_2$  concentration are quite high.

Recently, Evans et al. [18] made a distinction between FC (or MILD) and auto-ignition non-premixed flames by extending the proposition of Oberlack et al. [20], which was developed for premixed flamelets. Their definition imposes the S-shaped curve ( $Da$  vs.



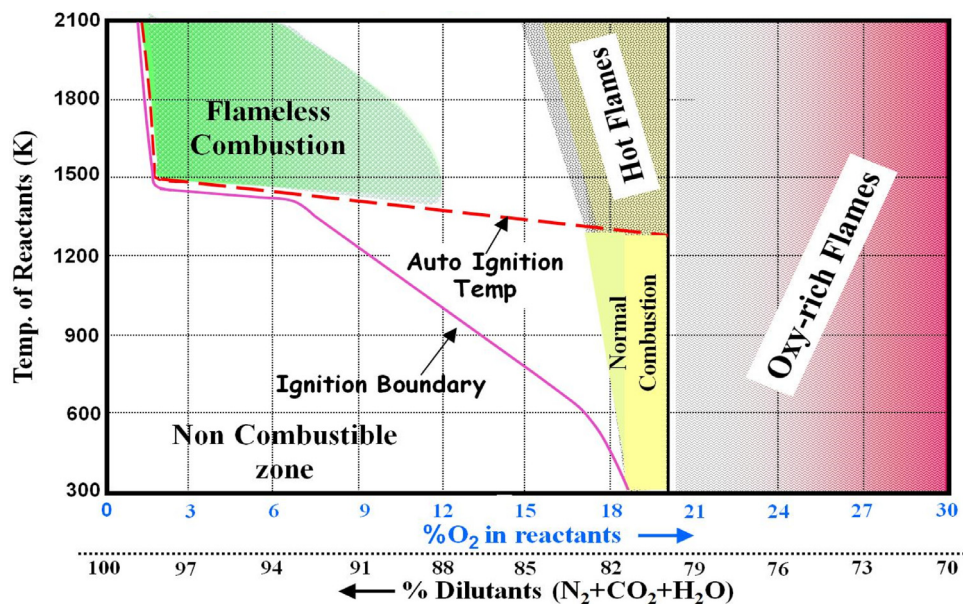


Fig. 2. Combustion regimes diagram proposed by Rao and Levy [19].

$T^*$ ) to be monotonic under the FC regime. Therefore, a strong and arguable assumption is made: FC flames do not exhibit auto-ignition and extinction in their structures. This has serious implications to the Jet-in-Hot-Coflow (JHC) experiments discussed in the following section of this paper since most of them would be outside the FC regime (as highlighted by Evans et al. [18]). Consequently, Evans et al. [18] considered the definition of Cavaliere and de Joannon [15] to be inaccurate, as it comprehends both auto-igniting and gradual combustion flames.

A comparison of the aforementioned definitions is shown in Fig. 3. The calculations are performed for methane combustion using the Cantera package [21] along with the GRI 3.0 mechanism [22], utilizing chemical equilibrium (for the PSR-like definition), premixed flamelets and non-premixed flamelets (for the S-shaped curve definitions). The considered value for the auto-ignition temperature and the one-step reaction effective activation energy were 1000 K and 40 kcal/mol, respectively, as previously assumed [15,18].

The plots for the S-shaped curve definition for premixed flames are made with an assumption for the non-dimensional heat of combustion introduced by Cavaliere and de Joannon [15]  $Q^* \approx \Delta T/T_{in}$ , while the original formulation defined  $Q^* = (QY_{Fin})/(c_p W_F T_{in})$ . As the criterion for a monotonic S-shaped curve is  $E^* \leq 4[(1 + Q^*)/Q^*]$ , the approximation neglects the influence of varying fuel mass fraction and  $c_p$  for different  $\Phi$  and  $O_2$  concentrations at the inlet. Therefore, the resulting FC region using these approximations is larger than without it. Moreover, it is worth highlighting that the formulation of Oberlack et al. [20] is valid only for lean mixtures.

The definition for non-premixed flamelets presents no difference between different  $\Phi$  as the regime is evaluated in relation to the temperature reached at stoichiometry. For low enough  $\Phi$ , the PSR definition [15] is only dependent on  $T_{in}$ , as the temperature increase is low enough for every  $O_2$  concentration considered, as shown when  $\Phi = 0.4$ . The only requirement is then to have  $T_{in}$  above auto-ignition temperature. For  $\Phi$  close to unity, the FC region is smaller, as the temperature increase is higher, which is also the case for the definition of Oberlack et al. [20].

All three formulations are ultimately dependent on initial temperature and temperature rise (once auto-ignition temperature and activation energy are given). Additionally, their assumptions are at first glance opposing: on one hand being

above auto-ignition temperature [15], and on the other hand not exhibiting ignition or extinction [18, 20]. However, that is not the case, as the definitions share common regions. Fundamentally, the assumption of Cavaliere and de Joannon [15] is that in FC the reactions energy barrier imposed by the activation energy should be surpassed by the reactants initial temperatures, while not reaching a final state of very high temperature, defined arbitrarily. On the other hand, the monotonic S-shaped curve assumption is to some extent concerned with how the energy release takes place, and not strictly with the initial and final states. The smooth heat release imposed by the monotonic S-shaped curve is especially translated into high  $T_{in}$  and low Zel'dovich numbers, as well as low fuel concentrations for premixed cases.

On a more fundamental standpoint, the Damköhler number ( $Da$ ) has been constantly pointed as a good indicator for the FC regime, as it has been shown that the interaction between turbulence and chemistry is strong under the regime. Therefore, values of  $Da$  are likely to be close to unity under the FC regime [23–25]. The analyses performed by Cavaliere and de Joannon [15], referred to by the authors as being “more suggestive than propositive”, focused largely on chemistry, while turbulence and its interaction with chemistry were left out of consideration. Many of their investigations were based on a  $Da < 1$  assumption. While such assumption is useful to simplify the study, most authors defend that the FC regime is fundamentally linked to turbulence-chemistry interaction.

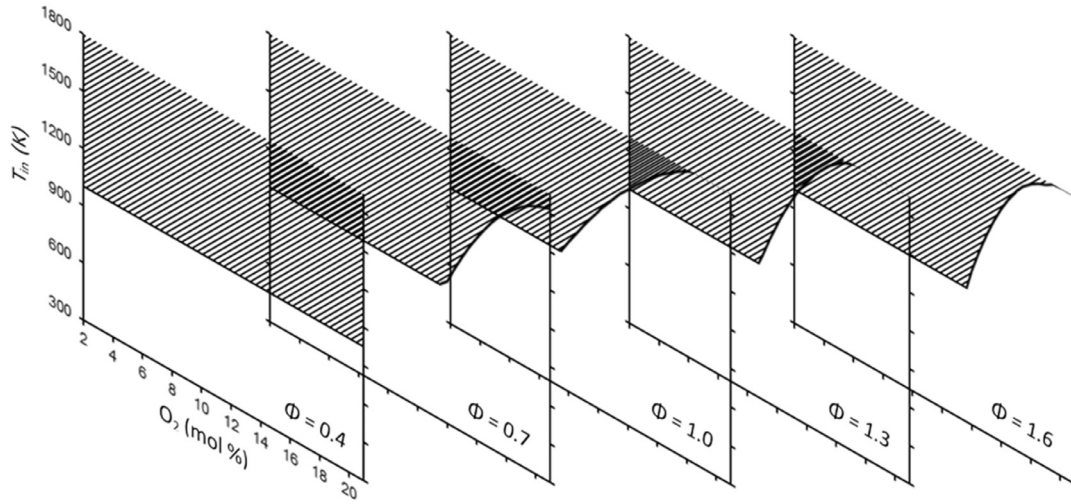
The generic definition of  $Da$  is the ratio between a flow (or turbulence) time-scale and a chemical time-scale. The difficulty dwells on how these time-scales are correctly defined to better represent the phenomena in FC. Examining the diagrams for conventional premixed (as proposed by Borghi [26] and Peters [27]) and non-premixed [28] flames (Fig. 4), the distributed reactions regime corresponds to values of  $Da$  near unity and high  $Ka$  (Karlovitz number), considering the flow time-scale of  $Da$  to be the integral time-scale ( $Da_T$ ).

Industrial applications usually have high Reynolds numbers ( $Re$ ) when compared to laboratory-scale burners. When considering  $Da$  close to unity, integral-scale  $Re$  is dependent only on the square of  $Ka$ , defined as the ratio between the chemical and the Komolgorov time-scales. To which extent the FC regime is

---

 PSR-like Definition [15]:
 

---



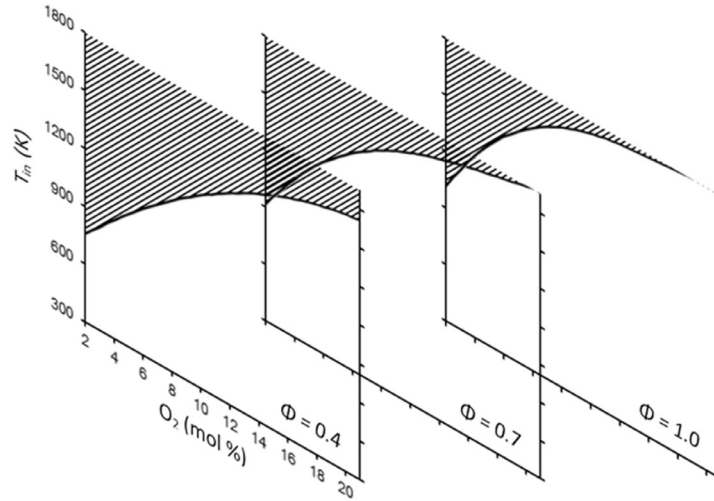

---

 Monotonic S-shaped Curve Definition
 

---

 Premixed Flamelets [20]:
 

---




---

 Non-Premixed Flamelets [18]:
 

---

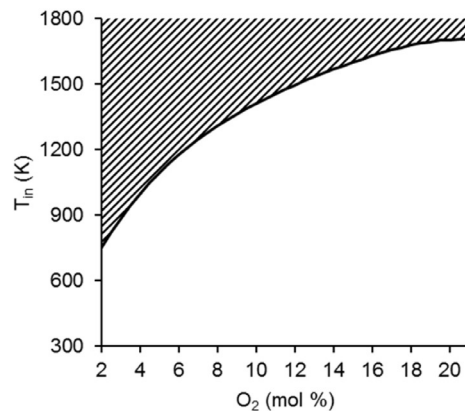


**Fig. 3.** Calculated regions where the FC regime occurs in relation to reactants temperature ( $T_{in}$ ), molar concentration of  $O_2$  in the oxidiser, and equivalence ratio ( $\Phi$ ) according to the definitions of Cavaliere and de Joannon [15], Oberlack et al. [20], and Evans et al. [18].

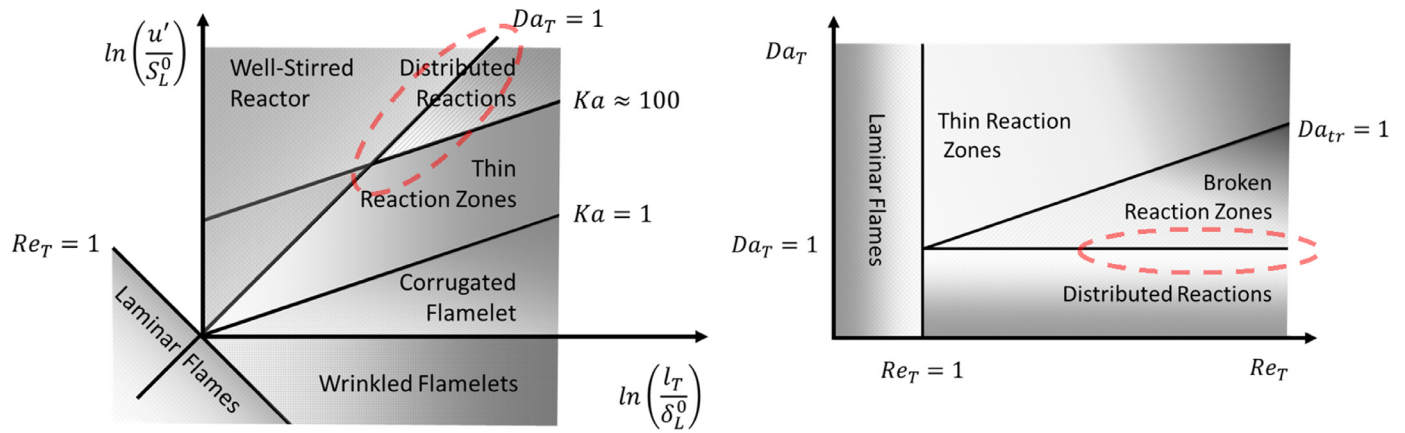


**Fig. 4.** Combustion regime diagrams for premixed flames (left) and for non-premixed flames, based on the diagrams proposed by Borghi [24], Peters [27] and Law [28]. If the FC regime is considered related to distributed reaction zones, the regions highlighted by the dashed lines are relevant for the regime.

dependent or affected by the value of  $Ka$  is still unknown due to the difficulties involved in achieving a broad range of conditions experimentally or through DNS. However, the high turbulence intensities normally associated with high  $Re$  have been reported to aid the attainment of the FC regime [29].

From the perspective of gas turbines, combustion is usually placed on the premixed diagram in the thin reaction zones region, with high  $Re$ ,  $Ka$  in the vicinity of 100, and  $Da$  greater than 1 [30–32]. In order to attain the region where FC is expected to occur, higher values of  $Ka$  and  $Re$  are expected, while  $Da$  has to drop. One can conclude that the chemical time-scales have to be increased in relation to the flow time-scales. The high pressures required in gas turbine combustors make that particularly difficult, as reactions tend to occur faster with pressure. Therefore, investigations in high-pressure conditions are necessary. However, as shown in Sections 3 and 5, there is a dearth of experimental investigations in high pressure environment.

As FC is classified as partially-premixed for most applications, the classical approaches employed for defining the flow and chemical time-scales for premixed flames are not necessarily valid, while the definition for non-premixed flames is not consensual. Isaac et al. [33] proposed a method to determine the chemical time-scale using the Jacobian of the chemical source term based on Principal Variable Analysis (PVA). As there is no possible validation for the method, its analysis comprised the application to simulation results of representative cases described to be in and out of the FC regime. They employed simulation results based on the experiments of Dally et al. [34] (discussed in Section 3.1) to represent FC conditions, while Direct Numerical Simulation (DNS) data of non-premixed jet flames were used for conventional combustion. A range of  $Da$  was then calculated by considering the full range of the turbulence (or mixing) scale between the Kolmogorov and integral scales. As expected, FC showed results close to unity, while conventional combustion exhibited higher values of  $Da$  for integral mixing scales.

Similarly, Li et al. [35] compared their proposed method for calculating chemical time-scales with others present in the literature (including the aforementioned PVA of Isaac et al. [33]). The input to the evaluations was a CFD simulation of a  $CH_4$  diffusion flame in a hot coflow, which was expected to operate under the FC regime. The authors' method presented  $Da$  values closer to unity, while the other methods had lower  $Da$ . However,  $Da$  was calculated considering the Kolmogorov scale as the flow scale, which is one of the many options to define it. Furthermore, the evaluation relied on many assumptions that eventually arrive at

the starting point: (i) the chosen case was assumed to be representative of FC; (ii) the CFD modelling was assumed to accurately capture the flame characteristics; (iii) the methods were compared based on the expected  $Da$  values for FC. Therefore, this work demonstrates well the difficulty related to defining FC solely based on  $Da$ .

The classification of combustion regimes has been disputed for decades, even when considering the aforementioned regime diagrams (Fig. 4), whose predictive value is limited because of the assumptions involved. More importantly, even canonical laboratory flames are spread over different regions of the diagrams instead of occupying a single point, since the conditions vary locally. Given the complexity involved in FC, perhaps global parameters alone cannot define its occurrence.

If a new FC definition would be based on  $Da$  and  $Ka$  numbers, the FC regime could be perceived as a local property. One could then set a global threshold or statistically determined value to define whether the system is under the FC regime. The inconsistencies found in all the aforementioned classifications are possibly a result of the simplifications incurred in estimating local characteristics using global parameters, a common and useful practice in many fields.

The importance of having a widely accepted definition goes beyond classification. As it is shown in the following sections, the conclusions of flame structure and modelling studies are not necessarily incremental if there is no certainty that the same regime was studied. Authors constantly disregard part of the previous works because of the inconsistencies in the classification or definition.

From a purely practical point of view, a definition including the advantages of the regime would be useful. Whether the reaction zones exhibit auto-ignition, are well-distributed, or have low visibility is of little importance if they do not yield lower emissions and acoustic oscillations. Evidently, a definition based solely on such advantages would certainly not be precise, as the conditions are not univocally achieved in combustion systems. However, this discussion is to point that while the debate on the boundaries of the FC is ongoing and requires more scientific support, the technological advance can take place exploiting the advantages provided by the regime.

### 3. Basic experimental investigations

The study of combustion often relies on measurements of simple canonical flame configurations, useful in providing an understanding of the physics involved in the combustion process and to



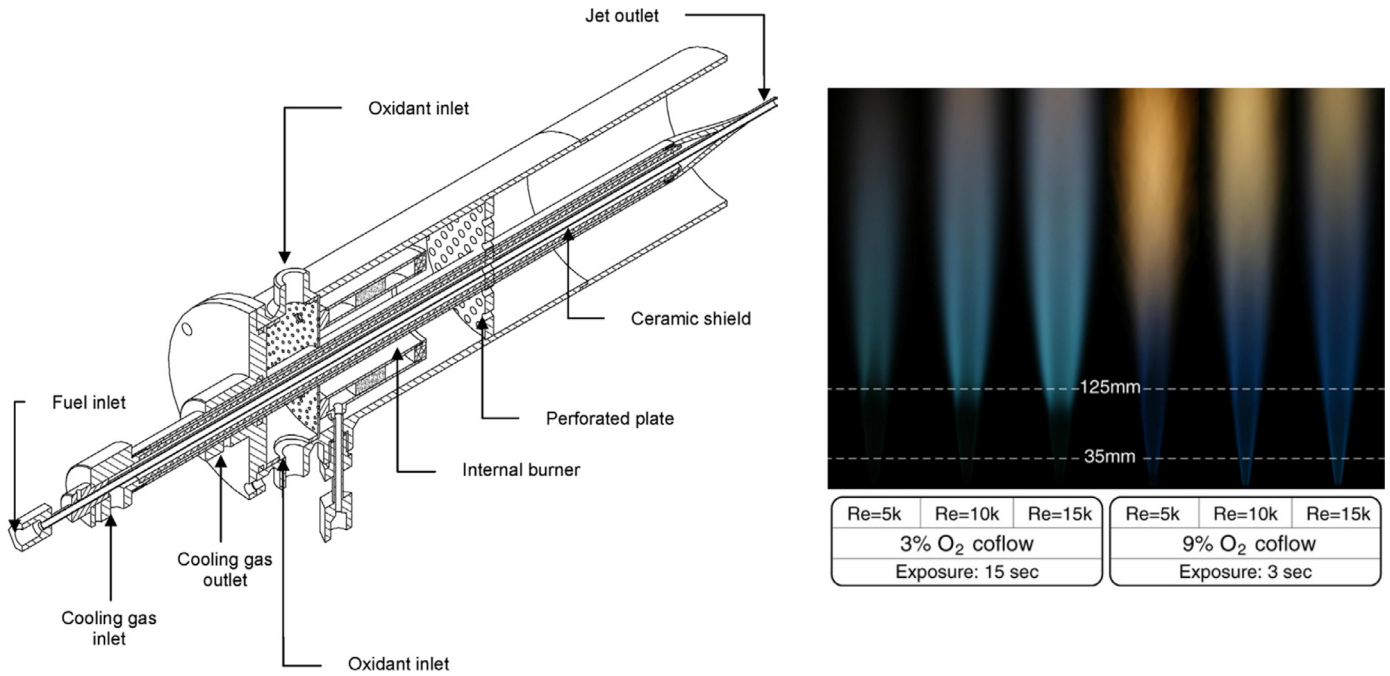


**Fig. 5.** The Adelaide JHC burner (left). Hot and vitiated coflow is generated by an internal burner [36]. Photographs of the flames for different fuel jet  $Re$  and coflow  $O_2$  concentrations [38].

systematically change the parameters that govern the flame characteristics, as well as to provide databases for model validation. Conventional combustion experiments of this type usually utilize burner stabilized flames for premixed cases, and opposing jets or lifted flames for non-premixed cases. This section is dedicated to reviewing experiments intended to investigate the FC regime.

### 3.1. Axisymmetric burners in non-enclosed environment

Researchers often take advantage of bi-dimensional and axisymmetric flame configurations in order to simplify measurements and simulations. Non-enclosed flames have been preferred due to the easier access for diagnostics. The most used approach to create the necessary conditions to achieve FC is to have a jet containing fuel within a coflow of oxidiser which may be preheated and/or diluted, as depicted in the example shown in Fig. 5. Usually called as Jet-in-Hot-Coflow (JHC), this configuration offers several advantages and unique features. The generation of vitiated gases in the coflow eliminates the need for aerodynamic recirculation of combustion products, thereby providing good control over the local composition. By applying low  $O_2$  concentrations in the coflow, it became clear that this type of experiment could be suitable to reach the FC regime.

JHC setups have many degrees of freedom as there might be several variations: fuel and coflow temperatures, ratio between fuel and coflow velocities, ratio between jet and coflow widths, fuel types, coflow composition, etc. For this reason, the identification of patterns and parameters that govern the attainment of the FC regime is still an open problem to some extent. Additionally, there is no consensus regarding the attainment of FC in all cases.

The first set of experiments using JHC to investigate FC was performed by Dally et al. [34], using a burner that is often referred to as the Adelaide burner. The experiments used a mixture of  $H_2$  and  $CH_4$  as fuel (equal in volume) and explored three different  $O_2$  concentrations (3, 6 and 9% in the mass base) in the preheated coflow, while maintaining temperatures and fuel jet Reynolds numbers. The coflow contained constant fractions of  $CO_2$  and water, while nitrogen concentration was varied. Radial profiles of species concentrations and temperatures were measured in few axial stations with point

measurements. The key findings of Dally et al. [34] were mostly related to consequences due to the decrease in reactivity with decrease in the  $O_2$  concentration: peak temperatures dropped and OH concentrations were lower (both due to a decrease in its overall quantity and to reactions becoming more distributed). The overall CO and NOx emissions were reduced, with NO showing distinct formation patterns in axial locations closer to flame. The case with the lowest  $O_2\%$  presented higher NO formation at axial stations closer to the inlet when compared to the cases with higher  $O_2\%$ . This fact pointed to the possibility of having different dominant chemical paths in the FC regime, as well as to the importance of the chosen diluent, since a different behaviour could take place if  $O_2$  concentration would be decreased by increasing  $CO_2$  or water.

According to the definition proposed by Evans et al. [18], this set of experiments is the only one to capture the transition from FC to auto-igniting flame when increasing the  $O_2$  concentration in the coflow. This observation was corroborated to some extent by the analysis of Parente et al. [37], in which an interesting statistical analysis of the data showed differences in the flame structures between the cases with 3 and 9%  $O_2$ .

The work of Medwell et al. [38] employed practically the same experimental setup of Dally et al. [34] to assess OH and formaldehyde ( $CH_2O$ ) distributions via LIF (Laser-induced Fluorescence). The comparison between the two works is an interesting example showcasing the multiple variables in such systems. The set of experiments had coflows with 3 or 9%  $O_2$  volumetric concentration, and different fuel jet Reynolds numbers were imposed by changing the fuel mass flow. The two data sets are not considering the same system configurations, as there were differences in fuel composition, coflow velocity and temperature.

Nevertheless, important conclusions arose by simultaneously acquiring temperature and intensities of OH and  $CH_2O$ . Lower  $O_2$  concentrations led to reduced levels of OH and thickening of the zone where OH is pronounced. Additionally, the high  $CH_2O$  levels pointed to a pattern in the reactions path similar to that found in auto-ignition. The role of the  $CH_2O$  radical in such conditions was further evidenced by other studies [39–41], which are discussed later in this review paper.

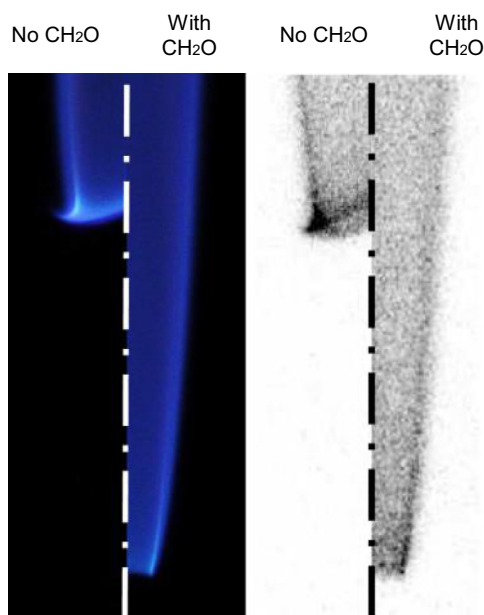


**Fig. 6.** Photographs (left) and  $\text{CH}^*$  imaging (right) comparing the flames with and without the addition of  $\text{CH}_2\text{O}$  to the fuel stream. NG as fuel, 12%  $\text{O}_2$  and 1300 K coflow, and fuel jet  $Re = 1300$  [43].

Medwell et al. [38] also discussed the effect of ambient air entrainment, which often caused local extinction in spite of the higher  $\text{O}_2$  concentration. The influence of ambient air is a limitation (or complication) of such experiments and was found to be mostly dependent on coflow Reynolds number and the ratio between the fuel and coflow pipe diameters.

In another paper [39], Medwell et al. used the Adelaide burner with the same measurement techniques to test the effect of changing the fuel stream composition. Ethylene was used in four conditions: pure, mixed with  $\text{H}_2$ , diluted with  $\text{N}_2$ , and diluted with air (partially premixed). The fuel jet Reynolds number was maintained and the coflow had 3 or 9% of  $\text{O}_2$ . The authors concluded that the flame stabilization mechanism in such conditions could be fundamentally different from that present in conventional diffusion flames. They identified a region with “weak” reaction (marked by the presence of  $\text{CH}_2\text{O}$  and low concentrations of  $\text{OH}$ ) upstream of the main reaction zone, at a position that would normally be identified as the lift-off height. This behaviour is related to the high temperatures of the reactants which cause auto-ignition in spite of the low  $\text{O}_2$  concentrations.

The levels of  $\text{CH}_2\text{O}$  below the apparent lift-off height were higher in the case of ethylene premixed with air, as expected, since  $\text{CH}_2\text{O}$  is a possible indicator of premixedness [42]. Interestingly,  $\text{H}_2$  addition showed its potential to radically change the behaviour. The  $\text{CH}_2\text{O}$  levels were the lowest when using  $\text{H}_2$  due to the increase in reactivity.

Further investigating the  $\text{CH}_2\text{O}$  formation in the conditions of these experiments [38], Medwell et al. [40] performed laminar flame calculations showing that the molecular transport of  $\text{O}_2$  to the rich side of the reaction zone plays an important role. Such transport occurred in larger proportions for lower  $\text{O}_2$  concentration in the coflow. Possibly, the lower reactivity under  $\text{O}_2$  deficient conditions allows enough time for the transport of  $\text{O}_2$  to the fuel side. In turn, the  $\text{O}_2$  availability regulates the production of  $\text{CH}_2\text{O}$  and, consequently, auto-ignition. The relation between  $\text{CH}_2\text{O}$ , auto-ignition, and  $\text{O}_2$  levels was further explained when experiments were conducted adding  $\text{CH}_2\text{O}$  to the fuel stream of the Adelaide burner [43]. The reaction zones moved upstream with increasing  $\text{CH}_2\text{O}$  and this

effect was more prominent for lower  $\text{O}_2$  concentrations. One example is shown in Fig. 6.

Moreover, the dependence on highly intermittent features became evident with the study, although these could not be precisely quantified. It was observed that the presence of  $\text{O}_2$  in the unburnt region increased with higher strain rates, which tend to be associated with large eddies. Therefore, one could expect the interaction between the largest turbulence scales and chemistry to be crucial.

The experiments using the Adelaide burner revealed important conclusions regarding stabilization and the overall behaviour of this JHC system. In parallel investigations, a slightly different configuration was developed by Cabra et al. [44] to study a jet of a  $\text{H}_2$ – $\text{N}_2$  mixture injected in a hot coflow generated by lean combustion of  $\text{H}_2$  and air to achieve a concentration of 14.74%  $\text{O}_2$ , thus much higher than those in the Adelaide burner. The burner is often referred to as the Cabra burner or the Dibble burner. The focus, according to the authors, was to replicate the coupling between chemical kinetics and turbulence (i.e. Damköhler numbers close to one) present in many applications. The coflow was created with many  $\text{H}_2$ /air lean laminar flames. Such coflow was shown to provide reasonably uniform fields, an important criterion for computational modelling.

The jet  $Re$  was considerably larger than that used by Dally et al. [34], as shown in Table 2. The fuel jet was another major difference between the two experiments, as Cabra et al. [44] employed  $\text{H}_2$  with approximately 25% molar fraction in the central jet, with the rest being  $\text{N}_2$  (contrasting with the  $\text{H}_2$ – $\text{CH}_4$  mixture used in the Adelaide burner). Simultaneous point measurements of temperatures and major species concentrations were performed, while planar measurements of  $\text{OH}$  and  $\text{NO}$  were done using LIF. Assisted by CFD modelling, the authors advocated that auto-ignition should be the mechanism responsible for stabilization, while turbulent mixing of products and reactants could be present, although they were unable to capture these features experimentally.

As a means of extending the data acquired with the  $\text{H}_2$ /N<sub>2</sub> flames, Cabra et al. [24] performed a complementary study using a  $\text{CH}_4$ /air mixture jet. As in the previous study, only point measurements were performed, and therefore the difference between the behaviour of the two fuels was shown by the larger scatter of the measured quantities in the stabilization region for the  $\text{CH}_4$  case. In accordance with what was later exposed by Medwell et al. [39], these results pointed to a different behaviour of  $\text{H}_2$  in relation to stabilization. Indications of this fact were already present in the experiments with Adelaide burner in which most of the experiments required an addition of  $\text{H}_2$  to allow stabilization of the flames. Further evidence arose as different fuel blends containing  $\text{H}_2$  showed similar behaviours [45], the stabilization of hydrocarbon JHC flames was shown to be dependent on stochastic ignition kernels [46], and when the effect of gradual  $\text{H}_2$  addition was studied [47].

The Cabra burner operating under similar conditions to those of Cabra et al. [44] was used by Wu et al. [48] with the objective of gathering data on the velocity fields. They employed LDV to measure velocity fluctuations and Reynolds stresses. They also tested the setup with non-reactive flows to draw a comparison. With the additional data, they further supported the conclusions of Cabra et al. [44] regarding auto-ignition as the possible stabilization mechanism. The most noteworthy result was related to the high sensitivity of the system. Using the same fuel jet and imposing a reduction of 13 K to the coflow temperature (from 1034 to 1021 K), the apparent lift-off height doubled and the profile of turbulent kinetic energy changed significantly. This change in the coflow was achieved by reducing the  $\text{H}_2$  molar fraction in the coflow pre-burner by only 0.2%. They suggested that the flame with the hottest coflow behaved as a conventional diffusion flame, while the other relied on auto-ignition for stabilization, as fluctuations were more intense.

**Table 2**

Summary of JHC experiments with gaseous fuels.

| Reference  | Coflow temperatures [K]               | Coflow O <sub>2</sub> concentrations (vol. or mass <sup>a</sup> ) | Fuel Jet Re          | Coflow Re <sup>a</sup>                 | Fuel jet composition  | Measured variables   | Measurement techniques                     | Computational modelling references <sup>b</sup> |
|--|---------------------------------------|---|----------------------|--|---|--|--|---|
| Adelaide Burner<br>Dally et al. [34]                             | 1300                                  | 3, 6, 9% (*)  | 9482                 | <b>1480, 1477, 1474</b>                | CH <sub>4</sub> /H <sub>2</sub>   | T, Y <sub>O2</sub> , Y <sub>N2</sub> , Y <sub>CO2</sub> , Y <sub>H2</sub> , Y <sub>CO</sub> , Y <sub>H2O</sub> , Y <sub>OH</sub> , Y <sub>NO</sub> , Z | Single point Raman-Rayleigh LIF            | [36, 104, 121, 124, 130, 133–142, 152]          |
| Medwell et al. [38]  | 1100                                  | 3, 9%   | 5000, 10,000, 15,000 | ~1400                                  | NG (92% CH <sub>4</sub> )/H <sub>2</sub>  | T, OH, H <sub>2</sub> CO   | LIF, Rayleigh scattering                   | –   |
| Medwell et al. [39]  | 1100                                  | 3, 9%   | 10,000               | ~1400                                  | C <sub>2</sub> H <sub>4</sub> , C <sub>2</sub> H <sub>4</sub> /H <sub>2</sub> , C <sub>2</sub> H <sub>4</sub> /air, C <sub>2</sub> H <sub>4</sub> /N <sub>2</sub> , | T, OH, H <sub>2</sub> CO   | LIF, Rayleigh scattering                   | [138]   |
| Medwell and Dally [45]   | 1100                                  | 3, 9%   | 10,000               | ~1400                                  | NG/H <sub>2</sub> , C <sub>2</sub> H <sub>4</sub> /H <sub>2</sub> , LPG/H <sub>2</sub> ,  | T, OH, H <sub>2</sub> CO   | LIF, Rayleigh scattering                   | –   |
| Medwell and Dally [61]   | 1100, 1200, 1300, 1400, 1500, 1600    | 3.0, 4.5, 6.0, 7.5, 9.0, 10.0, 11.0, 12.0%                        | 100 to 28,000        | <b>645 to 1702</b>                     | NG, C <sub>2</sub> H <sub>4</sub>   | Luminosity, CH*  | Filtering, Photography                     | –   |
| Medwell et al. [43]  | 1300                                  | 12%   | 7500, 13,000         | n/a                                    | NG, NG/CH <sub>2</sub> O  | Luminosity, CH*  | Filtering, Photography                     | –   |
| Ye et al. [65]   | 1250, 1315, 1385                      | 3, 6, 9, 11%  | 10,000, 30,000       | n/a                                    | Ethanol (pre-vaporized)   | Luminosity, OH*  | Filtering, Photography                     | –   |
| Evans et al. [56]  | 1250, 1315, 1385                      | 3, 6, 9, 11%  | 10,000               | <b>951 to 1135</b>                     | CH <sub>4</sub> , C <sub>2</sub> H <sub>4</sub> , CH <sub>4</sub> /C <sub>2</sub> H <sub>4</sub>  | Luminosity   | Photography                                | –   |
| Ye et al. [66]   | 1250, 1315                            | 3.0, 6.1, 9.1%  | 10,000               | n/a                                    | n-heptane (pre-vaporized)   | Luminosity, OH, CH*  | Filtering, LIF, Photography                | –   |
| Cabra / Dibble Jet in Hot Coflow Burner<br>Cabra et al. [44]     | 1045                                  | 14.74%  | 23,600               | <u>18,600</u><br><b>5188</b>           | H <sub>2</sub> /N <sub>2</sub>  | T, Y <sub>N2</sub> , Y <sub>O2</sub> , Y <sub>H2O</sub> , Y <sub>H2</sub> , Y <sub>OH</sub> , Y <sub>NO</sub> (single-point)                           | LIF, Raman scattering, Rayleigh scattering | [44, 128, 129, 131, 145]                        |
| Cabra et al. [24]  | 1350                                  | 15%   | 28,000               | <u>23,300</u><br><b>5168</b>           | CH <sub>4</sub> /N <sub>2</sub> / O <sub>2</sub> /H <sub>2</sub> O  | T, Y <sub>N2</sub> , Y <sub>O2</sub> , Y <sub>H2O</sub> , Y <sub>OH</sub> , Y <sub>CO</sub> (single-point)   | LIF, Raman scattering, Rayleigh scattering | [24, 126]                                       |
| Wu et al. [48]   | 1034, 1021, 300                       | 14.74%  | 22,600               | <u>5340, 5380</u><br><b>5541, 5589</b> | H <sub>2</sub> /N <sub>2</sub>  | V, Reynolds stresses (single point)  | LDV  | –   |
| Gordon et al. [49]<br>Delft Jet in Hot Coflow                    | 1475, 1395, 1355                      | n/a   | 13,500               | n/a                                    | NG/CH <sub>4</sub> /He  | T, OH, H <sub>2</sub> CO   | LIF, Rayleigh scattering                   | –   |
| Oldenhof et al. [54]   | 293, 1540 (max.), 1460 (max.)         | 7.6, 8.8% (*)   | 3000 to 9500         | <b>1656, 1762</b>                      | CH <sub>4</sub> /N <sub>2</sub> , CH <sub>4</sub> /N <sub>2</sub> /C <sub>2</sub> H <sub>6</sub>  | V, T, Luminosity   | CARS, LDV, Photography                     | [99, 125, 130, 132, 146–148]                    |
| Oldenhof et al. [46]   | 1540 (max.), 1460 (max.), 1395 (max.) | 7.6, 8.8, 10.9% (*)   | 2500 to 8800         | <b>1656, 1742, 1820</b>                | CH <sub>4</sub> /N <sub>2</sub> /C <sub>2</sub> H <sub>6</sub>  | V, T, OH, Luminosity   | CARS, LDV, LIF, Photography                | [99, 125, 132, 146–148]                         |
| Oldenhof et al. [57]   | 1540 (max.)                           | 7.6% (*)  | 8800, 9000, 5900     | <b>1656</b>                            | CH <sub>4</sub> /N <sub>2</sub> /C <sub>2</sub> H <sub>6</sub> , CH <sub>4</sub> /N <sub>2</sub> /C <sub>2</sub> H <sub>6</sub> /air                                | V, OH (planar, simultaneous)   | PIV, PLIF                                  | –   |
| Arteaga Mendez et al. [47]                                       | 1460 (max.)                           | 8.8% (*)  | 5700, 5650           | <b>1762</b>                            | NG, NG/H <sub>2</sub>   | V, T, Luminosity   | CARS, Photography, PIV                     | –   |
| DLR-JHC<br>Arndt et al. [58]                                     | 1655 (adiab.)                         | 9.4%  | 13,000               | <b>1335</b>                            | CH <sub>4</sub>   | OH, OH*, CH*   | Filtering, Photography, PLIF, Schlieren    | –   |
| Arndt et al. [59]  | 1566 to 1810 (adiab.)                 | 7.77 to 10.21%  | 13,000               | <b>1134 to 1466</b>                    | CH <sub>4</sub>   | OH, OH*  | Filtering, Photography, PLIF               | –   |
| Arndt et al. [60]  | 1490                                  | 10.2%   | 15,400               | <b>1553</b>                            | CH <sub>4</sub>   | OH*, T, Z, $\chi$  | Filtering, Rayleigh scattering             | –   |
| Distributed and Flameless Combustion Burner<br>Duwig et al. [62] | 1850                                  | 4.7%  | 2810, 5620           | <b>178</b>                             | CH <sub>4</sub> /air  | T, OH, H <sub>2</sub> CO (planar, simultaneous)  | PLIF, Rayleigh scattering                  | –   |

<sup>a</sup> Values reported by the authors are underlined and calculated values are bold. Values are calculated based on the reported compositions, temperature, diameter, and velocity or mass flow. If temperature and velocity profiles are available, mean values are adopted. Properties (density and viscosity) were calculated using the GasMix library along with FluidProp [64].

<sup>b</sup> Selected works discussed in Section 4.

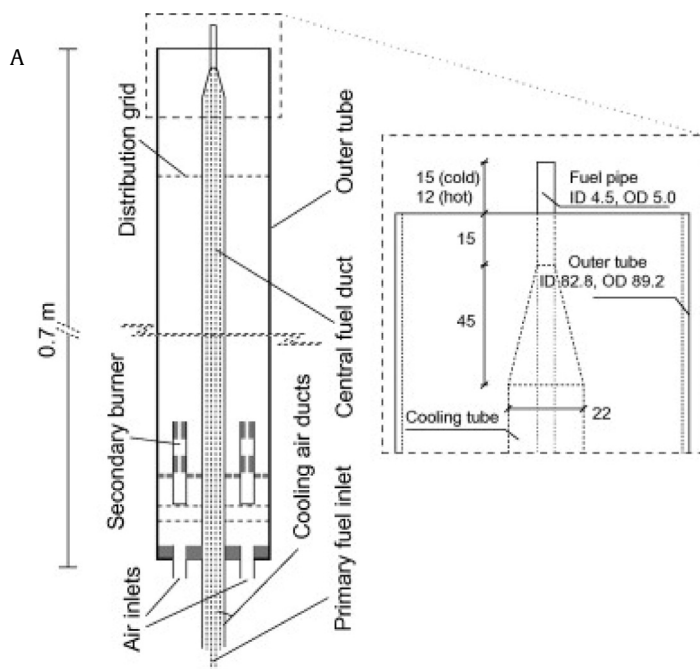


Fig. 7. Sketch of the DJHC burner [46].

more detailed experimental campaign using the same burner was presented by Gordon et al. [49]. They were able to simultaneously acquire temperature and to perform OH and CH<sub>2</sub>O imaging. The experiments were conducted using a natural gas, CH<sub>4</sub> and He mixture instead of the H<sub>2</sub>–N<sub>2</sub> mixture used in the previous experiments. This mixture was developed to match the fuel and coflow Rayleigh cross-section, in order to minimize errors and allow quantification of temperature and OH. The results showed the presence of CH<sub>2</sub>O and ignition kernels early in the jet. Supported by transient laminar simulations, these characteristics were speculated to be necessary for the formation of a stable flame further downstream. The authors analysed the flames statistically and identified three distinct regions. Such regions were located sequentially downstream the jet and were based on the frequency of structures. The first region was characterized by the presence of CH<sub>2</sub>O with practically no OH and was related to the “building of a radical pool”. Further downstream, ignition kernels were frequent, marked by the presence of OH radical in an intermittent fashion. The last region was identified as the stabilized flame, with a discernible flame front. Therefore, Gordon et al. [49] provided insights into the structures and mechanisms involved in auto-ignition and stabilization for that particular system.

By comparing the works of Gordon et al. [49] and Medwell et al. [39], it is again possible to identify how difficult it is to reach a general conclusion. Although measured quantities were the same, the techniques employed had different capabilities. Moreover, fuel composition, jet velocities, Reynolds numbers and coflow composition were different. Therefore, two different structures have been reported: (i) flames with a weak region of OH followed by a stronger reaction zone [39] and (ii) flames with the three regions as described by Gordon et al. [49]. However, the apparent difference could be a result of different setups and measurement systems.

As an attempt to reach more general conclusions, Gordon et al. [41] further analysed the obtained data [49] while also comparing to data from other sources. The authors used the product of the OH and CH<sub>2</sub>O images to represent the heat release rate (HRR), as first suggested by Najm et al. [50]. They verified the validity of this approach on the auto-igniting flames and concluded that while the progression of these flames is different from well-known lifted diffusion

flames, they behave similarly from the height where medium-sized kernels appear. Moreover, the flame structures had similarities with triple flames (as described by Dold [51]), evidencing the partially-premixed nature of the JHC flames analysed. The correlation between species concentrations and HRR was recently studied by Sidey and Mastorakos [52]. They performed extensive calculations comparing conventional flames and flames under FC conditions to correlate HRR and chemical species. They found HCO to be a poor marker, while CH<sub>2</sub>O performed better. Additionally, OH\* emission was significantly lower than in conventional flames, even when OH peaks were similar, further explaining the low luminosity of flames under FC. Therefore, the analysis of Gordon et al. [41] is in line with the most recent developments.

Another series of experiments was introduced by the work of Oldenhof et al. [53]. The authors presented the Delft-Jet-in-Hot-Coflow (DJHC) burner (shown in Fig. 7) and results regarding the symmetry of the velocity and temperature fields, key for good quality of the experiments. Further investigating the stabilization characteristics mentioned by Medwell et al. [39] and Gordon et al. [49], Oldenhof et al. [46,54,55] compared flames in cold and hot coflows, the formation of ignition kernels, and the stabilization mechanisms especially relying on a statistical approach. The studies made use of velocity, temperature, flame luminescence and OH radical data to draw conclusions regarding the effects of fuel jet *Re* and fuel composition (natural gas and CH<sub>4</sub>–C<sub>2</sub>H<sub>6</sub> blends were tested) on flame stabilization.

The works of Oldenhof et al. [46,54,55] were able to demonstrate that the mechanism of stabilization in the investigated hot diluted coflows is fundamentally different from that of conventional diffusion flames, supporting previous works [40,41,49]. In conventional lifted flames, the propagation of energy and radicals from the reaction zone to the incoming reactants is responsible for stabilization. In most of the hot coflow flames, the entrainment of coflow into the fuel stream causes auto-ignition at sparse random regions due to the low reactivity of the mixture and its high temperature. The stabilization is then a combined effect of both auto-ignition and flame propagation. The main particularity of this series of experiments was the combined use of PIV and OH measurements, as well as comparisons with ambient temperature coflows.

Usually, a precise prediction of lift-off height for diffusion flames is a good indicator for assessing the modelling accuracy as it is dependent on turbulent mixing, chemistry and their interaction. In a hot coflow environment, as the reactions become distributed and the gradients decrease, such definition is not as straightforward and the different possible definitions give rise to large discrepancies. Medwell et al. [39] pointed out that the definition used to define the lift-off is arguable for hot coflow conditions. This issue was later approached by Oldenhof et al. [54]. The proposed lift-off height evaluations were statistically derived based on several instantaneous chemiluminescence snapshots, instead of an average image. One of the definitions proposed was the height in which the probability of finding flame luminescence was 50%.

The effect of fuel jet *Re* on lift-off heights was found to be rather remarkable and is explained by the stabilization mechanism. The lift-off height was lower with increasing *Re* up to a certain value of *Re*, after which the lift-off height started to increase. With jet *Re* higher than 5000 (bearing in mind this value is case-dependent) the lift-off height increased with increasing *Re*. The initial reduction in the lift-off heights is explained by the entrainment of hot coflow caused by the fuel stream momentum, which compensates the increase in convection. The authors pointed that higher jet *Re*, and consequently higher turbulence levels, decrease the growth of ignition kernels and even extinguish nascent kernels.

These conclusions pointed to possible difficulties in computational modelling. As stabilization in such conditions is highly dependent on local stochastic phenomena, RANS approaches would tend



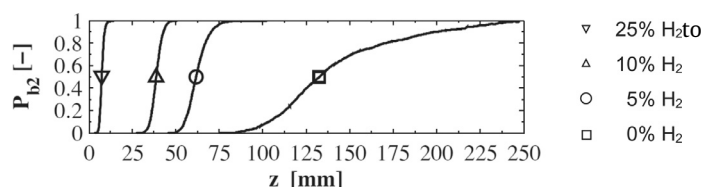


Fig. 8. Probabilities of flame luminance as a function of the height above the fuel nozzle in the DJHC for decreasing  $H_2$  concentration in the natural gas fuel stream [47].

fail, unless a robust statistical treatment can be employed. Additionally, the local transient entrainment should be well predicted [54], further pointing towards unsteady RANS or LES approaches.

The effect of having higher alkanes in the fuel stream was also investigated by Oldenhof et al. [54], by adding  $C_2H_6$  to  $CH_4$  or natural gas. Such investigations are interesting from a practical point of view since commonly used fuels are more complex than  $CH_4$  or  $H_2$ . As result of the  $C_2H_6$  addition, the chemical time-scales were reduced, causing a reduction in the lift-off height (similar effect as raising coflow temperature). Evans et al. [56] observed the same behaviour for  $CH_4$ – $C_2H_4$  blends in the Adelaide burner with the increase of  $C_2H_4$ : the visual lift-off height of the flames decreased substantially and the luminosity gradients increased, suggesting the  $C_2H_4$ -rich flames are more similar to conventional diffusion flames. Such behaviour can be expected as the auto-ignition temperatures tend to decrease for higher hydrocarbons. Therefore, the use of higher hydrocarbon fuels can prevent or impair the attainment of FC, especially for configurations that mainly rely on mixing prior to ignition.

The effect of fuel composition was approached differently by Medwell and Dally [45]. The Adelaide burner was used to compare the behaviour of natural gas, ethylene, and LPG, all diluted in a 1:1 volumetric ratio with  $H_2$ . The coflow had again 3 or 9% oxygen in volume and jet  $Re$  was constant for all cases. They found the behaviour to be similar between the three fuels in terms of OH,  $CH_2O$ , and temperature, probably due to  $H_2$  addition. Notably,  $H_2$  addition was necessary to avoid flame blow-off, pointing to its high influence in the overall behaviour. The authors performed laminar flame calculations to analyse conditions with and without  $H_2$ , as an attempt to determine its effect. Although the auto-ignition temperature of  $H_2$  is relatively high, the analysis showed that  $H_2$  improves reactivity by increasing the concentration of essential radicals as  $CH_2O$  and HCO.

Given the unique behaviour of  $H_2$  in such systems, Arteaga Mendez et al. [47] compared different proportions of  $H_2$  feeding the DJHC setup. Natural gas was used undiluted or blended with 5, 10 or 25%  $H_2$  (in volume). Ignition kernels were clearly visible for the flame with no  $H_2$  addition, and were only discernible for the flame with 5%  $H_2$ , while it was not possible to capture kernels in the 10 and 25%  $H_2$  flames.

Interestingly, when calculating the lift-off height as proposed by Oldenhof et al. [54], the probability of spotting flame luminance was much more distributed for the case without  $H_2$  (Fig. 8). Therefore,  $H_2$  either shifts the stabilization mechanism to that present in conventional lifted flames, or the occurrence and development of auto-ignition kernels happen in a much shorter length. How such differences would affect pollutant emissions is not completely clear. However, the temperature data provided by Arteaga Mendez et al. [47] shows larger gradients of temperature for the case with more  $H_2$ , which would potentially increase  $NO_x$  emissions. Moreover, it is also not clear whether the cases are actually operating under the FC regime.

As the importance of auto-ignition and sparse ignition kernels in the JHC configuration became evident, the interest in the transient response of such systems emerged [57–60]. Especially, the difference

(if any) between conventional and auto-ignited FC is not clear, and studying the development of a fuel jet can reveal the mechanism regulating flame stabilization. Although the analysis of transient conditions is complex, it allows a simplification related to the stabilization mechanisms: as there is no developed flame, the energy transfer from the downstream reactions is limited. Such studies shall continue to help identify conditions in which auto-ignition occurs. For example, Oldenhof et al. [57] pointed out that ignition tends to occur in regions where the velocities are close to that of the coflow, which means less shear.

Remarkably, in view of the objective of this review, the most important conclusion derived from the experiments with the DJHC is regarding how representative JHC flames are in relation to industrial applications. Analysing velocity data conditional to the presence of flame zones, Oldenhof et al. [55] concluded that most of the flame was not exposed to strong turbulence, since reactions occurred mostly in the low  $Re$  coflow streams entrained by the jet. The highest coflow  $Re$  had been achieved with the Cabra burner and were below 6000, as shown in Fig. 9. Therefore, many JHC flames studied so far may not be representative of conditions encountered in industrial applications and thus conclusions derived from their analysis and modelling should be extrapolated cautiously. JHC burners operating at higher  $Re$  and  $Ka$  may overcome this limitation, as discussed below.

Medwell and Dally [61] also dealt with how well JHC flames represent FC. They proposed a distinction between lifted flames and FC flames (treated by the authors as MILD) in the experiments using the JHC configuration. According to the authors, the experiments performed with the Cabra burner and the DJHC [44,24,46,54] should be considered as lifted flames, while the experiments with the Adelaide burner [34,38,39] are in the FC regime. However, this classification was based on the observed lift-off heights, which is an arguable parameter, as pointed out by Oldenhof et al. [54].

Interestingly, the authors extended the conditions previously experimented with the Adelaide burner (from 3 to 9% up to 11 and 12%), attempting to analyse the change from FC to conventional lifted flame. The work of Medwell and Dally [61] is the responsible for the broader range of  $O_2$  concentration and fuel jet  $Re$  in the Adelaide burner, depicted in Fig. 9. It was difficult to identify patterns in the lift-off height behaviour while varying coflow temperatures, coflow  $O_2$  concentration, and fuel-jet  $Re$  separately. This could be either a result of the complex physics not regulated by single variables, or by limitations in the definition of the lift-off height. Anyhow, the lack of a good definition for the FC regime once again impedes the interpretation of results.

Duwig et al. [62] presented a coflow burner with a premixed central jet surrounded by a McKenna burner to generate the coflow (Fig. 10). The burner was named Distributed and Flameless Combustion Burner (DFCB). Attempting to address the problems mentioned by Oldenhof et al. [55], this burner was able to operate at high  $Ka$  (estimated to be up to 14,000), with increased levels of turbulence as compared to previous experiments. Premixed mixtures were injected through the central plug, thus, the setup shares similarities with the piloted premixed jet burner, studied by Dunn et al. [63].

Different  $CH_4$ /air equivalence ratios were explored in the central jet composition, with two lean mixtures (0.6 and 0.8) and one rich (6.0). The premise was to compare FC under very lean conditions, created by the lean central jets and the vitiated coflow (gas turbines), and conditions close to stoichiometry (furnaces). The authors showed that the cross-correlation of the OH and  $CH_2O$  signals was negative, pointing that OH starts to increase as the initially produced  $CH_2O$  begins to decay in these flames, corroborating the aforementioned findings of Gordon et al. [49]. The differences between the lean and rich jets were mostly exhibited in the joint PDF of the estimated layer thicknesses of OH and  $CH_2O$  at the axial location with the lowest values of cross-correlation. A thicker  $CH_2O$  brush

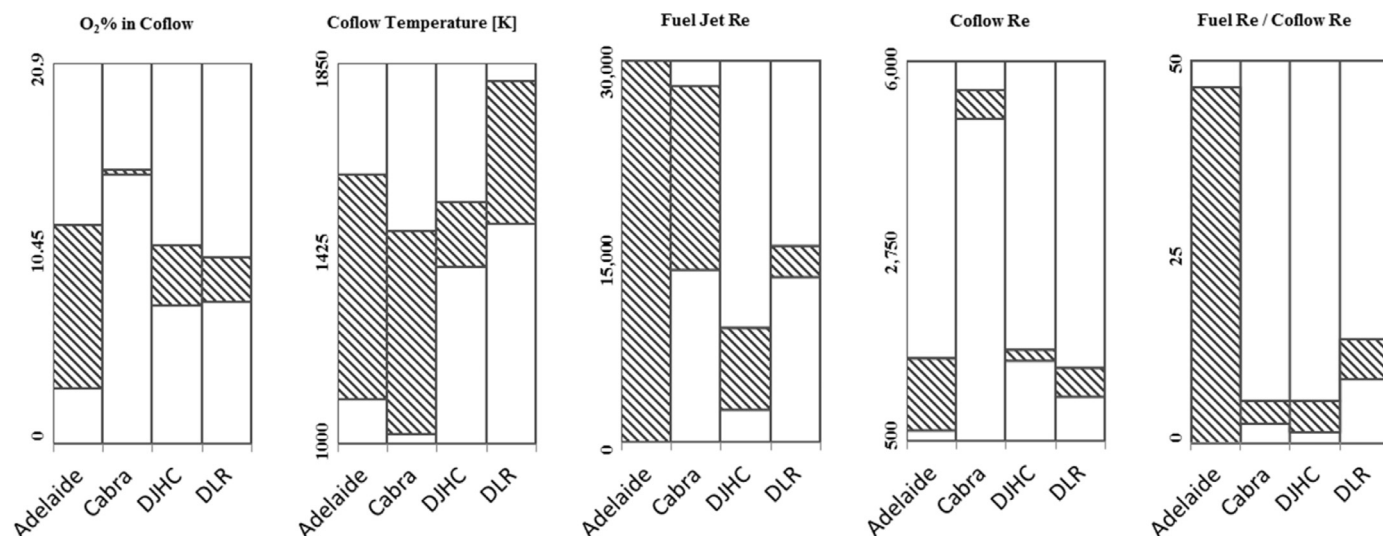


Fig. 9. Comparison of the ranges covered by the experiments performed with the most important JHC setups. Ranges displayed in accordance to the calculated values on Table 2.

followed by a thinner and more defined OH brush was found in the rich case, as opposed to the thinner CH<sub>2</sub>O region followed by a wrinkled and less intense OH brush for the lean cases.

The authors concluded that the turbulence-chemistry interaction would therefore be fundamentally different between a gas turbine application and a furnace in the FC regime. However, full validation of such statement requires more studies, especially on the influence of higher  $Ka$ , which is still unclear. Furthermore, the lean and rich cases also differ in the degree of premixedness. This fact is one of the possible explanations for the differences in the size and characteristics of the CH<sub>2</sub>O and OH regions. The higher premixedness of the lean cases possibly allowed auto-ignition to occur closer to the injection (causing a thinner CH<sub>2</sub>O brush).

In order to simplify experiments and modelling, gaseous fuels were chosen for the first sets of experiments with JHC. To study fuels that are normally in the liquid state without getting into the complications of the spray dynamics, a burner analogous to the Adelaide burner was employed using pre-vaporized ethanol [65] and *n*-heptane [66]. The ethanol flames showed behaviour similar to previous investigations when varying coflow O<sub>2</sub> concentrations (3, 6, 9 and 11% by volume). The apparent lift-off height peaked at 6% O<sub>2</sub>, thereby exhibiting a non-monotonic behaviour. The same was observed for CH<sub>4</sub> and C<sub>2</sub>H<sub>4</sub> [61], but not for *n*-heptane [66], for which the lift-off height decreased with increasing O<sub>2</sub> in the coflow. The authors had previously related the non-monotonic behaviour of lift-off height in relation to O<sub>2</sub> coflow concentration in the Adelaide burner to a shift between FC and conventional lifted flames [61]. Regardless of the dispute concerning the lift-off height definition, these results indicate anew that attaining FC is possibly more challenging with more complex hydrocarbons.

As fuels in the liquid state are very important for a series of applications, the use of vitiated coflows along with fuel sprays was also addressed with JHC burners. Cabra et al. [67,68] performed droplet-size measurements using methanol in the Cabra burner as early as 2000. However, more in-depth experiments with sprays were only performed later, first focusing on auto-ignition [69,70], followed by investigations related to FC [71,72].

The spray structure and stabilization were discussed through a comparison between non-preheated air coflow and diluted hot coflow [71] on an improved burner compared to the DJHC with respect to increased coflow diameter and more uniform temperature and velocity profiles in the coflow. Gas phase velocities on the plane of the fuel atomizer were measured, data was acquired on

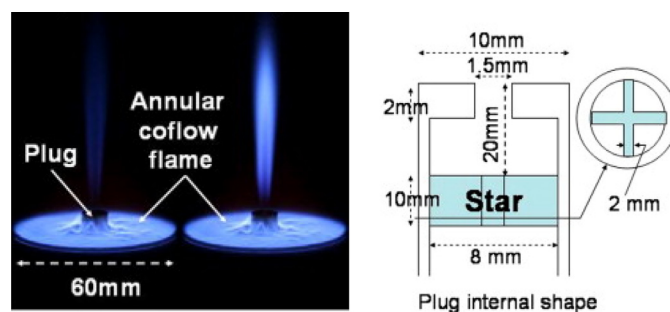


Fig. 10. The burner employed by Duwig et al. [62]. The central jet plug was placed in the centre of a McKenna burner. Premixed methane and air was injected through the plug.

droplets velocity and sizes, as well as temperatures. Similar to the stabilization mechanism for gaseous fuels, the authors concluded that auto-ignition plays a central role, as there was sufficient energy to vaporize and ignite the fuel in the hot coflow case. The hot environment led to the faster breakup of the liquid sheets as the coflow temperature affected fuel viscosity, similarly to what Cavaliere and de Joannon [15] predicted to happen under FC. Such characteristics change the velocity field near the atomizer, altering the entrainment of coflow. These experiments pointed to the need of an accurate spray model for such conditions. Such models would be useful for application in gas turbines.

Analysing the studies using the JHC mentioned so far, it is evident that the gap between these laboratory scale experiments and conditions that would be encountered in practical applications is not yet bridged. Despite the fact that JHC burners provide the most detailed databases and a relatively simpler configuration for modelling, its suitability for gas turbine related conditions is arguable. Furthermore, most experiments disregard pollutant formation, a key aspect in the analysis and application of FC.

### 3.2. Experiments in enclosed environment

The conventional JHC open-air configuration is certainly the most studied related to FC conditions. However, a range of experiments was performed using laboratory devices with enclosures. Their complexity tends to be higher than for JHC in terms of geometry and flow characteristics, while optical access is rather limited. Usually,

there is a trade-off between complexity and diagnostics: more complex geometries and enclosed flames are not easily accessible for advanced combustion diagnostics techniques, but are potentially more representative of the actual application. Importantly, data on emissions is usually present. Experiments in enclosures were performed in both axisymmetric and non-axisymmetric environment.

The experiments discussed in the following two sub-sections often focus on pollutant emissions, as this is one of the main benefits of using enclosures. The emissions generated in such systems is to some extent dependent on residence times (especially to allow CO to be converted into CO<sub>2</sub>) and recirculation (especially due to NO<sub>x</sub> reburning, further discussed in Section 4.2). Changing operational conditions of systems such as equivalence ratio, inlet temperatures, velocities, etc., inevitably modifies residence times and/or recirculation, partly explaining the difficulties in achieving low emissions for broad operational range. This is also the case for the designs discussed in Section 5.

The works reviewed in the next two sub-sections are summarized in Table 3. As can be seen, most of the experiments are still conducted at atmospheric pressures, which indicates that the field is nascent.

### 3.2.1. Axisymmetric environment

A fuel jet surrounded by a hot coflow in an enclosure was presented by Rebola et al. [73]. Preheated air surrounding a methane jet entered the combustion chamber at the same axial location. The setup did not have optical access as priority was given to thermal insulation. Temperatures and species (including CO, NO<sub>x</sub> and UHC) were point-measured at axial and radial stations, for several operating conditions. The type of data available is entirely different from the aforementioned JHC experiments. The focus was on measuring pollutant emissions, while flame structure and intermediate species could not be accessed. Although model validation is hardly possible using the dataset, its focus on emissions provides an opportunity to assess some relevant aspects for FC. The NO<sub>x</sub> emissions were observed to be lower than 10 ppm throughout all operational conditions. On the other hand, CO emission levels reached thousands of ppm for the leaner operation conditions.

Some works reported the use of reverse flow combustion chambers. This configuration is better suited for FC as the recirculation ratio is higher due to the geometry. Kruse et al. [74] adapted a laboratory scale rig (Fig. 11) previously used to study furnaces [14,75] for gas turbine relevant operating conditions. As the optical access was limited, only OH\* chemiluminescence was measured in a small portion of the chamber. The most valuable output of this experiment was related to the behaviour of CO and NO<sub>x</sub> emissions in relation to equivalence ratio and operational pressure. The NO<sub>x</sub> emissions dropped for increasing pressure and a low-emission operating window was identified.

Ye et al. [76] explored the same setup but employing pre-vaporized fuels (ethanol, acetone and n-heptane). Fuel was injected up to a pressure of 5 bar in the combustion chamber. The results showed a comparison between the fuels operating at different pressures and equivalence ratios. Interestingly, the NO<sub>x</sub> emissions increased with operating pressure, in contrary to what was observed in some of the cases using CH<sub>4</sub> explored by Kruse et al. [74].

Comparison between the different fuels is difficult due to the fixed geometry. If the equivalence ratio is to be kept constant, air-flow rate has to be varied, thereby influencing the velocity fields, residence times and reaction zones. Castela et al. [77] evidenced the limitation of such geometries using a similar reverse flow configuration. The experiments were carried out at atmospheric pressure as the combustion took place within a quartz-glass cylinder to allow optical access. The coupling between air inlet temperature, air velocity and equivalence ratio does not allow to easily extrapolate the results to different systems. However, some

patterns could be identified. Increasing air inlet velocity caused a reduction in NO<sub>x</sub> emissions for the same inlet temperatures. This behaviour is expected since equivalence ratio decreased as air velocity was increased.

Verissimo et al. [78] introduced a series of experiments carried out in a combustor very similar to the one used by Castela et al. [77] but with a direct flow configuration. The geometry shares similarities with the FLOX<sup>®</sup> architecture (presented in Section 5 of this paper), having one central air jet surrounded by 16 radially distributed fuel jets. Until recently, the only optical diagnostics were performed was OH\* chemiluminescence, while temperatures and species were point-measured with probes. The authors focused on the effect of changing operating parameters on pollutant emissions and OH\* distribution: namely equivalence ratio [78], air jet velocity [79], power input [80], and air temperature [81], although it is important to note that these parameters are not necessarily independent in such a system.

Their first set of experiments [78] focused on the combustion regime and emissions, while equivalence ratio was altered. The power input was constant, as well as inlet air temperature. Therefore, lower equivalence ratios represented higher air flow. Due to increased mixing, the reaction zone moved upstream (closer to the injection) with lower equivalence ratios. The intensity of the reactions was also higher in terms of OH\* (Fig. 12).

Regarding the emissions, while NO<sub>x</sub> increased up to a certain level of excess air ( $\Phi = 0.53$ ) and then decreased slightly, the CO emissions exhibited an opposite behaviour. This is in contrast with what is expected from typical combustion systems in which the NO<sub>x</sub> emission increases with equivalence ratio and peaks at around an eq. ratio of 1. The authors mentioned that, possibly, the effect of enhanced entrainment competed with the reduction in global residence time for decreasing equivalence ratios, and the balance between the two shifted, explaining the behaviour of CO emissions. The increase in NO<sub>x</sub> is consistent with increased intensity and possible generation of hotspots. However, the reason for its slight reduction with further decrease in equivalence ratio is not clear.

Subsequently, Verissimo et al. [79] attempted to systematically investigate the effect of heat input on the emissions. They kept the air-fuel-ratio constant throughout all conditions, as well as inlet temperatures. As thermal input was increased, reactions moved downstream as a result of increased momentum. While the NO<sub>x</sub> emissions exhibited little variations, the CO emission increased with thermal input. Hypothetically, maintaining the ratio between air and fuel, as well as their jets momenta did not change the overall mixing pattern much and therefore the emissions were not affected. In the case of NO<sub>x</sub>, the shift in the reaction zone downstream did not affect the final value of NO<sub>x</sub>, but the CO formation increased, probably due to a lower residence time. These results once again point to difficulties in attaining a systematic variation of operational parameters in combustors with jet induced mixing (subject also discussed in Section 5).

Maintaining mass flows while increasing air flow velocity (by decreasing the nozzle area), did not shift the reactions downstream. The peaks of OH\* occurred at the same location, while the reactions were more distributed for higher air velocities. The CO emissions also increased with velocity, but NO<sub>x</sub> emission reduced due to the distributed reaction zone. Hence, the works of Verissimo et al. [79,80] are another indication that mixing and recirculation drive the emissions behaviour in FLOX<sup>®</sup> type combustors.

The effect of air preheating was also analysed [81] at a chosen  $\Phi$  of 0.77. Due to the change in density, increasing air temperature increased jet velocities, thereby enhancing the mixing. At this equivalence ratio, an increase in the oxidiser inlet temperature caused an increase in both CO and NO<sub>x</sub> emissions. The NO<sub>x</sub> increased due to higher initial temperatures and higher peak temperatures, as

**Table 3**  
Summary of experiments in enclosed environments displayed chronologically.

| Reference                 | Reactants temperature [K]           | Oxidiser O <sub>2</sub> concentrations (vol.) | Pressure (bar)*    | Recirculation / Stabilization technique | Enclosure geometry          | Power (kW)   | Fuel composition  | Measured variables  | Measurement techniques                |
|---------------------------|-------------------------------------|---|--------------------|---|-----------------------------|--------------|---|---|---------------------------------------|
| Veríssimo et al. [78]     | 673 (air)                           | atm   | 1                  | Jet momentum                            | Cylinder (L/D = 2.8)        | 10           | CH <sub>4</sub>   | CO, CO <sub>2</sub> , NOx, O <sub>2</sub> , OH*, T                | Filtering, Photography, Thermocouples |
| Castela et al. [77]       | 298 to 798 (air)                    | atm   | 1                  | Jet momentum / Reverse flow             | Cylinder (L/D = 3.4)        | 8            | NG  | CO, UHC, NOx, OH*   | Filtering                             |
| Rebola et al. [73]        | 813 to 993 (air)                    | atm   | 1                  | Jet momentum                            | Cylinder (L/D = n/a)        | 8 to 13      | CH <sub>4</sub>   | CO, UHC, NOx  | Thermocouples                         |
| Veríssimo et al. [79]     | 298 and 673 (air)                   | atm   | 1                  | Jet momentum                            | Cylinder (L/D = 2.8)        | 10           | CH <sub>4</sub>   | CO, CO <sub>2</sub> , NOx, O <sub>2</sub> , OH*, T, V (cold-flow) | Filtering, Thermocouples, LDV         |
| Veríssimo et al. [80]     | 673 (air)                           | atm   | 1                  | Jet momentum                            | Cylinder (L/D = 2.8)        | 7 to 13      | CH <sub>4</sub>   | CO, CO <sub>2</sub> , NOx, O <sub>2</sub> , OH*, T                | Filtering, Photography, Thermocouples |
| Khalil and Gupta [89]     | 600 (air)                           | atm   | 1                  | Cyclonic chamber                        | Cylinder (L/D = 0.5)        | 6.25         | CH <sub>4</sub>   | CO, NO, OH*   | Filtering                             |
| Kruse et al. [74]         | 873, 923, 973 (air)                 | atm   | 1.0, 2.5, 5.0      | Jet momentum / Reverse flow             | Parallelepiped (L/x = 3.5)  | ≈ 4          | CH <sub>4</sub>   | CO, NOx, OH*, T, V  | Filtering, PIV, Thermocouples         |
| Ye et al. [76]            | 873 ± 50 (air), 443 (fuel)          | atm   | 1.0, 2.5, 4.0, 5.0 | Jet momentum / Reverse flow             | Parallelepiped (L/x = 3.5)  | 4.7          | Acetone, Ethanol, n-heptane   | CO, NOx, T  | Thermocouples                         |
| Veríssimo et al. [81]     | 373 to 973 (air)                    | atm   | 1                  | Jet momentum                            | Cylinder (L/D = 2.8)        | 10           | CH <sub>4</sub>   | CO, CO <sub>2</sub> , NOx, O <sub>2</sub> , OH*, T                | Filtering, Photography, Thermocouples |
| Khalil and Gupta [83]     | 300, 600 (diluent)                  | 12.38 to 21.00                                | 1                  | Swirler                                 | Cylinder (L/D = n/a)        | 3.250, 4.875 | CH <sub>4</sub>   | CO, NOx, OH*, T   | Filtering, Photography, Thermocouples |
| Sidey and Mastorakos [88] | 1234 to 1997 (crossflow, adiabatic) | 3.7 to 8.7                                    | 1                  | Jet in crossflow                        | Cylinder (L/D = 5.0)        | n/a          | CH <sub>4</sub>   | OH, OH*   | Filtering, PLIF                       |
| Khalil and Gupta [84]     | 300, 450, 600, 750                  | 8.92 to 21.00                                 | 1                  | Swirler                                 | Cylinder (L/D = n/a)        | 3.25         | CH <sub>4</sub> , C <sub>3</sub> H <sub>8</sub> , CH <sub>4</sub> /H <sub>2</sub> | CO, NOx, OH*  | Filtering, Photography                |
| Khalil and Gupta [86]     | n/a                                 | 14.5, 21.0                                    | 1                  | Swirler                                 | Cylinder (L/D = n/a)        | n/a          | CH <sub>4</sub>   | OH, OH*, V  | Filtering, Photography, PIV, PLIF     |
| Sorrentino et al. [91]    | 850 to 1250 (oxidiser)              | ≈ 3.6 to 5.9                                  | 1                  | Cyclonic chamber                        | Parallelepiped (L/x = 0.25) | 2            | C <sub>3</sub> H <sub>8</sub>   | T   | Photography, Thermocouples            |
| Zhou et al. [82]          | 673 (air)                           | atm   | 1                  | Jet momentum                            | Cylinder (L/D = 2.8)        | 10           | CH <sub>4</sub>   | C <sub>2</sub> *, CH*, CH <sub>2</sub> O, OH, OH*                 | Filtering, Photography, PLIF          |
| de Joannon et al. [92]    | 500 to 1100                         | ≈ 4 to 21                                     | 1                  | Cyclonic chamber                        | Parallelepiped (L/x = 0.25) | n/a          | C <sub>3</sub> H <sub>8</sub>   | T   | Thermocouples                         |
| Khalil and Gupta [85]     | 700                                 | 9.18 to 21.00                                 | 1                  | Swirler                                 | Cylinder (L/D = n/a)        | 3.25         | Ethanol, JP-8   | OH*   | Filtering                             |

\* Experiments performed in atmospheric conditions were considered to be at 1 bar.



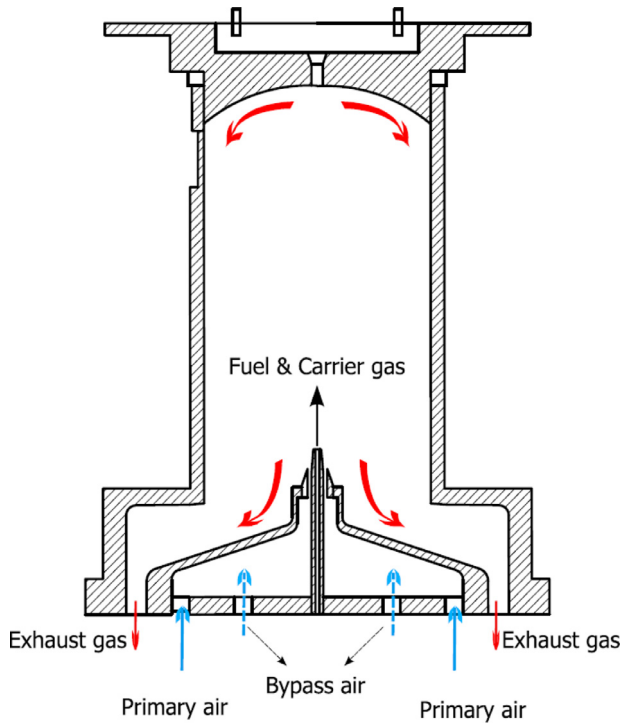


Fig. 11. Reverse flow combustion chamber employed with gaseous fuels [74] and with pre-vaporized liquid fuels [76].

denoted by the higher gradients in  $\text{OH}^*$ . The increase in CO is probably caused by the reduction in the residence time.

The works of Veríssimo et al. [78–81] provide a good database for model comparison and for descriptive analysis, especially regarding pollutant emissions. However, the varied parameters are coupled with other variables in such systems, hindering the comprehension regarding why each parameter variation yields a certain effect, also the heat loss from the combustor is an important parameter which is not measured in detail during the experiments. In order to provide more information related to this geometry, the work of Zhou et al. [82] presented measurements of OH and  $\text{CH}_2\text{O}$  for three cases previously explored, named “conventional”, “transitional”, and “flameless” ( $e$ ,  $c$  and  $a$  in Fig. 12, respectively). As pointed in various JHC experiments, the formation of  $\text{CH}_2\text{O}$  occurred upstream in relation to the region with higher  $\text{OH}^*$  for the “flameless” case. Also in line with previous experiments, the standard deviation of the OH signal was larger in the “flameless” case, indicating higher intermittency. By increasing the operational parameters and measured variables of this experimental setup, it would be possible to build a valuable database.

Swirl stabilized flames are common in gas turbines, and experiments were performed to explore this technique [83–87], in the geometry schematically shown in Fig. 13. The use of vitiated oxidiser is especially interesting for land-based gas turbines, as external recirculation is a possibility to attain the required dilution and preheating of the reactants. Again, oxidiser was diluted with  $\text{N}_2$  and  $\text{CO}_2$  at various ratios [83], while  $\text{CH}_4$ ,  $\text{C}_3\text{H}_8$ , a  $\text{H}_2$ – $\text{CH}_4$  mixture [84], ethanol and JP-8 [85] were used as fuels. The reactions took place in a transparent tube to enable acquisition of OH chemiluminescence, while emissions were monitored. A more detailed analysis was carried out having only  $\text{CH}_4$  as fuel, as velocity fields under reactive and non-reactive flows were assessed using PIV [86]. Additionally, OH was measured with PLIF. To some extent, these works share similarities with the above-mentioned jet-stabilized experiments by Veríssimo et al. [78–82],

in terms of the difficulty encountered in generalising the results of the experiments due to the large number of dependencies encountered in the system.

### 3.2.2. Non-Axisymmetric environment

The advantages of having axisymmetric configurations were previously mentioned. However, not every condition can be achieved with such geometries, especially those involving large recirculation rates. Furthermore, several engineering application of FC have non-axisymmetric geometries and experiments aimed at replicating their conditions occasionally have to adopt non-axisymmetric configurations.

Sidey and Mastorakos [88] tested a canonical three-dimensional configuration: a jet in crossflow Fig. 14. A methane jet was studied for several crossflow compositions (from 3.7 to 8.7%  $\text{O}_2$ ) and temperatures. Both steady and transient conditions were assessed via OH PLIF and  $\text{OH}^*$  chemiluminescence, and the findings were in line with most of other JHC experiments. The geometry was highly three-dimensional, posing complex flow patterns as compared to JHC cases. The main advantages of using such configuration are the examination of pollutant formation in an enclosure and the attainment of possibly higher Ka numbers. To the best of our knowledge, this is the only work that reported such configuration specifically to study FC. There is extensive literature concerning auto-ignition in cross-flow, as reported by Medwell and Dally [61], but not with a focus on examining FC. Therefore, it is still not clear if such 3D configuration would be able to provide more relevant insights or if it would be more suited to operate in the FC regime.

Khalil and Gupta [89] explored another configuration to achieve the FC regime in a relatively simple design. They used a cylindrical chamber with relatively low aspect ratio and a nearly tangential air inlet, while the exhaust was placed in the centre of the cylindrical chamber. They tested four configurations of fuel inlet, including a premixed case, coaxial injection (partially-premixed) and different injection positions for non-premixed. The location and direction of fuel injection was shown to directly affect the emissions. As the premixed case had the lowest emission values, one can argue that the mixing between products and incoming fuel and air was poor, leading to the existence of hot-spots (higher  $\text{NO}_x$  emissions) and incomplete combustion (higher CO emissions). Furthermore, whether the experiments come under the FC regime is uncertain.

Another cyclonic combustion chamber was presented by Sorrentino et al. [90,91]. The prismatic chamber had oxidiser jets positioned along opposing corners to generate swirling motion, while the exhaust was positioned at the centre of the top face (Fig. 15). The design intended to achieve relatively high residence times. The chamber was operated with several levels of dilution (by either  $\text{CO}_2$  or  $\text{N}_2$ ) and preheating temperatures, with propane as fuel. As a result, they were able to build diagrams indicating the combustion regime as a function of equivalence ratio and inlet temperature (Fig. 16). With temperatures lower than approximately 925 K, no combustion occurred. Between 925 and 1000 K, reactions took place but were not complete as temperature rise was not significant, while for higher inlet temperature, reactions were sustained and the authors considered it to be under the MILD regime. An intermediate region was identified for a range of equivalence ratios categorized as “dynamic” because of the large intermittency.

As far as gas turbine application is concerned, dilution with  $\text{CO}_2$  is more interesting than with  $\text{N}_2$ . Due to different behaviours in relation to third body reactions, the results for each diluent had slight dissimilarities. The regimes showed less dependence on the equivalence ratio when using  $\text{CO}_2$ .

The system presented hysteresis when altering the inlet temperature [92]. The CO emissions increased up to a certain level when gradually increasing the inlet temperature. After a given value of inlet temperature, CO emissions suddenly decreased. On the other

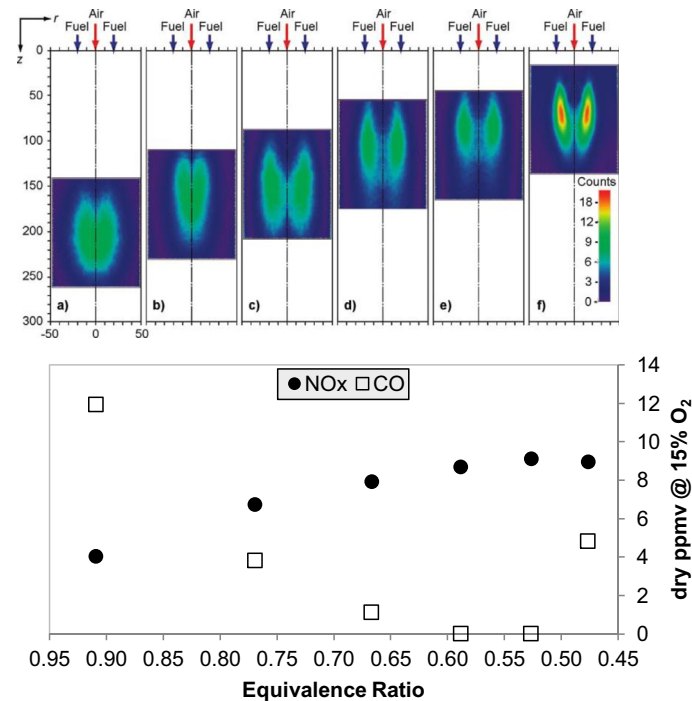


**Fig. 12.** Mean OH\* images for diverse global equivalence ratio values. From left to right,  $\Phi = 0.91, 0.77, 0.67, 0.59, 0.53, 0.48$ . Emissions of NOx and CO in dry volumetric ppm. Adapted from Verissimo et al. [78].

hand, if temperatures were decreased starting from the highest temperatures the emission levels remained low. The NOx emissions were reported to be low for most of the operational range. A drawback of this experiment is its large residence time (average of 0.5 s), which does not corroborate with the residence times encountered in gas turbines.

Notably, this kind of setup does not allow to clearly follow the path-lines of incoming reactants and their mixing pattern with recirculated combustion products as in e.g. JHC experiments. Quantifying the recirculation of products is one of the main difficulties. Therefore, these configurations are not suited for understanding auto-ignition or reaction progress. However, they can be useful to the development of concepts relying on large recirculation zones, such as FLOXCOM, FOGT and AHEAD, discussed in Section 5.

### 3.3. Observations and recommendations

The aforementioned works provide valuable information and data for model validation and comparison. Further investigation should be performed in order to make this type of experiment even more useful towards the application of FC to gas turbines. As an example, having a JHC operating in an enclosed and pressurized environment, while employing conventional and candidate alternative fuels could provide valuable indications for future gas turbine designs. It is notable that most experiments performed in enclosures had atmospheric conditions.

Many works point to the fact that stabilization under the FC regime depends on auto-ignition kernels, which in turn are highly dependent on local fluctuations and conditions. Disregarding the dispute related to the definition of the FC regime (discussed in Section 2), this hints to the need of using statistical models or unsteady approaches to achieve successful modelling.

However, it is not proven if it is necessary to model all the features of the flame in order to predict the emissions accurately. From a design point-of-view, experiments should also contain emissions measurements, which unfortunately is not provided by most of the JHC experiments. Data on pollutant emissions from JHC flames are

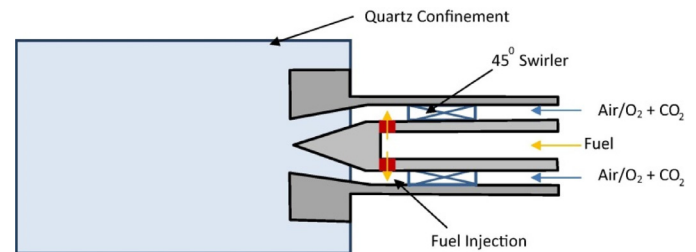


**Fig. 13.** Scheme of the swirl stabilized combustion chamber employed by Khalil and Gupta [87].

not necessarily the most relevant due to the fact they are non-enclosed and, therefore, not representative of any application. On the other hand, modelling could benefit from comparisons with such data, as the literature lacks detailed data combining flame morphology and structure with pollutant formation. If these would be combined with an enclosed and pressurized environment, the resultant data would be even more relevant.

The huge gap between laboratory scale experiments and gas turbine operating environment is evident. On one hand, effort should be concentrated to determine the conditions in which FC would take place in gas turbines in terms of energy density, turbulence intensity,  $Da$ ,  $Ka$ , and recirculation ratios. On the other hand, the design of experimental setups able to replicate these conditions in simplified configurations, while allowing range modulation and state-of-the-art diagnostics, are required. These two combined can provide the necessary bridge to enhance our understanding of the FC regime and enable us to come-up with design methods.

## 4. Computational modelling

The challenge of modelling reacting flows is often related to how simplifications and assumptions impose discrepancies in relation to the actual behaviour and how these deviations change for different

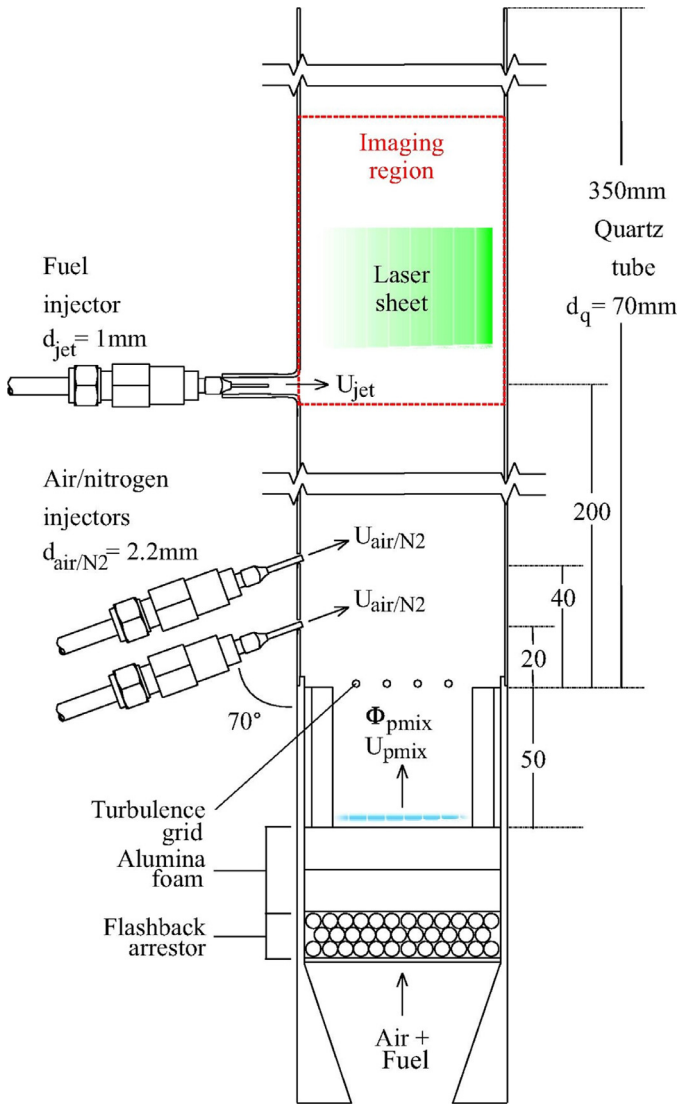


Fig. 14. The jet in crossflow experimental setup employed by Sidey and Mastorakos [88,83].

operating conditions. The comparison between computational modelling and experimental data is not only interesting to assess the validity of models, but also to provide information on variables that were not measured or are difficult to measure during an experiment. Throughout the years the effect of possible simplifications in the modelling of premixed and diffusion flames has become clear. However, development of models able to yield good results across different regimes (partially premixed combustion) or for a broad range of operational conditions still remains a challenge.

Typically, the main interest in simulating gas turbine combustors is for predicting temperature fields and emissions. The latter is especially important for FC, since it is the main reason why the combustion regime is attractive. However, no consensus exists on which features of the flow field and chemical reactions must be accurately modelled in order to have accurate pollutant emissions prediction.

Taking the previous remarks into account, in this section we give an overview of modelling approaches, report on new developments that have been made especially aimed towards representation of FC conditions. Subsequently, an overview of the main results obtained with direct numerical simulation and in the various model evaluation studies, which most often are done using the experiments discussed in Section 3 as validation database.

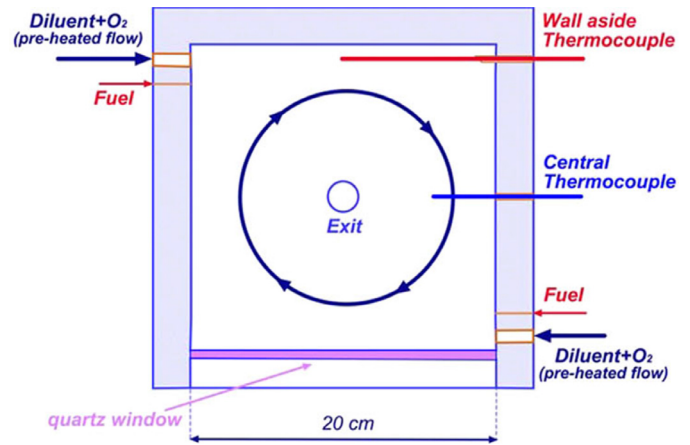


Fig. 15. Scheme of the prismatic combustion chamber designed by Sorrentino et al. [90].

#### 4.1. Overview of modelling approaches

Due to the uncertainties regarding the underlying physics, virtually every known approach has been tried for modelling the FC regime. Bilger et al. [93] have very well summarized such approaches or paradigms, and the theoretical background is not discussed in details here. The models discussed in this work are presented in the schematic of Fig. 17. Different models are given a location considering two criteria: the level of detail in the description of turbulence and the level of detail in the chemistry. The size of the boxes given to a model reflects the actual practice in published works related to modelling of the FC regime. The colour shading gives an indication of the complexity of the description of the turbulence-chemistry interaction.

Solving the flow field via Direct Numerical Simulation (DNS) provides a complete description of the turbulence. The computational cost is very high and therefore most often is carried out in combination with simple chemistry. The configurations that can be handled have a simple geometry, relevant for fundamental studies and far away from practical applications. Chemical Reactor Networks (CRN) on the other hand put the computational effort in the detailed kinetics and handle flow effects via mass flow rates between reactors and the residence time in each reactor. Their parameters have to be calibrated for specific applications. The combination of turbulent flow and chemical reaction can be handled in many different ways, working either in a Reynolds Averaged Navier–Stokes (RANS) framework or using Large Eddy Simulation (LES). In both approaches, the closure of the mean or filtered chemical source term is the main issue [93]. The simplest option is to use RANS with an eddy dissipation model (EDM) considering a comparison of chemical time scale deduced from very simple chemistry and flow time scale from a turbulence model to find the effective global reaction rate.

In flamelet models and their generalisations like Flamelet Generated Manifold (FGM) [94] or Flamelet Progress Variable Approach (FPVA) [95], a laminar flame structure is considered and all important thermochemical properties and source terms are tabulated as a function of a few independent variables using detailed chemistry. These approaches fall in the more general category of ‘tabulated chemistry methods’. Detailed chemistry can be included in these flamelet calculations. The types of flamelets can cover both premixed and non-premixed or partially premixed situations. To properly represent differential diffusion effects it is important to use detailed laminar transport properties (non-unity Lewis numbers) in the calculation of the laminar flames. To represent the combined effect of mixing and ignition in JHC flames, an igniting mixing layer (IML) has been proposed as a canonical flame

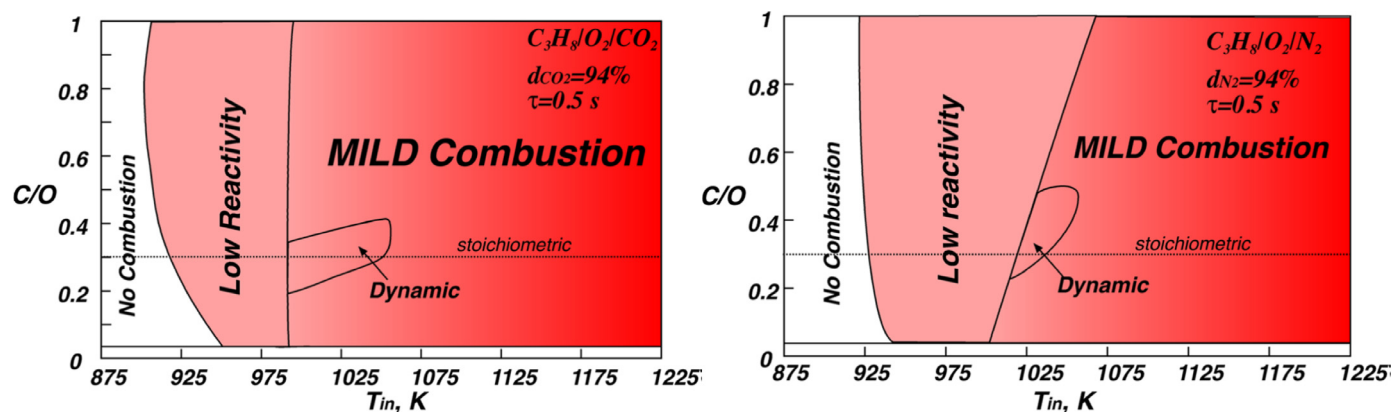


Fig. 16. Operation diagram of the prismatic combustion chamber developed by Sorrentino et al. [91] as a function of C/O (moles of carbon atoms in the fuel over the moles of oxygen atoms coming from O<sub>2</sub>). Dilution with N<sub>2</sub> (left) and CO<sub>2</sub> (right). MILD combustion region defined as in the PSR-like definition [15].

structure [96] as alternative for the unsteady counterflow diffusion flame. The mean or resolved turbulent flame structure is computed using the state or the source terms of the laminar flames and performing ensemble averaging. The turbulence chemistry interaction is taken into account via the probability density function (PDF) of independent variables, which is most often taken as an assumed mathematical function depending on a few parameters, typically mean and variance of mixture fraction and progress variable. For low Reynolds number flames it may be important to keep the mean laminar diffusion term including differential diffusion in the mean scalar transport equations. However, it has lower impact than including the differential diffusion in the creation of the lookup table [97]. Having the relatively low computational cost as an advantage, these approaches have been extended and tested under several conditions. A priori, it would seem that flamelet-based models for FC are not a recommended option because the high mixing intensity and dilution are supposed to lead to well-mixed conditions or at least widely distributed reaction zones. However, some of the DNS studies discussed in the next section concluded that thin reaction zones are also present in FC conditions.

In contrast, many other models are built upon a micromixing model. In principle, the importance of proper handling of the micromixing of reacting scalars is high in FC because the chemical and flow time-scales are in the same order of magnitude. In the Eddy Dissipation Concept (EDC) model the micromixing model distinguishes between reaction zones, often modelled as perfectly stirred or plug flow reactors and their non-reacting environment. The time-scale of the large and small turbulent eddies is taken into account to find the mass exchange rate between the reaction zones and their surroundings. In the EDC framework, skeletal or even more detailed chemistry can be afforded, but the role of turbulent fluctuations on determining effective reaction rates is not well represented. Transport equations for mean mass fractions are solved and it is straightforward to include a detailed laminar diffusion term when necessary. Calibration of model constants is often needed and this aspect has received attention for FC, as is discussed in the section on RANS applications below. More involved representations of turbulent fluctuations are used in Conditional Moment Closure (CMC) [98] and Conditional Source Estimation (CSE) [99] and in transported PDF models [100]. Especially the transported PDF models allow for a wide variety of micromixing models and their performance has received a lot of attention in the past decades. CSE has similarities with CMC in its formulation. Both CSE and CMC use conditional averages to compute the chemical source term, while the conditional fluctuations are assumed to be negligible

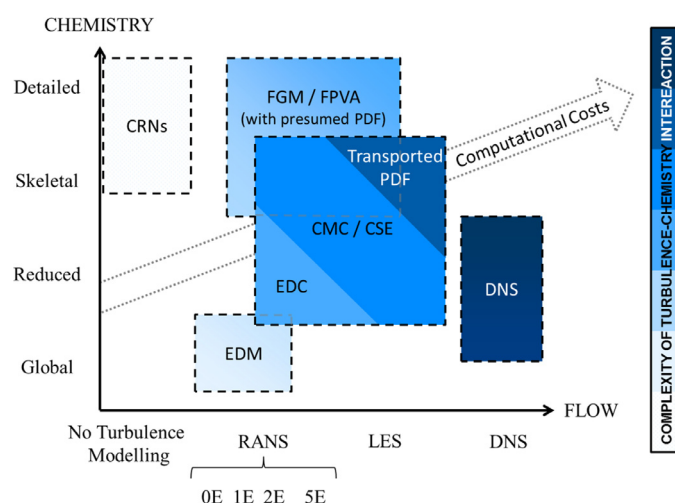


Fig. 17. Schematic of the most used approaches for modelling FC in relation to turbulence, chemistry, turbulence-chemistry interaction, and computational costs.

(conditioned to mixture fraction). In the CMC, transport equations for the conditional means of species and temperature are solved, while in the CSE these conditional means are obtained by inverting the integral equation that relates the unconditional to the conditional mean in a relation involving the (presumed) PDF. In the sections below, each addressing one of the types of models mentioned in Fig. 12, more detailed description of the different models is given and results reported. But before doing so the selection of chemical kinetic scheme for FC is discussed in the next section.

#### 4.2. Chemical kinetics

Here we briefly review the progress in the selection and performance of detailed and reduced chemical kinetic schemes for combustors working in the FC mode. Using appropriate chemical kinetics is crucial, especially for emission predictions. It is known that under FC reaction pathways and the interaction with transport phenomena are different if compared to canonical premixed and diffusion flames. However, there is no complete consensus on the exact nature of these differences and their influence on combustion and emissions.

Idealised reactors incorporating detailed kinetics on the one hand are an affordable tool to study the relative importance of kinetic



pathways and on the other hand, are often considered representative of intensely mixed conditions in FC. Such models are expected to be able to predict trends in pollutant formation as overall parameters change, making them suitable for sensitivity analysis. Nicolle and Dagaut [101] presented ideal chemical reactor simulations performed to analyse the NO<sub>x</sub> formation and destruction mechanisms under FC conditions. Based on the definition of Cavaliere and de Joannon [15], they employed a Partially Stirred Reactor (PaSR) model to evaluate the behaviour of NO formation. The study pointed to the relevance of chemical pathways that are frequently neglected in conventional applications, such as the NNH and N<sub>2</sub>O pathways.

The reburning of NO<sub>x</sub> was also found to be relevant. Since the beginning of the investigations on the FC regime, reburning has been pointed out as an important mechanism [17], having more relevance than in conventional combustion. Several works acknowledged the need to include reburning reaction pathways in simulations related to FC. Earlier works reported the use of simple approaches, as a single global reaction representing reburning [102], while more recent works included several reactions and analysed their relative contributions [103]. Despite the tangible advances, there is no consensus regarding which reactions should be included to a “reburning mechanism” in order to achieve accurate predictions.

Recognizing the necessity of including usually neglected reactions, Galletti et al. [104] proposed two new reduced chemical mechanisms for CH<sub>4</sub>/H<sub>2</sub> to be used under FC conditions, based on their analysis of ideal chemical reactors. They analysed reaction rates at various temperatures and pressures using detailed mechanisms in order to select the most important reactions. Each of the two new mechanisms was developed based on a different detailed mechanism (namely, the POLIMI and the Glarborg mechanisms). The developed mechanisms were then compared to other contemporary reaction mechanisms used in CFD simulations related to the Adelaide burner. The newly developed mechanisms showed better (and very similar) results. Again, the NNH pathway proved to be relevant for the overall values, while the inclusion of HNO and NO<sub>2</sub> pathways was pointed as the responsible for the better results with the developed reduced mechanisms. Although deviations in relation to experimental data were still present, it is not possible to attribute them solely to the chemical mechanisms, as deviations could be a result of the CFD models and their implementation.

Calculations of laminar flames with a simple flow pattern also present an opportunity to validate detailed mechanisms by comparison with measurements. Sepman et al. [105] reported experimental measurements and detailed computations of laminar jet flame of CH<sub>4</sub> diluted with N<sub>2</sub> in either preheated air or in a hot coflow containing products of lean combustion of CH<sub>4</sub>. The calculations were performed with two detailed mechanisms, GRI-mech 2.11 [106] and GRI-mech 3.0 [107], with well-documented modification of the NO chemistry, based on recent literature, in the latter. The rate-of-production analysis demonstrated that the Fenimore mechanism is the dominant pathway of NO formation in all flames studied. The NO formation in the MILD flame appears to be negligible (few ppm). The reported detailed results obtained with the modified GRI-mech 3.0 mechanism were found to be in good quantitative agreement with the measurements. It would be of interest to investigate whether the same level of agreement is achieved with different detailed and reduced mechanisms mentioned above.

#### 4.3. Direct numerical simulation

The DNS studies can provide valuable insight into the physical behaviour of the FC regime rather than directly aiding the design. This approach avoids the uncertainties of turbulence modelling by employing a computational grid that is able to capture the smallest turbulence scales, without necessarily capturing the details of the flame structure.

Due to the immense computational cost of such simulations, the domain size is limited. Therefore, DNS is not suited to compute most of the laboratory scale experiments or (semi-) industrial scale applications. Nevertheless, valuable conclusions can be drawn from DNS studies, especially concerning the interaction of flow and reaction zones. They provide detailed databases to check the validity of combustion models and provide inspiration for the development of new models. However, the uncertainty in the definition of the FC regime affects the relevance of DNS investigations. Many works use the conditions of JHC experiments as a baseline to perform DNS and, therefore, may be out of the range of interest from a design point of view, as highlighted in the previous section.

One of the first DNS related to FC, based on JHC configurations was presented and analysed in a series of papers by Yoo et al. [25,108], Lu et al. [109] and Luo et al. [110]. Using rectangular domains (a typical requirement of DNS codes), H<sub>2</sub> combustion in hot and diluted coflow was simulated [25]. Jets and coflows were not round, but rectangular as in slot-burners. Chemical Explosive Mode Analysis (CEMA) was performed later to reach conclusions regarding the presence of auto-ignition [109]. Similar steps were taken for an ethylene flame [108,110], providing an interesting comparison between the behaviour of two fuels.

The findings were in line with the most recent JHC experiments: auto-ignition and quenching were identified for both cases in a region with high intermittency. The difference between C<sub>2</sub>H<sub>4</sub> and H<sub>2</sub> was on the base structure of the flame. The H<sub>2</sub> flames showed both auto-ignition and upstream propagation of the kernels, while ethylene flames exhibited no propagation. The comparison shown in Fig. 18 exhibits the sudden variations in ethylene flames with step-like shapes, while H<sub>2</sub> had smoother spikes. Both the stabilization point (defined by a threshold value of OH mass fraction) and the mixture fraction exhibited such behaviour.

The CEMA results discussed for both cases [109,110] further supported the conclusions and showed that this may be a powerful method to identify the type of ignition structures present in DNS and LES. The delimitation of auto-igniting and diffusion flame regions is done via the local evaluation of the eigenvalues of the chemical source term Jacobian. The application of this method should be further investigated as it has the potential to provide insights into the boundaries and definition of the FC regime.

Another set of investigations [111,112] was performed using mixing layers to mimic conditions found in the Adelaide experiments [34]. Both 2D and 3D simulations were performed to evaluate the effect of preferential diffusion, especially due to the presence of H<sub>2</sub>. In the 2D simulations [111], the effect of preferential diffusion was more important, as H<sub>2</sub> chemistry was shown to be dominant for the occurrence of ignition. However, such effect was shown to be less prominent in the 3D simulations by Göktolga et al. [112] as turbulence structures were able to cascade to smaller scales as compared to 2D. Such difference causes higher interaction between chemistry and turbulence (as expected under the FC regime). Therefore, 2D DNS is an incorrect representation of this case.

In the same investigations, the authors included the cooling effect caused by the entrainment of ambient air in the coflow by imposing a non-uniform temperature profile to the layer representing the coflow. The results pointed to large differences in ignition behaviour when including heat loss, once again pointing at the shortcomings of JHC configurations and their consequences on simulations. Additionally, these studies were the base for improving the definition of progress variables for chemical tabulations discussed in the following section, as the role of radicals as HO<sub>2</sub> was highlighted.

Focusing on the flame structures present in FC, a series of DNS was performed for comparing representative conditions of FC and conventional premixed flames. Boundary and initial conditions typical of these regimes were carefully created before allowing the solutions to evolve [113–116]. The procedure to create such conditions

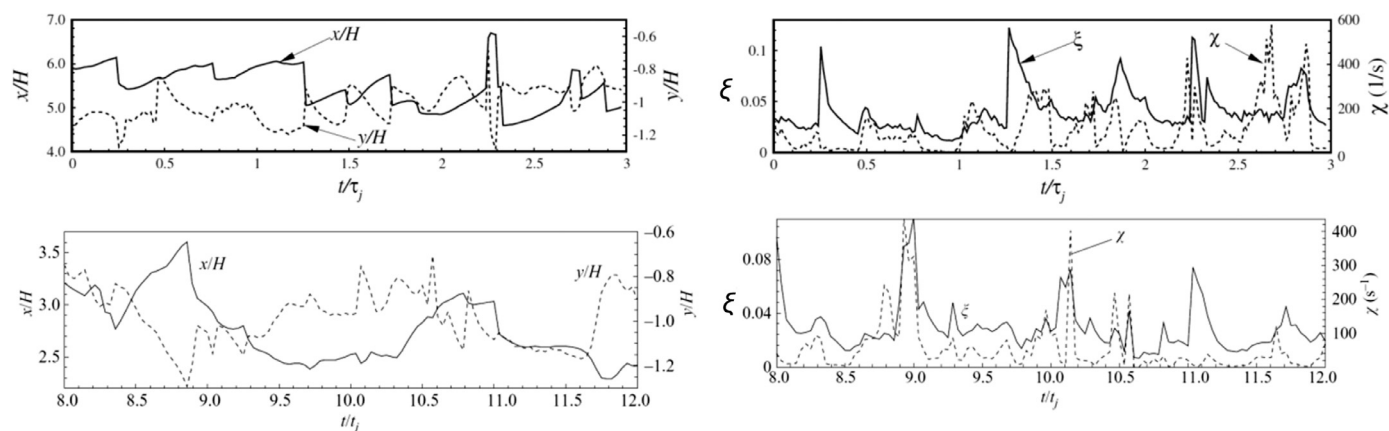


**Fig. 18.** Comparison of temporal progressions between an ethylene flame (up) [108] and hydrogen (down) [25]. Stabilization point in axial  $x/H$  and radial coordinates  $y/H$  (left). Mixture fraction  $\zeta$  and scalar dissipation rate  $\chi$  (right).

involved the evaluation of 1D laminar flames, which were referred to as MIFE (MILD Flame Element) for the FC cases.

One of the most important conclusions from these works [113,114] was that the flames in FC conditions displayed thin structures with frequent interaction between each other, having a complex reaction front (Fig. 19) providing a surprising physical picture of the typical portrayal as ‘well-distributed’. The interaction between the flamelets locally increases the reaction rates and thickens the reaction zones [115].

Interestingly, the authors attempted to draw conclusions about LIF by extracting the signal that would be acquired from 2D slices of their DNS. In accordance with previous investigations, they concluded that it is necessary to have signals from both OH and  $\text{CH}_2\text{O}$  to represent the heat release in FC conditions since OH gradients are not as large as in conventional combustion.

In another creative approach, the DNS data was treated mathematically to evaluate the shapes of the reaction zones [116]. While the classical premixed case pointed to well-defined thin surfaces, FC was shown to be composed of several shapes (distinguished by values of planarity and filamentarity), while the probability of having ‘pancake-like’ structures (intermediate values of planarity and low values of filamentarity) is the highest. The analysis pointed to a relation between temporal progression and the probability of the shapes.

Following their findings using DNS, Minamoto and Swaminathan [117] attempted to reproduce filtered DNS data. The PSR approach with presumed PDF showed better results, especially for intermediate species concentrations. The lack of interaction between the flamelets was said to be the cause of the poor results for the MIFE approach. The authors pointed that flamelet models should be modified to successfully represent FC, with a formulation capable of taking the interaction between flamelets into account.

As a conclusion, DNS may deliver more detailed information than experiments and is extremely valuable for understanding and assessing FC. However, in all mentioned works,  $Re$  and  $Ka$  are lower when compared to most experiments and applications. Additionally, there are always sensitivities with respect to chemistry modelling and numerical treatment that should be considered before generalizing the results.

#### 4.4. Extension of tabulated chemistry

Both FGM and FPVA are examples of tabulated chemistry methods. These methods combine detailed treatment of reactions and diffusion with a relatively low computation cost because of the use of a

low-dimensional representation of the set of states accessed in a flame (depending only on a selected set of controlling variables). In short, they can provide an efficient and simplified description of the thermochemical state of the reacting flow. They can be used in combination with any type of flame calculation, from laminar flow and DNS, to RANS and LES. In the case of RANS and LES, they have to be supplied with a model for the fluctuations of the independent variable. In this section, we only consider the novel developments needed in the creation of the lookup tables, whereas the applications in RANS and LES are discussed in subsequent sections.

Even when a given detailed mechanism is chosen, the application of tabulated chemistry methods can be performed according to different procedures. The set of laminar flames or other idealised reactors used as input must be chosen and also the set of progress variables selected as independent variables in the representation of the laminar flame results must be chosen. Some new developments were needed in order to address dilution and ignition aspects encountered in the FC regime.

First, in order to represent the influence of dilution (due to external or internal recirculation in applications), it is possible to introduce diluted streams as boundary conditions in flamelets. This leads to an extra independent variable representing the degree of dilution. Locci et al. [118] and Colin et al. [119] and also Lamouroux et al. [120] introduced such approaches with the objective of simulating furnaces operating in FC mode. These works resulted in equations describing mixture fraction, progress variable and dilution variable. The model was applied to the furnace experiments of Verissimo et al. [78–82]. An FGM model with dilution variable proposed by Huang et al. [121,122] is included in the comparative study presented in Section 4.8.

In the case of the JHC configuration the dilution of the oxidiser stream is predefined by the settings of the secondary burner and it would seem that a dilution variable taking a range of values would not be needed, but in practice the coflow is not perfectly homogeneous in composition and an additional independent scalar to describe the deviations from homogeneity is needed to accurately represent this. If the inhomogeneity is describing a local excess of oxygen, to very good approximation the same extra variable can also be used to describe entrainment of air from the surroundings further downstream. Ihme et al. [123,124] developed this extension in the frame of the FPVA. The chosen progress variable was a linear combination of  $\text{CO}_2$ ,  $\text{H}_2\text{O}$ ,  $\text{CO}$  and  $\text{H}_2$  mass fractions. Sarras et al. [125] introduced a similar approach in the frame of FGM based on unsteady igniting flamelets and steady flamelets as inputs for the tabulation. An additional independent scalar was

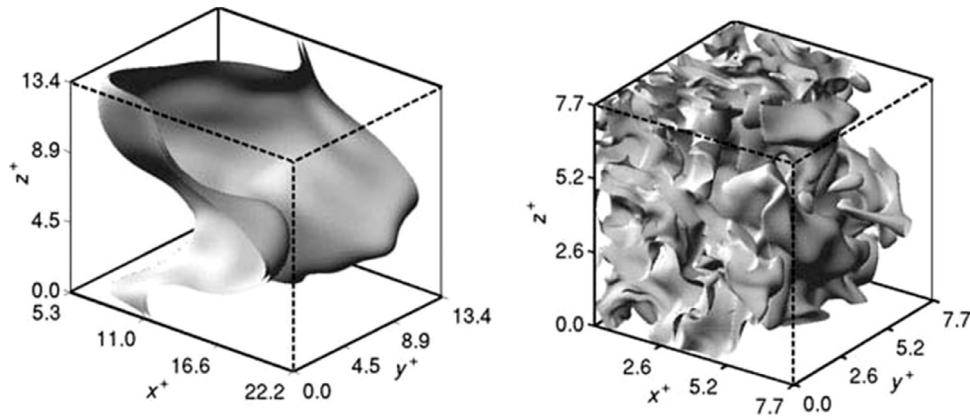


Fig. 19. Comparison of reaction rate isosurfaces between DNS of a classical premixed flame (left) and a case within the FC regime (right). [114].

introduced representing normalised  $O_2$  concentration in the range between minimal value occurring in the coflow and in air. The progress variable was based on  $CO_2$ ,  $H_2O$ , and  $H_2$ . They also added normalised enthalpy loss as a fourth independent variable in the FGM, in order to represent the inhomogeneous profile of mean and standard deviation of temperature in the coflow. The results obtained by Ihme et al. (using LES) and Sarras et al. (using RANS with transported PDF) are discussed in Sections 4.6 and 4.5.3, respectively.

Domingo et al. [126] proposed the combination of auto-ignition chemistry (using PSRs) and premixed flamelets as input for the creation of tabulated chemistry for auto-igniting flames. The relative weight of PSR and premixed flamelet was then made dependent on the value of progress variable, assuming a larger contribution of the auto-igniting regime for low values of progress variable, while the premixed tabulation was dominant for high values of progress variable. The results are discussed in the section on LES (4.6).

The use and extension of the FGM approach for FC conditions was investigated by Göktolga et al. [127], based on some of the conclusions from the DNS study presented by Göktolga et al. [112]. The conditions of the JHC experiment performed by Dally et al. [34] were considered, and the authors investigated the behaviour of the solution with different definitions of progress variable. As pointed by Göktolga et al. [112], the studied FC combustion cases were more suited to have  $H_2O$  and/or  $HO_2$  present in the definition of progress variable instead of carbon compounds. The authors compared the DNS solution using detailed chemistry or FGM with different combinations of  $H_2O$  and/or  $HO_2$  mass fractions as progress variable. They concluded that it was not possible to accurately model the reaction using a single progress variable, due to the characteristics of pre-ignition and post-auto-ignition zones in this FC case. The authors proposed a method to incorporate two progress variables in the model, each of interest in a different part of the flame, with a transition between them in the final model. Transport equations of both were solved across the whole domain, and a threshold value (maximum  $HO_2$  mass fraction) was established to make the transition between the two pre-calculated lookup tables. This type of solution demonstrates that based on a prior investigation, it is possible to create a tabulated chemistry model able to cope with a qualitative change in flame structure at an a priori unknown spatial position. This appears to be an attractive feature from a design point of view. The application of this approach has to be explored further.

#### 4.5. RANS-based modelling

##### 4.5.1. Early studies

Along with the early JHC experiments, many simulations were carried out using the models already available for calculation of canonical premixed and non-premixed flames. Especially the joint scalar transported PDF models were employed as they are in principle independent of the combustion regime. Their relatively high computational cost was not a severe constraint for the simple JHC configuration as the geometry could be simplified to a 2D axisymmetric case in RANS. Variations of PDF and EDC approaches along with RANS dominated most of the works related to the JHC configuration in the past 15 years.

Cabra et al. [44] together with their experimental results presented computational results on a comparison between a transported PDF model and the EDC model using the  $k-\epsilon$  turbulence model. A Reynolds stress model (RSM) for turbulence was also applied but only with the EDC model. None of the approaches was able to replicate the experimental data with a high degree of accuracy. Especially the OH mass fraction showed major discrepancies. The comparison regarding mixture fraction and  $O_2$  concentration extracted from point measurements at radial stations suggested that the turbulence modelling had a significant influence. The best results were obtained when using the RSM turbulence model, as both PDF and EDC approaches with  $k-\epsilon$  showed large disagreement. Further studying the behaviour of the PDF model in these conditions, Masri et al. [128] assessed the use of the storage and retrieval algorithm ISAT and the choice of the chemical reaction mechanism. The tolerance imposed in ISAT had a significant influence on the results as well as on computational time, pointing to the need for convergence studies.

Similarly to Cabra et al. [44], Christo and Dally [36] performed a comparison between a PDF model, a flamelet-based model, EDM and EDC, in an attempt to replicate the Adelaide burner results [34]. Using EDM with three-step chemistry, different versions of the  $k-\epsilon$  model were compared and using the value of 1.6 for the model constant  $C_{\epsilon 1}$  provided the best results. This comparison was made based on the results of the mixture fraction field. Next, it was shown that EDM performs best among the turbulence-chemistry interaction models. This illustrates the difficulty, commonly encountered in turbulent reacting flow studies, of attributing deviations to a given sub-model. For example, the calibration of a turbulence model could be sensitive to the chosen turbulence-chemistry interaction model, and

conclusions regarding which model performs the best might be sensitive to the case studied.

Along with the experiments on the Cabra burner using  $\text{CH}_4$ , Cabra et al. [24] presented simulations using a PDF method. A comparison between micromixing models was performed and the influence of such models was shown to be significant. The results showed that the modified Curl micromixing model performed slightly better than other common micromixing models. Interestingly, the effect of modifying the chosen micromixing model was shown to be unimportant for the Cabra burner  $\text{H}_2$  flame [129].

Using data from both the Adelaide burner and the DJHC, De and Dongre [130] investigated the EDC, steady-flamelet with presumed-PDF, and transported-PDF models. Additionally, micromixing models were compared in detail. The comparison pointed to better predictions by the Lagrangian transported PDF, along with either the EMST (Euclidian Minimum Spanning Tree) or the IEM (Interaction by Exchange with the Mean) mixing models. However, the authors pointed to the need of providing the temperature fluctuations as a boundary condition to enhance the accuracy. Whether or not this can be done depends on the type of model and the completeness of experimental information. Furthermore, the prediction of minor species was relatively poor, representing a challenge for prediction of pollutant formation (especially CO).

#### 4.5.2. Application of EDC

The EDC model has been popular since the early works on JHC flames. Comparisons were carried out in relation to turbulence models and chemical reaction mechanisms [131–134]. The computational costs are highly dependent on the chosen chemical mechanism, but are usually lower than those of PDF-based models.

In several JHC cases, the standard EDC model was found to predict ignition far upstream, leading to a clear peak in the radial mean temperature profile not present in the experiments. This is not surprising as EDC by its definition in no way represents ignition by separate local events (ignition kernels) responsible for the ignition in many JHC flames. Nevertheless, several authors have remedied the failure by paying more attention to the role of turbulent boundary conditions and the role of differential diffusion or by modifying the model constants in the EDC model [36,125,130,132–137]. Indeed, in the EDC model, two model parameters appear. The key model features are the volume fraction of the reaction zones ( $\gamma$ ) and the residence time in these zones ( $t$ ), which are dependent on two constants,  $C_t$  and  $C_\gamma$  respectively. Aminian et al. [134] proposed adjusting the value of  $C_t$ . Similarly, Evans et al. [138] investigated a range of values for the model constants and recommended values for  $\text{CH}_4/\text{H}_2$  and  $\text{C}_2\text{H}_4/\text{H}_2$  flames. Both works were based on the Adelaide burner experiments and showed improvement in relation to the standard constants.

The proposed changes of model constants in the EDC model were not only purely empirical but were also motivated by the argument that the FC combustion regime is different from the conditions for which the EDC was formulated originally. Indeed, as pointed out by Minamoto et al. [116] in their DNS study, the modification of EDC models can potentially take into account the increased volumes caused by the different shapes of the reaction zones in the FC regime. This was in corroboration with earlier findings, also pointed in the conclusions of De and Dongre [130]. Being characterized by distributed reactions, FC has  $Da$  close to unity, when calculated using the integral time-scale, as discussed in Section 2 and shown in the diagrams of Fig. 4.

Recently, more comprehensive modifications were suggested. Aminian et al. [139] proposed the modification of the extinction criterion of the EDC model. They employed the PaSR (Partially Stirred Reactor) concept to the fine scales instead of the PSR assumption. In this approach, both a finite rate mixing process and a finite-rate

chemistry are taken into account. Therefore, the critical residence time (which ultimately determines extinction) has different values as it is dependent on the required time for chemistry within the fine structures.

Parente et al. [140] compared two different approaches with the Adelaide flames as test cases: global and local model constant evaluation. For the first approach, the  $C_t$  and  $C_\gamma$  were determined based on values of the turbulent  $Re$  and Kolmogorov scale  $Da$ . They employed the fuel jet as a reference for the  $Re$  calculation, while the method of Isaac et al. [33] was used to calculate a global  $Da$ . Therefore such approach requires a previous model solution in which the chemical analysis can be performed in order to calculate  $Da$ . For the second approach of calculating model constants locally, the turbulent  $Re$  was calculated for each domain cell. However, the calculation of  $Da$  would ideally require using the same method employed for the global approach at each location. The method involves evaluating the Jacobian of the chemical source term, and would be very expensive for cell-based calculations. As a consequence, the authors opted for an estimation of the chemical time-scales based on one-step chemistry and the local conditions of temperature and concentration. Both global and local approaches showed improved results in relation to the standard EDC model.

Also employing the Adelaide JHC as a test case, Li et al. [141] assessed the performance of EDC for varying parameters: formulations of the EDC with respect to the mass fraction on the fine structures, EDC model constants,  $k$ - $\epsilon$  model  $C_{1\epsilon}$  constant, chemical reaction mechanisms, assuming the fine structures to be PSRs or PFRs, and including or not differential diffusion. While adjusting the EDC and  $k$ - $\epsilon$  constants have shown to affect the solutions, the other parameters did not considerably influence it. The prediction of minor species was still sub-optimal for all cases. Additionally, they performed a comparison of EDC to a PaSR model, which notably performed better in the prediction of NO.

Having the DJHC as test case, Bao [142] presented another formulation of the EDC with locally determined constants. The difference in relation to the model developed by Parente et al. [140] is on how the laminar flame speed is calculated in order to evaluate the constants. While Parente et al. [140] had  $C_\gamma$  proportional to the square-root of the Kolmogorov scale  $Da$ , Bao [142] derived a relationship in which  $C_\gamma$  is proportional to  $Da^{3/4}$ . The temperature predictions were shown to be superior in comparison to the formulation of Parente et al. [140] for the chosen test case. Some of the results of Bao [142] are further discussed in Section 4.8.

The improvement of the EDC model is promising if the calculation of local constants can be made more consistently and at a low computational cost. All the aforementioned developments were performed using RANS simulations and could possibly be validated using DNS or transferred to LES.

#### 4.5.3. Application of statistical models (CMC, CSE, PDF)

Kim et al. [143] were the first to apply the Conditional Momentum Closure (CMC) model to FC flames. The CMC is a general modeling approach that in principle is suitable for flames in all regimes. In this approach, closure assumptions are made concerning the conditional expectation values of thermochemical variables, conditional on values of a few key variables. The model allows its validity throughout combustion regimes, as it has no a priori assumptions regarding turbulent or chemical time or length-scales. This fact makes the approach attractive for FC applications, given the complexity of the regime characterisation. However, the number of investigations dealing with CMC for FC is relatively low. This fact is possibly due to its theoretical complexity in combination with the need to solve transport equations in a space with the conditioning variables as extra dimensions. Additionally, the associated computational costs are relatively high, although being lower than transported PDF models with similar chemistry [144].



The work of Kim et al. [143] showed results obtained for the three cases explored during the first experiments with the Adelaide burner [34]. Considering the fact that a RANS approach was adopted, the results were consistent with the experimental observations. Even the usual difficulty with the predictions of CO and NO profiles was overcome and the simulation results had a reasonable agreement.

A similar approach was used to simulate experiments with the Cabra burner. Patwardhan et al. [145] compared their results to those of transported-PDF [128]. The CMC approach showed slightly better results while none of the models were good at predicting lift-off heights. This could also be an artefact of the turbulence model, as both combustion models employed only  $k-\epsilon$  model.

Sarras et al. [125] simulated the DJHC experiments for cases with natural gas and a synthetic biogas as fuel using a transported-PDF approach in combination with the extended FGM method using up to four independent variables (two mixture fractions, a progress variable and enthalpy deficit). The FGM was a means to reduce the high computational cost usually associated with transported PDF methods. A comparison between a 3D FGM (without enthalpy deficit) and a 4D tabulation (with enthalpy deficit) was carried out. The progress variable was based on  $\text{CO}_2$ ,  $\text{H}_2\text{O}$  and  $\text{H}_2$  mass fractions. Additionally, the authors investigated the effect of including effects of differential diffusion. Agreement with the experimental data was achieved only when the 4D approach with differential diffusion was considered.

Labahn et al. applied CSE to model the DJHC flames with natural gas fuel in the frame of RANS [99] and LES [146]. Their approach employed two mixture fractions as conditioning variables: the first was the conventional mixture fraction and the second was a variable representing at the same time the oxygen profile and temperature (or enthalpy deficit profile) at the inflow boundary. Handling oxygen and temperature profile with only one variable induces an approximation but was found to be effective. Chemistry was tabulated with an approach called Trajectory Generated Low Dimension Manifold (TGLDM), which was stored as a function of the two mixture fractions and mass fractions of  $\text{CO}_2$  and  $\text{H}_2\text{O}$  as progress variables. This RANS-CSE approach was found to perform very well. Remaining discrepancies were attributed to inaccuracies in the turbulent mixing due in RANS. The RANS-CSE results of Labahn et al. [99] are included in the comparative study presented in Section 4.8.

#### 4.6. LES-based modelling

After the very first attempts to model JHC flames with RANS, researchers employed LES. Kulkarni et al. [147] used an Eulerian formulation of the transported PDF method (stochastic field method) along with tabulated chemistry based on PSRs was. Later Bhaya et al. [148] performed a comparison between a Lagrangian and an Eulerian formulation (particle method versus moment method), along with the effect of two chemical reaction mechanisms and mixing models. The Lagrangian approach was shown to be superior to the Eulerian, and, as expected, the LES results were better than their RANS counterparts.

In the framework of LES, Domingo et al. [126] presented simulations intended to reproduce experiments performed on the Cabra burner [24]. Chemistry was tabulated using their approach combining auto-ignition chemistry (using PSRs) and premixed flamelets in the tabulation, described above. The results were fairly good. The largest deviations in relation to experiments were present in intermediate species and pollutants, as OH, CO and NO were not correctly predicted.

Using LES, Ihme et al. [121] applied the extended FPVA to the Adelaide JHC flames and compared to the usual approach (with only two controlling variables). The results with three controlling variables were superior, particularly in predicting CO. However, to achieve better results for every measured variable, the mean values

and the turbulent intermittency of the three controlling variables imposed as boundary conditions proved to be important and were optimized based on the experimental results.

Possibly the best simulation results achieved so far related to the DJHC experiments were achieved using CSE in combination with LES [146]. This approach was able to capture most of the features observed in the experiments, pointing to CSE and related approaches as very promising. Compared to the RANS-CSE results of [99], the peak temperatures and shape of the temperature profiles were better captured in LES-CSE. The fact that temperature fluctuations were assumed absent in the inlet boundary conditions was mentioned as an area for improvement. The LES-CSE results of Labahn and Devaud [146] are included in the comparative study presented in Section 4.8.

#### 4.7. Chemical reactor networks

Application of a CRN to describe the reacting flow in a combustor requires a definition of the network parameters (number and type of reactors, mass flow rates and residence times). To provide these parameters, insight on the flow field has to be used. The type of information used can be derived from overall characteristics of flow patterns such as expected presence of a recirculation zone or based on a separate CFD simulation of the flow field, either inert or with simple chemistry. Some works have focused on post-processing of CFD solutions by splitting the computational domain according to certain criteria to form a CRN. Detailed chemistry can then be employed in CRNs at relatively low computational cost, while the same CRN can be used to quickly simulate variation in operating conditions.

Within this framework, Frassoldati et al. [135] developed a postprocessor for NO<sub>x</sub> prediction by building a CRN using the same grid as the one employed in CFD simulation. The CFD was done using a simple kinetic scheme and their detailed kinetic mechanism (PolimiC1C3HT1201) was adopted to predict the NO<sub>x</sub> formation. The tool was first applied to the Adelaide burner with  $\text{CH}_4/\text{H}_2$  as fuel. The approach was further developed by using the splitting criteria based on temperature and species concentrations to build CRNs with lower number of reactors [149]. Their method included a correction to the temperature due to turbulence interaction (based on the temperature variance) that should be available from the CFD solution. In addition to this imperfect mixing was represented by considering a fraction of the PSRs as inert. The volume of reacting portion was determined by the estimated volume of the fine structures, calculated based on local turbulence parameters. This clearly comes close to the procedure used in the EDC model. The authors compared their results with experimental data from laboratory flames and also to the experiments performed by Verissimo et al. [78]. The predictions of CO and NO showed deviations from experimental data, which were attributed to the insufficient accuracy in the mean temperature prediction.

In conclusion, both mean and variance of temperature should be correctly predicted before the CRN NO<sub>x</sub> post-processor can give accurate predictions. Because of the dilution and strong mixing in FC conditions the level of temperature fluctuations is not so strong and simple variance models would be sufficient. However, more comparisons and validation should be accomplished using experimental data to come to clear conclusions on the way to represent the role of temperature fluctuations in the CRN approach. Furthermore, in the approach using a reactor associated with clusters of CFD cells, the criteria for clustering the CFD cells and the use of information contained in the CFD simulations should be optimized.

**Table 4**  
Compared modelling approaches for the DJHC-I flame [46,54].

| Reference              | Turbulence model                | Chemistry simplification approach   | Number of independent thermo-chemical scalars | Turbulence chemistry interaction model |
|------------------------|---------------------------------|---|---|--|
| Bao [142]              | RANS $k-\varepsilon$ , RANS RSM | Kinetic scheme DRM19 [150]  | 19 + 1  | EDC, EDC-LP                            |
| Labahn et al. [99,146] | RANS $k-\varepsilon$ , LES      | TGLDM 2 mixture fractions   | 2   | CSE                                    |
| Huang et al. [121,122] | RANS $k-\varepsilon$ , LES      | DA-FGM (mixture fraction, progress variable, enthalpy, and a dilution variable) | 4   | Assumed PDF                            |

#### 4.8. Modelling comparison of a DJHC flame

The JHC experiments discussed in Section 3.1 have served as canonical test bench for model validation. In this section we present results for the DJHC-I flame [46,54], coming from different research groups. A representative set of modelling approaches to date was selected in order to showcase their capabilities.

The modelling approaches compared in this section are listed in Table 4. They comprise EDC with RANS [142], CSE with RANS or LES [99,146] and an FGM-method using “diluted air” flamelets (DA-FGM) with RANS or LES [121,122]. This DA-FGM model builds the FGM from non-premixed flamelets diluted at the air boundary with a diluent which is defined as products of stoichiometric combustion [146] and differs from the approaches proposed in [118–120]. The EDC with RANS cases presented here are taken from [137] and comprise standard EDC with either  $k-\varepsilon$  or Reynolds Stress Model (RSM) and an EDC with local modified model constants (here abbreviated to as “local parameters”: EDC-LP. In the following some key aspects of the base case DJHC flame are discussed via a comparison of the relative performance of the models. Results are presented in Figs. 20–24.

##### 4.8.1. Velocity predictions

The prediction of the radial profile of axial velocity (Fig. 20) is generally good for all the approaches. The differences are related to the well-known problem of predicting the spreading rate of a round jet in RANS and the influence of temperature prediction on the density.

On the other hand, the agreement between model and experiment in the profile of radial velocity (Fig. 21) is not good close to the burner. This might be explained by a bias in the experimental results due to an unequal density of seeding particles in the fuel jet compared to the coflow, leading to an underestimation of the radial spreading close to the nozzle. However, the experimental paper of Oldenhof [46] explains that careful attention was paid to the equal seeding density of fuel and oxidiser.

Further downstream ( $x = 90$  mm) the CSE-LES prediction deviates significantly from other model predictions and from the experiments. This might be due to insufficient averaging time for constructing the mean values.

##### 4.8.2. Temperature predictions

A key problem in the prediction of mean radial temperature profiles is the identification of the height at which the ignition is sufficiently strong to significantly affect the mean temperature. In the experiments, the presence of ignition kernels (detected via their chemiluminescence) affected only the high temperature tail of the temperature PDF (measured using CARS) and did not have significant effect on the mean profile. The EDC model in combination with standard  $k-\varepsilon$  tends to over predict the ignition and lead to a clearly visible peak in the radial temperature profile already at  $x = 30$  mm, which becomes clearer at  $x = 60$  mm (Fig. 22). Choosing the Reynolds Stress Model (RSM) instead of  $k-\varepsilon$  does not eliminate the early temperature peak but predicts its position closer to the centreline in

agreement with the prediction of a smaller spreading rate of the cylindrical jet. The more elaborate EDC model with local parameters (EDC-LP), as discussed in Section 4.5.2, does lead to a prediction without a too early peak.

The conditional source term estimation (CSE) model in combination with RANS gives a lower peak. The CSE in combination with LES and the DA-FGM give no peak, as shown in Fig. 23. The agreement between model predictions and experiments for mean temperature in the core of the coflow is not as good at  $x = 60$  mm as it is at  $x = 30$  mm. This is rather caused by a shift in the temperature level of the experimental results than caused by recognisable model features. All models assume a coflow in chemical equilibrium at the outlet of the coflow annulus, but the evolution of the experimental profiles shows an increase between  $x = 15$  mm and 30 mm which tend to indicate a heat release effect not compatible with the equilibrium assumption made in the model calculations. The differences in predicted temperature can partly be explained by the different ways in which experimental information on mean oxygen profile is converted into the model boundary conditions employing mixture fractions and/or a dilution variable.

Laboratory air is entrained at the outer edge of the coflow leading to reduction of the mean temperature. The rate of entrainment depends on the boundary conditions in the air region. At the inlet the laboratory air should be given a low non-zero axial velocity in order to properly describe the entrainment of stagnant air into the coflow stream. In the CSE approach the air inlet velocity was set to 0.5 m/s which led to the best results. On the other hand, the mean temperature at the centreline at axial distance 60 mm and 120 mm is better predicted by the RANS approaches compared to the LES approaches.

The experimental radial profile of temperature standard deviation at  $x = 15$  mm (Fig. 24) is flat and more than 100 K, similar to what is present in the measured profile at  $x = 3$  mm (not shown). None of the models presented here has taken this initial level of temperature fluctuations into account or is able to predict the initial development of temperature rms correctly (See Sarra et al. [125] for a simulation including the temperature rms profile as a boundary condition at the inlet). Nevertheless, the increase in temperature rms due to the presence of the mixing layers between fuel and coflow and between coflow and air is predicted in agreement with the experiments by both CSE and DA-FGM.

We can conclude that the reviewed simulations of the DJHC base allow the identification of the key aspects to be taken into account to reach agreement with the experiment: jet spreading rate, ignition delay, and entrainment. The available DJHC database contains cases with different  $Re$ , coflow composition and temperature and allow for further analysis to identify whether the models also capture all trends correctly. A deeper understanding of the differences between the predictions of CSE and FGM approaches could be achieved by extending the comparison to the probability density function of temperature as done by Sarra et al. [120].

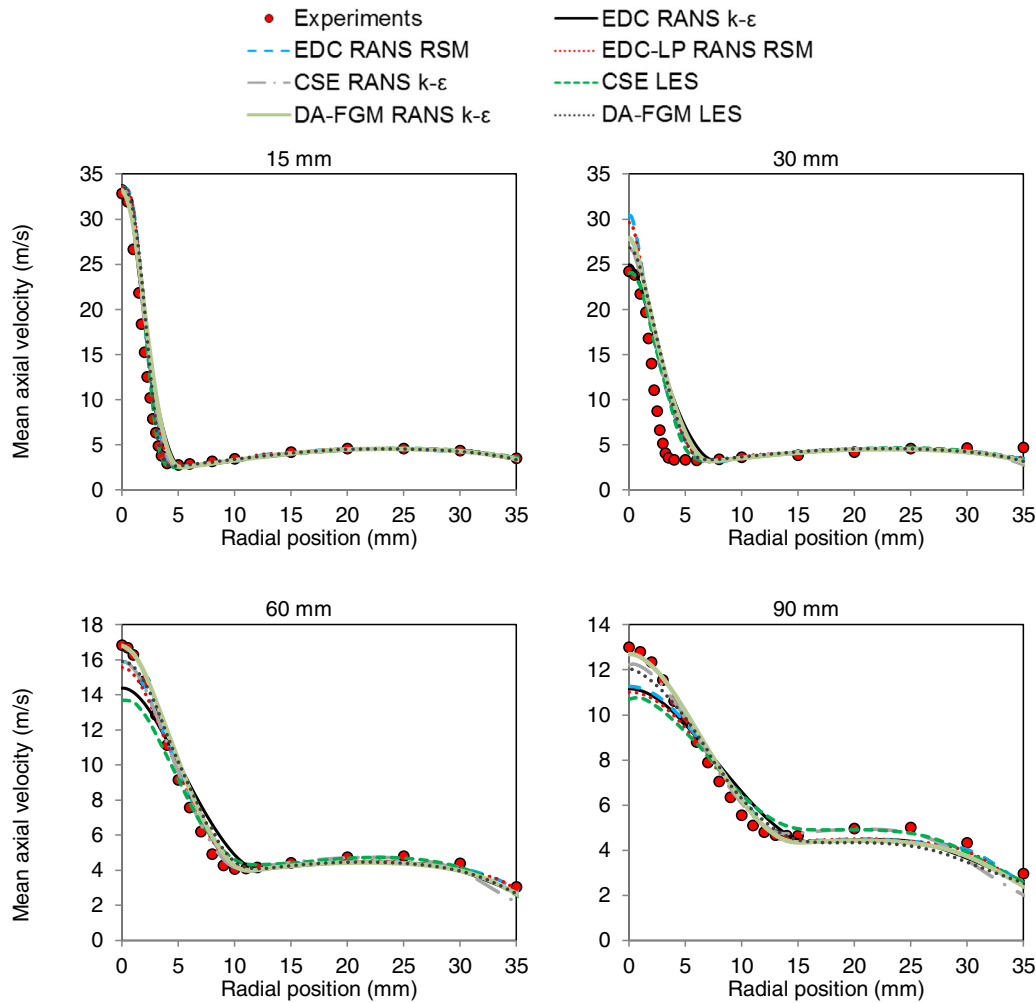


Fig. 20. Plots of mean axial velocity for four different axial locations of the DJHC-I flame [46,54]. Results for different turbulence modelling and turbulence-chemistry interaction approaches: EDC and EDC-LP [142], CSE [99,146] and DA-FGM [121,122].

#### 4.9. Conclusions and future outlook for computational models

The review and discussions provided above are concerned about simulations of FC in canonical configurations and lab-scale experiments. In this section we comment on which models perform best and in which directions more efforts are needed. Next, we make an attempt to formulate recommendations towards computation modelling in support of designing new combustors.

As has been explained, several types of models, based on widely different (and occasionally contradictory) assumptions have been employed to simulate FC and numerous authors reported to have been successful in reproducing experimental data. For several reasons, the reported success of a given model does not necessarily make it recommendable for all cases related to FC. The final evaluation is sometimes difficult due to the lack of consistency in the definition of FC. Additionally, the results reported have not been benchmarked to a specific level of accuracy, and are thus subjective.

The following conclusions and recommendations can be made:

- Possibly, the most used turbulence-chemistry interaction model is the EDC, due to its availability in commercial codes, its long standing tradition in the field, and the possibility of using diverse chemical reaction mechanisms. The EDC with suitable model constant calibration, as already has been attempted

[139–142], is relatively straightforward to use and reasonably accurate. If a robust and flexible modification of the model can be developed, this model can become even more popular.

- Tabulated chemistry models, especially FGM, are attractive because they are computationally efficient and can be relatively easily extended with a model for turbulent fluctuations (presumed PDF). But to be accurate, it is necessary that the applicable local flame structure and the related progress and control variables can be determined for a given case with little a priori information. However, one must be aware that the flamelet structure ceases to exist or at least is strongly affected in FC applications.
- CMC/CSE approaches seem to offer optimal combined representation of chemistry and turbulent fluctuations at (just) affordable cost. Given the high quality of the reported results, they can become popular if the knowledge on their implementation and operation spreads and if further investigations confirm their good performance.
- It can be effective to use a different modelling approach for the predictions of flow and heat release, and the predictions of emissions. The CRNs are attractive for predicting emissions, especially in situations where the role of fluctuations is low or easy to represent. Under FC conditions, due to the characteristics of the regime (lower temperature and species gradients), this

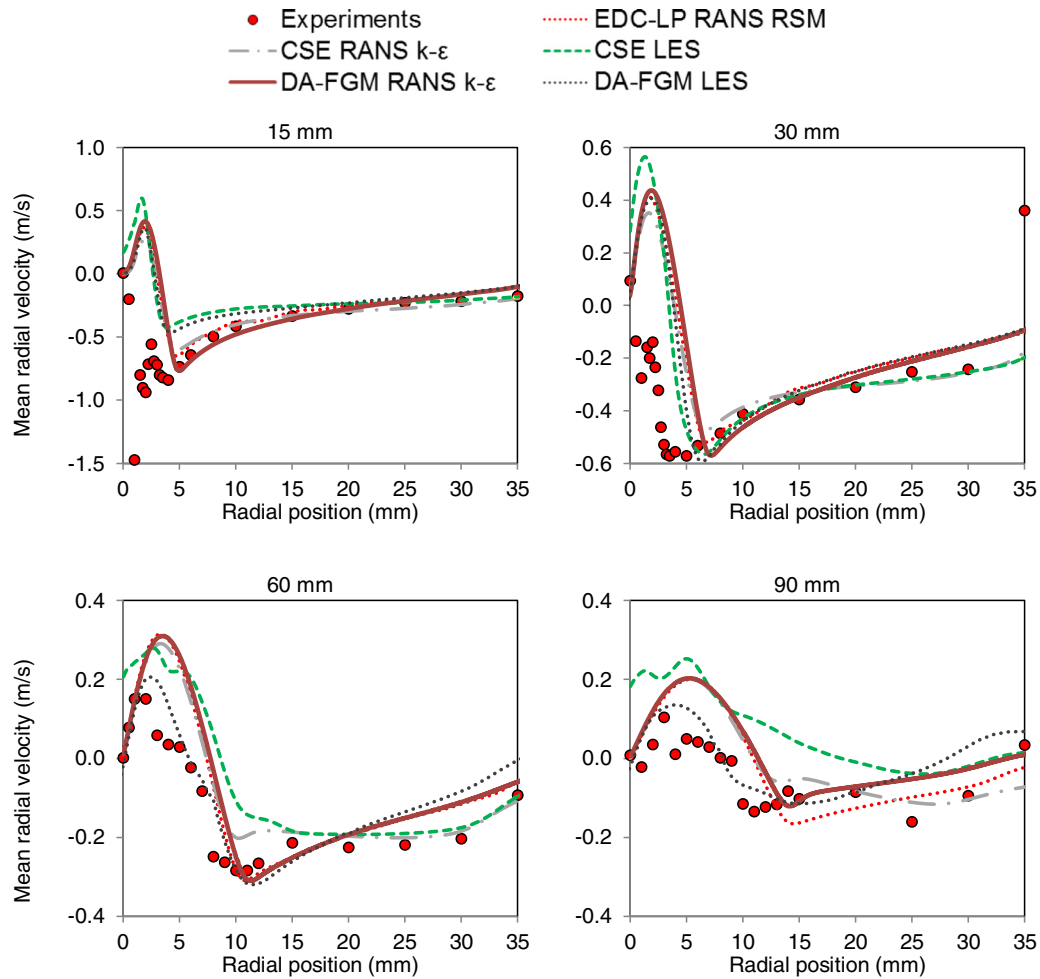


**Fig. 21.** Plots of mean radial velocity for four different axial locations of the DJHC-I flame [46,54]. Results for different turbulence modelling and turbulence-chemistry interaction approaches: EDC-LP [142], CSE [99,146] and DA-FGM [121,122].

seems to be the case. The development of recommended strategies for clustering CFD domain cells into the idealised reactors that form the CRNs might help in the handling of practical flow configurations in a sufficiently accurate way.

An important question is whether it is worth using LES instead of RANS. The more complex the flow field, the more one can expect a clear benefit from LES. Until now the use of LES related to the design attempts is not common, although there are exceptions [151]. This is mainly due to its larger computational cost, which is aggravated by the higher complexity in the geometries. Therefore for several design studies where multiple simulations are needed, the RANS approach will be preferred. Additionally, RANS approaches may be sufficiently accurate (as shown in Section 4.8). It should be stressed though that the usual difficulties in predicting the intermediate species are closely related to the influence of turbulent fluctuations [152]. Using sufficiently resolved LES, the sensitivity to different choices of turbulence-chemistry interaction model will be smaller because the modelling only concerns the subgrid scale phenomena.

## 5. Conceptual designs for gas turbine FC combustors

A number of concepts and designs of Flameless combustors for gas turbines have been proposed, simulated or tested. The lessons learned through these attempts are key to the possible success of

future designs. This section presents the most relevant aspects and findings of the previous design attempts.

In contrast with industrial furnaces, there is no easy solution for preheating and diluting the reactants in a gas turbine combustor. The design is far more challenging because:

- Gas turbines usually operate with an overall equivalence ratio of 0.3–0.4 close to peak power settings, which hinders the reduction of  $O_2$  concentration in the recirculated combustion products.
- The heat density (thermal energy density) of gas turbine combustors is an order of magnitude greater than that of industrial furnaces and this hinders the application of FC to gas turbines. This is especially true for aero engines as aircraft performance is sensitive to any increase in the volume and weight of the propulsion system.
- Unlike in most furnaces, the gas turbine combustor is adiabatic, which means that the recirculated combustion products are at a high temperature. This can become a problem when increasing the recirculation ratio as the temperature after mixing of incoming fresh mixture and recirculated combustion products can reach significantly higher temperature than the auto-ignition temperature, which can increase the  $NO_x$  emission from the combustor.
- Pressure losses due to the recirculation in the combustor can degrade the gas turbine efficiency.



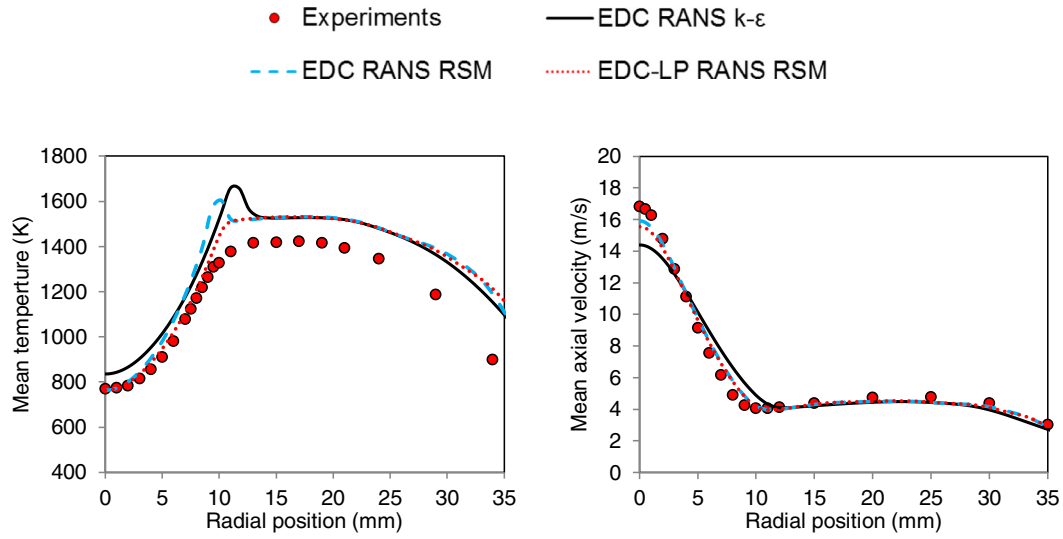


Fig. 22. Plots of mean temperature and mean axial velocity at  $x = 60$  mm of the DJHC-I flame [46,54]. Results for different EDC approaches [142].

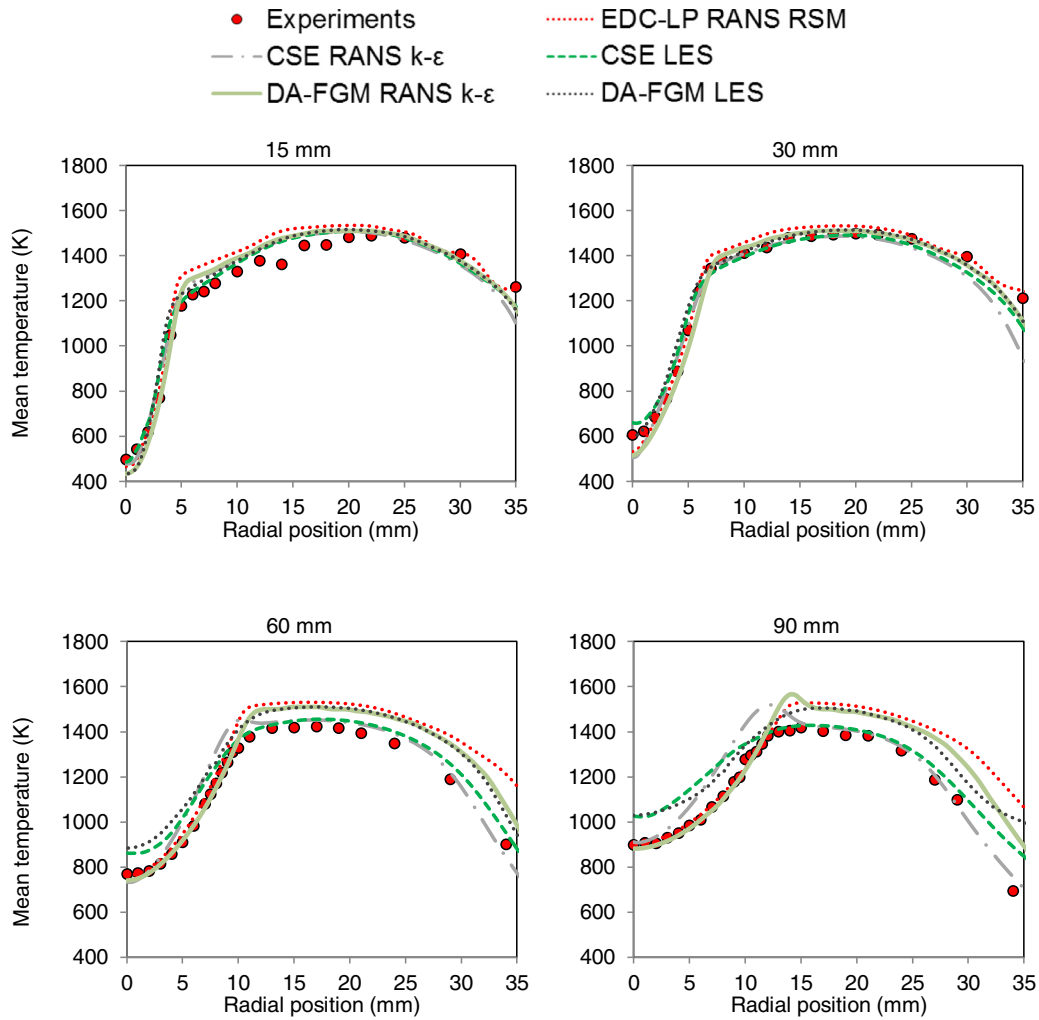


Fig. 23. Plots of mean temperature for four different axial locations of the DJHC-I flame [46,54]. Results for different turbulence modelling and turbulence-chemistry interaction approaches: EDC-LP [142], CSE [99,146] and DA-FGM [121,122].

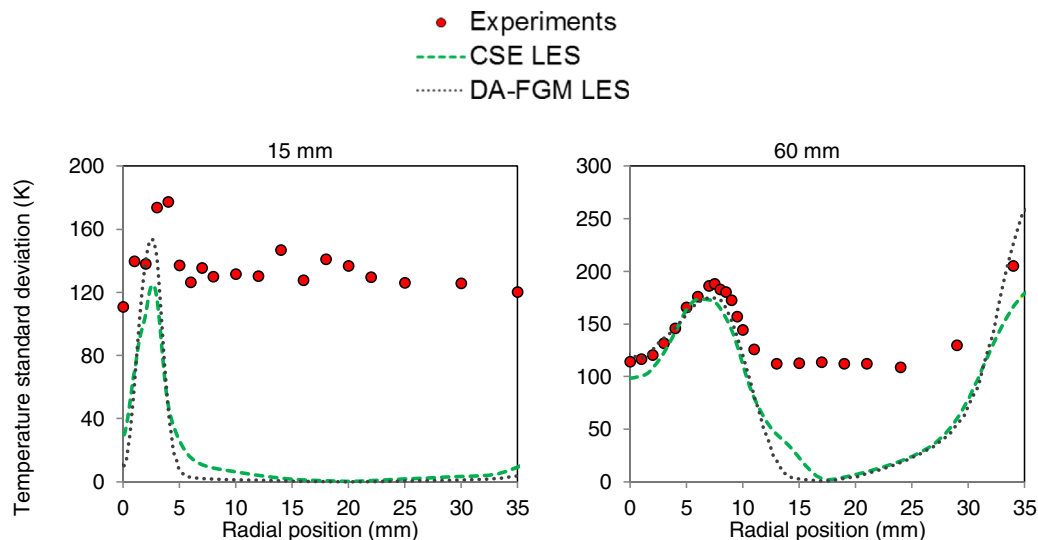


Fig. 24. Plots of temperature standard deviation for two different axial locations of the DJHC-I flame [46,54]. Results for LES using CSE [99,146] and DA-FGM [121,122].

worth highlighting the differences in the requirements between aero engines and land-based gas turbines. The latter has less restrictions in terms of combustor volume and weight, and no requirement for re-light capabilities. Additional restrictions could be imposed due to cycle differences (recuperation or intercooling, for example)[153]. Other differences are the possibility of having external recirculation (EGR) in land-based gas turbines, which may have a major impact on design constraints and strategies, and their usual longer residence times [154]. Until recently, land-based gas turbines required narrower operational range. However, as mentioned in Section 1, gas turbines shall be employed along with renewable energy sources to cope with the inherent intermittency of solar and wind energy. Therefore, the gas turbine operation will have to be more flexible. The main differences between the requirements of land-based gas turbines and aero engines are summarized in Table 5.

The FC-based combustor design attempts for gas turbines often rely on the internal recirculation of combustion products. Mixing air with combustion products is an obvious solution as it increases temperature of the reactants and reduces  $O_2$  concentration. The challenge is in designing a combustor that is able to promote mixing at the required rates without excessive pressure losses and within the limited available volume.

The requirements for operational range in aero engines is one of the main challenges for combustor design, and that is also the case for FC application. The attainment of low emissions while maintaining stability at part-load conditions is crucial. However, this joint requirement has not been extensively evaluated for most design concepts herein reviewed. This is partly explained by the fact FC-based combustors are still in an early stage of development. On the other hand, it will become clear that the success of design concepts would be more likely if such central issues would be addressed already from the conceptualization phase.

The adopted strategies to recirculate gases internally within the combustion chamber are: (i) recirculation induced by jet momentum and (ii) recirculation induced by geometry. In the first category, the FLOX<sup>®</sup> type combustors have been proposed and are primarily derived from industrial burners. These burners rely on high momentum jets to promote recirculation and the mixing between oxidiser, fuel and combustion products. Combustors with FLOX<sup>®</sup> burners oriented to gas turbine applications were tested and simulated with different approaches.

In the FLOX<sup>®</sup> burners, the fuel is injected through radially distributed nozzles in a pre-chamber section, where it is partially premixed

with the oxidiser stream. Both fuel and oxidiser promptly enter the combustion chamber via larger nozzles, positioned in the same axes as the fuel nozzles (Fig. 26). This concept was first developed for gaseous fuels. The axial distance between the fuel nozzles and the main nozzles (through which both air and fuel enter the combustion chamber) determines the premixedness. The radial position of the nozzles is related to mixing behaviour inside the chamber and, consequently to the chamber volume, which determines the intended energy density of the combustor. However, these design parameters were never openly discussed in literature and their effect on performance is not precisely known.

Lückerath et al. [163] presented one of the first investigations regarding the adaptation of the FLOX<sup>®</sup> concept to gas turbines. A FLOX<sup>®</sup> burner with 12 nozzles was adapted to a combustion chamber with optical access and was operated at 20 bar. Using natural gas as fuel they concluded that the low emission range (for both CO and NO<sub>x</sub>) was extended with increasing jet velocity (shown in Fig. 25), which influenced the mixing behaviour. This fact points to issues regarding pressure losses, which increase with jet momentum.

Additionally, the operational range was relatively narrow. The reported variation in equivalence ratio is shown in Fig. 25 as well. The behaviour of emissions with varying excess air ratio was usual: increasingly leaner mixtures yielded lower NO<sub>x</sub> and higher CO emissions. These results are in contrast with those of Veríssimo et al. [78], discussed in Section 3.1. Although the geometries of Lückerath et al. [163] and Veríssimo et al. [78] share similarities, the latter was non-premixed, while the former had a significant level of premixedness. Essentially, Lückerath et al. [163] pointed out that the largest difficulties of the FLOX<sup>®</sup> concept for gas turbine conditions are emissions and operational range. Instabilities and flame blow-offs took place while altering the equivalence ratio and power in settings that would be required for a gas turbine operation. In most enclosed systems the rate of recirculation almost solely depends on the jet momentum which relates to the jet diameter and the heat capacity of the system. Hence, these systems end up having a limited operational range. Duwig et al. [151] also pointed to the problem of narrow operational range, while estimating the required amount of recirculated products to be approximately the same as the incoming reactants in order to sustain FC.

Lammel et al. [164] tackled the problem of having low power densities in FLOX<sup>®</sup> by increasing the diameter of the fuel nozzle to allow more fuel. However, this led to stability problems and higher emissions as the partial premixing was impaired. The burners were

**Table 5**

Comparison of requirements and operational aspects between aero engines and land-based gas turbines.

|  | Aero engines   | Land-based gas turbines  |
|--|--|--|
| High priority emission reduction [153] | CO, CO <sub>2</sub> , H <sub>2</sub> O, NO <sub>x</sub> , SO <sub>x</sub> , Soot | CO, CO <sub>2</sub> , NO <sub>x</sub>                          |
| Typical residence time (ms)            | ≈ 3 to 5 [154]   | ≈ 10 to 20 [155,156]   |
| Weight constraints [153]               | Very strict [157,158]  | Flexible   |
| Volume constraints [153,154]           | Strict [157]   | Flexible   |
| External recirculation                 | Not possible   | Possible [159]   |
| Fuel flexibility [154]                 | Liquid hydrocarbons (kerosene, biofuels) [160]                                   | Virtually any gaseous or liquid fuel. Flexibility is required. |
| Emission regulations [154]             | Regulated only for the Landing and Take-Off (LTO) cycle [161]                    | Regulated for all operating conditions [162]                   |

then redesigned to a configuration with air surrounding the fuel nozzle. The reactants further mixed in mixing tubes before entering the chamber. This design was named HiPerMix<sup>®</sup>. The authors experimentally analysed the performance of the design from 5 to 7 bar, using OH chemiluminescence, temperature and velocity measurements, as well as flue gas concentrations. The fuels tested were natural gas, natural gas-H<sub>2</sub> mixture, and natural gas-C<sub>3</sub>H<sub>8</sub> mixture.

Lammel et al. [164] pointed that the temperature fields displayed inhomogeneity due to the mixing characteristics of the HiPerMix<sup>®</sup>. Further improving the mixing would increase pressure losses to undesirable levels. Nevertheless, they showed that low NO<sub>x</sub> emissions were low (< 10 ppm) for the cases in which peak local temperatures were below the global adiabatic flame temperature. In practice, these conditions were translated to equivalence ratios lower than approximately 0.6, as their analysis maintained oxidiser mass flows and varied fuel input. For low equivalence ratios local temperatures were less likely to reach temperatures close to the global adiabatic flame temperature. This was probably due to the mixing characteristics of the design. This work showcased the compromise between mixing, pressure loss and emissions using the FLOX<sup>®</sup> concept. However, more detailed studies are still required in order to develop this concept, as the results are not generalized easily.

In the experiments described by Lammel et al. [164] different fuels were compared based on their NO<sub>x</sub> emission characteristics. Sadanandan et al. [165] further investigated the effect of fuel composition using a preceding FLOX<sup>®</sup> combustor operating at 20 bar to determine the effect of H<sub>2</sub> addition to natural gas in various proportions while maintaining the thermal power. Additionally, two types of nozzles were tested: partially premixed, with a fixed axial distance between fuel inlet and combustion chamber inlet, and non-premixed, with fuel and air entering at the same plane directly in the combustion chamber (Fig. 26). Once again, the addition of H<sub>2</sub> increased the levels of NO<sub>x</sub> emissions and moved the reactions upstream because of higher reactivity. Thus, such addition should be followed by adaptations in the jet velocities. In turn, the effect of having partial or no premixing on emissions was minor as compared to the recirculation ratio (for a given equivalence ratio). Emissions were lower for higher recirculation ratios, achieved by higher jet velocities.

As narrow operational range is a common problem faced by FLOX<sup>®</sup> based combustors, the EZEE<sup>®</sup> configuration was developed [166] in an attempt to improve the operational range of the high energy density HiPerMix<sup>®</sup> design. The design retained the 12 inlets to the combustion chamber as in previous designs, but each of the premixing tubes was fed by two fuel nozzles placed in the same plane and radial coordinate. These fuel nozzles were tested both in centric and excentric configurations, as shown in Fig. 27. The idea was to extend the power modulation by regulating the fuel distribution between the nozzles. The fuel partitioning was able to enhance the operational range using natural gas and was regarded as satisfactory by the authors.

Yet another attempt using a modified FLOX<sup>®</sup> design was explored by Roediger et al. [167] and Zanger et al. [168]. The idea was to have

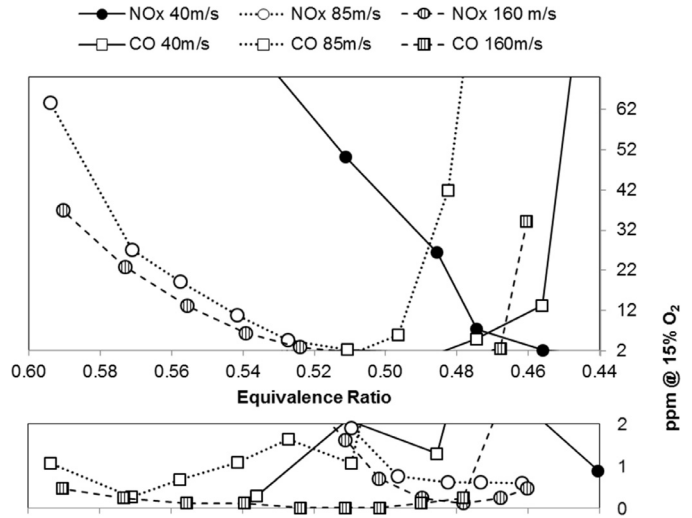


**Fig. 25.** Emission results of CO and NO<sub>x</sub> of a FLOX<sup>®</sup> setup, as functions of the equivalence ratio for three different jet velocities. Adapted from Lückerrath [163]. The vertical axis was split to aid visualization and clearly show the low emissions window.

staged combustion with a swirler-stabilized flame in the centre of the combustor, upstream of the axial position at which the usual concentric FLOX<sup>®</sup> jets were positioned. It is worth highlighting the relevance of the experiments done with JHC discussed in Section 3.1 for configurations intended to employ staged combustion, as the (fuel) jets are injected in a vitiated environment. Such architecture provides more freedom to extend the operational range and stability as the core is similar to a conventional combustor. The authors reported that a good operational range and relatively low NO<sub>x</sub> emissions was obtained. They suggested that CO could be reduced further by optimizing the split between the swirler burner and the FLOX<sup>®</sup>. These results were achieved in an atmospheric pressure test rig and requires further testing, especially with respect to the complexity involved in fuel splitting. This concept shares similarities with the design studied by Guillou et al. [169] in which the oxidiser was injected through a swirler positioned at the centre of the burner, while the fuel jets were displaced radially and injected tangentially in order to increase the swirling motion.

These concepts [166–169] are examples of how the FLOX<sup>®</sup> approach could incorporate solutions to broaden the operational ranges similarly to pilots employed in modern lean-premixed combustors. These candidate solutions must also be evaluated with respect to emissions, as low emissions should be maintained throughout the whole LTO cycle for aero engines.

The FLOX<sup>®</sup> combustors are primarily suited for gaseous fuels. Using liquid fuels would require a different architecture as the fuel jet momentum and evaporation play an important role in the partial premixing, which is essential for this type of combustors. Attempting to overcome this limitation, Zizin et al. [170] tested possible configurations and designs that would allow the use of liquid fuels. Different atomizers and nozzles were tested for a single-nozzle and

a

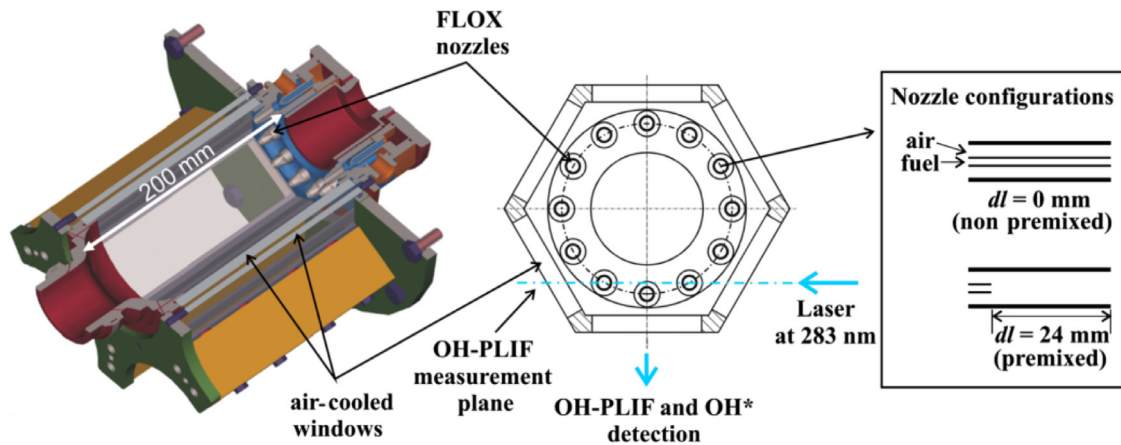


Fig. 26. FLOX® combustor employed by Sadanandan et al. [165] and the two nozzle configurations.

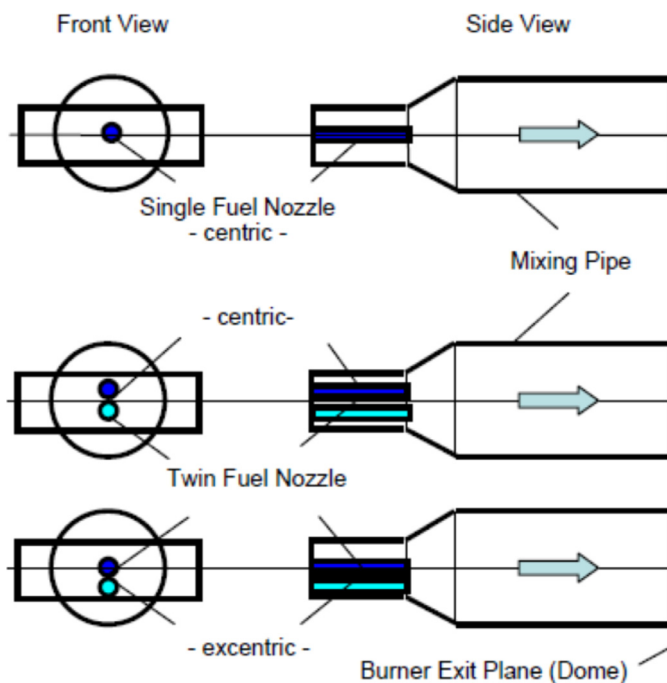


Fig. 27. The configurations of the partially premixed nozzles studied by Schütz et al. [166] in the EZEE® concept.

12-nozzle configuration with diesel, light heating oil and kerosene fuels. The authors reported no clear advantage of one configuration over the others.

Gounder et al. [171] further developed the study performed by Zizin et al. [170] and performed measurements in a 8-nozzle square-shaped combustor (shown in Fig. 28) intended for a micro gas turbine. The authors mentioned that the spray atomizers could be easily incorporated in large FLOX® gas turbines due to the large ratio between air nozzle diameter and atomizer diameter. However, the usual difficulties faced in previous works with gaseous fuels were still present.

Apart from the above mentioned difficulties, the applicability of FLOX® based gas turbine combustors is still uncertain. The integration of an FC combustor within a gas turbine has not been discussed in detail by researchers, especially for aero engines, which use annular type combustion chambers.

Other experimental variations relying on jet-mixing are present in the literature. The architectures of such concepts were

summarized by Arghode and Gupta [173], with variations being mostly in the relative positions of oxidiser jets, fuel jets, and exhaust. The overall difficulties and strategies to tackle them in such concepts are similar to those presented for the FLOX® configuration. Along with their summary, the authors explored the challenge of achieving high energy density inside the combustors, an important requirement of gas turbine engines.

Examining the works mentioned in this section, the gap in relation to the basic experiments (Section 3) is evident. For example, formaldehyde ( $\text{CH}_2\text{O}$ ) was not measured in realistic setups, while its role was shown to be of great importance. A better correspondence between canonical and applied experiments would also be of great value to discuss the FC regime itself and to check the validity of fundamental experimental conditions to applications. The most important experiments are summarized in Table 6.

The designs with recirculation induced by jet momentum were studied in more detail than those based in primary flow recirculation and the difficulties with operational range, combustion efficiency and engine integration are still significant obstacles. Attempting to bridge the gap between designs and basic experiments in combustors based on jet momentum, a single-nozzle premixed burner in a non-symmetrical combustion chamber was designed to represent one of the nozzles found in the FLOX® concept. An early work provided data on OH, OH\* and velocity fields [174], being useful for model validation, while a study on jet-flapping was presented using the same measurement techniques [175].

Interestingly, the setup was employed to study the combustion regimes by varying the jet velocity [176]. With increasing velocity, transitions from laminar premixed flames to turbulent premixed jets that could not be stabilized occurred. Further increase in the jet velocity caused flame stabilization possibly due to the increase in recirculation, with evidence of auto-ignition kernels. The authors suggested that the no-flame region corresponds to jet velocities higher than the flame propagation velocity and too low to cause enough recirculation. Furthermore, the authors estimated positions of the investigated conditions on the Borghi diagram. They pointed that the flames with the lowest jet velocities populated the laminar flame region. A gradual increase in velocity made the flames unstable until velocities were high enough to achieve stable combustion through recirculation, and the flames populated the corrugated flamelet and thin reaction zone regions of the diagram (see Fig. 4). Although the methodology to calculate  $Ka$  and  $Da$  is arguable (as discussed in Section 2), it is certainly valuable to relate the fundamentals of the FC regime with an experiment similar to an application. Therefore, this type of experiment shall provide better



**Table 6**

Summary of experiments related to proposed FC combustors intended to operate in gas turbines displayed chronologically.

| Reference               | Power (kW)  | Fuels  | Recirculation Strategy | Pressure (bar) <sup>a</sup> | Power Density (MW/m <sup>3</sup> bar) <sup>b</sup>           | Measured Variables <sup>c</sup> | Measurement Techniques                                  |
|-------------------------|-------------|--|------------------------|-----------------------------|--|---------------------------------|---|
| Vaz et al. [190]        | 82 / 106    | NG   | Jet momentum           | 1                           | < 16   | T                               | Thermocouples   |
| Li et al. [191]         | 8.3 to 49.3 | C <sub>3</sub> H <sub>8</sub>  | Jet momentum           | 1                           | 3.5 to 20.9  | OH*, V                          | Filtering, PIV  |
| Vaz [192]               | 69 to 464   | NG   | Jet momentum           | 1.00 to 4.74                | up to 70   | T                               | Thermocouples   |
| Duwig et al. [151]      | 463.5       | C <sub>3</sub> H <sub>8</sub>  | Jet momentum           | n/a                         | p n/a<br>(vol. = 2.356•10 <sup>-3</sup> m <sup>3</sup> )     | OH*, p, V                       | PIV, Filtering  |
| Lückerath et al. [163]  | 100 to 475  | NG, NG/H <sub>2</sub>  | Jet momentum           | 20                          | 3 to 14  | OH*, Y <sub>OH</sub>            | Filtering, PLIF   |
| Guillou et al. [169]    | n/a         | C <sub>3</sub> H <sub>8</sub> , C <sub>4</sub> H <sub>10</sub> , C <sub>5</sub> H <sub>12</sub> , C <sub>6</sub> H <sub>14</sub> , C <sub>6</sub> H <sub>5</sub> —CH <sub>3</sub> , C <sub>9</sub> H <sub>20</sub> , Jet A | Jet momentum / Swirl   | 1                           | Power n/a<br>(vol. = 1.456•10 <sup>-2</sup> m <sup>3</sup> ) | OH*, T                          | Filtering, Thermocouples                                |
| Melo et al. [180]       | 4 to 32     | CH <sub>4</sub>  | Geometry               | 1                           | 2.6 to 21.2  | V                               | LDV   |
| Lammel et al. [164]     | 600 to 1300 | NG, NG/H <sub>2</sub>  | Jet momentum           | 5 to 7                      | 53 to 117  | OH*, p, T, V                    | CARS, Filtering, PIV                                    |
| Melo et al. [181]       | 10 to 21.5  | CH <sub>4</sub>  | Geometry               | 1                           | 6.6 to 14.2  | V, T                            | LDV, Thermocouples                                      |
| Sadanandan et al. [165] | 141 to 500  | NG, NG/H <sub>2</sub>  | Jet momentum           | 20                          | 4.15 to 14.69  | OH*, Y <sub>OH</sub>            | Filtering, PLIF   |
| Schütz et al. [166]     | < 1400      | NG   | Jet momentum           | 2 to 8                      | 60.53 to 101.90  | OH*                             | Filtering   |
| Roediger et al. [167]   | 907, 978    | NG   | Jet momentum / Swirler | < 10                        | 172.38   | OH*                             | Filtering   |
| Zanger et al. [168]     | n/a         | NG   | Jet momentum / Swirler | 1, 4                        | n/a  | OH*                             | Filtering   |
| Zizin et al. [170]      | < 40        | Diesel DIN EN 590  | Jet momentum           | 1                           | 18.8   | OH*, T <sub>walls</sub>         | Filtering, Mie Scattering, Temperature Sensitive Paints |
| Gounder et al. [171]    | 90 to 236   | Light Heating Oil  | Jet momentum           | 3.5                         | 25.6 to 67.1   | OH*, V (spray)                  | Filtering, Mie Scattering, Spray PIV, PDI               |
| Zhou et al. [193]       | 161 to 381  | CH <sub>4</sub>  | Jet momentum           | 1                           | 11 to 26   | —                               | —   |
| Seliger et al. [194]    | 2.07 / 3.00 | NG   | Jet momentum           | 1                           | n/a  | OH*, Y <sub>OH</sub> , V        | Filtering, PIV, PLIF                                    |

<sup>a</sup> Experiments carried at atmospheric pressure are assumed to be at 1 bar.<sup>b</sup> If not reported, values are calculated based on estimated combustor volumes.

understanding and modelling databases for the relevant conditions of FC applications.

As previously mentioned, another possible strategy to attain FC in gas turbines is to impose a large recirculation to the primary flow. This strategy was adopted by the FLOXCOM combustor [177–181]. The authors were able to define a preliminary geometry as well as some key design parameters like air split, recirculation ratio and the temperatures of the different streams. By means of a CRN analysis, Levy et al. [179] pointed out that increasing recirculation ratio (condition necessary to attain FC using this concept) could have negative impact on CO emissions. This trend was later confirmed by Melo et al. [180]. The central idea of the design was the generation of a large recirculation zone inside the combustor and to have the fuel injected in a region where the incoming air is already mixed with combustion products. Such design would allow the combustor to be annular and would therefore be easier to integrate into an engine. The concept was developed into a prototype [180].

The experiments performed by Melo et al. [180] employed 60° sectors of the annular concept as shown in Fig. 29. They investigated different configurations of air inlets (using slots or holes in different angles) while retaining fuel injection and key geometrical features. The cold flow recirculation ratios, as well as emissions for a range of equivalence ratios for different configurations were compared. Recirculation ratios and emissions showed significant sensitivity to the air inlet design. However, there was no assessment in terms of pressure losses, an important parameter for the application to gas turbines.

In another work, Melo et al. [181] focused on velocity and turbulent kinetic energy distributions on different conditions in relation to power input for one of the air inlet configurations previously studied (Melo et al. [180]). Additionally, point measurements of temperature and main species were performed inside the combustor

using probes. The authors identified relatively uniform temperature profiles, suggesting attainment of the FC regime. In both works, the experiments confirmed low NO<sub>x</sub> emissions, while the attained combustion efficiencies and CO emissions were not at acceptable levels. The authors suspected that the residence times within the combustion zone were too low and could be improved by changing dimensions or fuel injection location. Therefore, it is yet to be proven if the concept is able to attain high combustion efficiencies, broad operational range and low pressure losses. Furthermore, the FLOXCOM concept would require further tests in high pressure environment and possibly using liquid fuels.

On a more conceptual level, Levy et al. [182,183] studied the idea of having smaller recirculation zones where fuel would be injected. According to the analysis performed with the aid of CRNs, having a smaller portion of the gases being recirculated to generate local low O<sub>2</sub> regions could reach a compromise between achieving FC and the pressure losses caused by recirculation. The concept (Fig. 30) also explored imposing heat transfer to the secondary air flow, which would allow combustion to take place at near-stoichiometric conditions without excessive temperature increase. In principle, such solution could improve stability and broaden the operational range, one of the largest concerns faced by the FLOX<sup>®</sup> concept. However, a proof of concept is required to back the preliminary analyses performed.

A more recent concept relying on a large recirculation zone was presented by Levy et al. [184], and was referred to as FOGT (Flameless Oxidation Gas Turbine) combustor. The authors employed the same analyses developed by Levy et al. [174–179], but developed a different geometry as compared to the FLOXCOM (Fig. 31). The central idea was to have an annulus with a recirculation zone and the outlet in a direction opposite to the air inlet, thereby forcing mixing

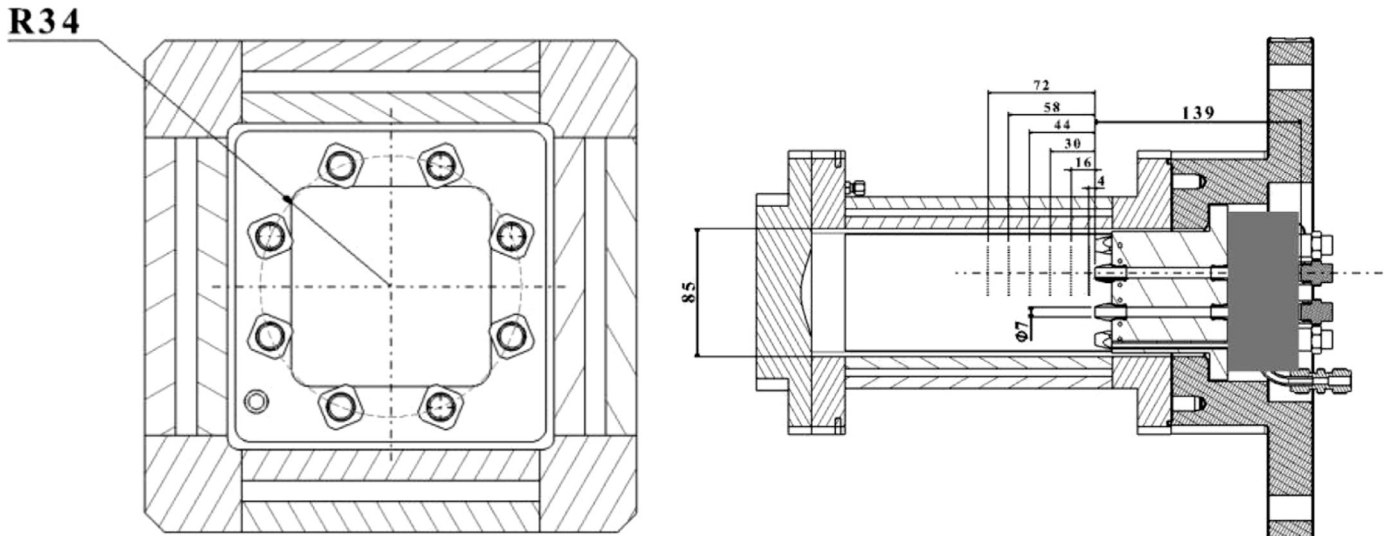


Fig. 28. The 8-nozzle square-shaped FLOX® combustor employed by Gounder et al. [172] to study fuel spray characteristics. Top view (left) and lateral view (right).

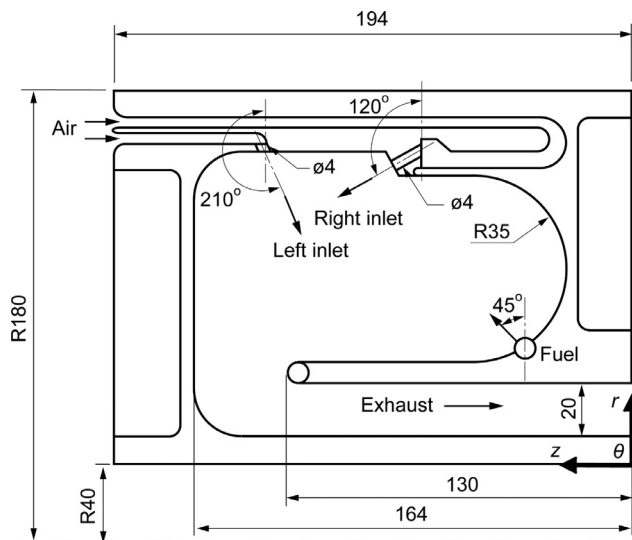


Fig. 29. Cross section of the 60° sector employed by Melo et al. [181].

with burnt gases. The authors proposed the fuel injection to be either along with the air inlet, or inside the recirculation zone.

The computational analysis performed using CFD showed promising results in terms of emissions and pressure losses. However, the concept requires a rigorous experimental analysis involving conventional fuels and assessment of the operational range. Additionally, the integrational aspects within the engine should be looked into.

Most of the proposed designs did not include aspects related to the integration in the gas turbine or modifications on the engine architecture strategies that would contribute to a successful design. The concept of staged combustion with turbine stages in between was explored by Joos et al. [185], as early as 1996, but with no focus on FC. Already pointed as a solution for reduction of NOx emissions, the authors reported on aspects of the design development of the ABB GT24 and GT26 design family, especially related to performance and emissions. Interestingly, the concept was presented in the review of Cavaliere and de Joannon [14] as one of the options to

achieve FC in gas turbines. Nevertheless, it was largely ignored in open literature for a long time.

Recently, the hybrid engine concept presented within the AHEAD project [186] employed a similar approach for aero engines. The project explored advantages and challenges of using cryogenic fuels in aviation, and proposed a multi-fuel blended wing body aircraft as a possible solution. The engine was conceptualised to have two sequential combustors separated by a turbine section as shown in Fig. 32. The first combustor would burn cryogenic fuels (natural gas or H<sub>2</sub>), while the second combustor, referred to as Inter-turbine Burner (ITB), would operate with Jet-A or biofuel under the FC regime.

The advantage of this strategy from a combustion point of view is that the gases entering the second combustor would have high temperature and reduced O<sub>2</sub> concentration. Such conditions would facilitate the attainment of the FC regime with lower recirculation thereby reducing the required volume and pressure losses. Additionally, the possibility of regulating the power in each combustion chamber could provide broader operational range if explored wisely [187].

The preliminary design of the ITB was presented by Levy et al. [188], and was based on chemical kinetics and CFD analysis. The authors were able to design the combustor and estimate emission values. The annular FC combustor would split the incoming vitiated oxidiser into the dilution and the combustion streams. The latter would enter a large recirculation zone where fuel is injected. The design of the ITB was evaluated by a comparison between experimental data on NOx and CO emissions with CFD and CRN simulations by Perpignan et al. [189]. The authors identified opportunities to improve the design and elaborated on the NOx formation pathways. Interestingly, the prompt pathway was shown to be dominant in the overall NOx formation, while the thermal pathway had relatively little contribution. This finding is related to the main reason why FC yields lower NOx emissions: abatement of the thermal pathway. However, a shift in the NOx formation chemistry due to the abundance of combustion products in the reaction zones is also an important factor.

Overall, the experimental assessment of concepts based on large recirculation zones is difficult due to their predominantly annular configuration, which limits diagnostics and makes the use of prototypes challenging. Therefore, the current trend is that these concepts are being explored with available numerical tools. Designs with

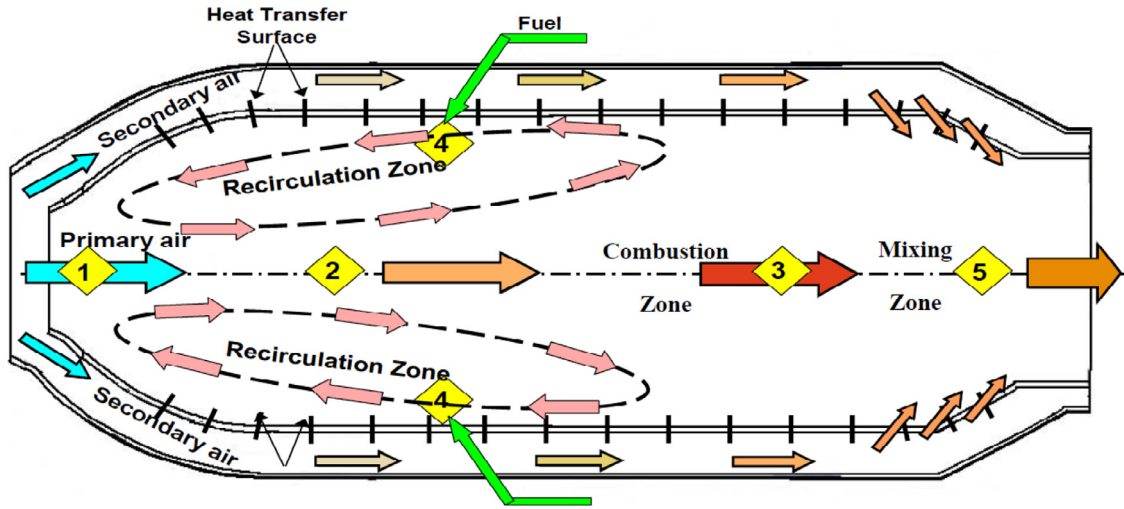


Fig. 30. The concept proposed by Levy et al. [183]. The numbers refer to the regions simulated in their analyses.

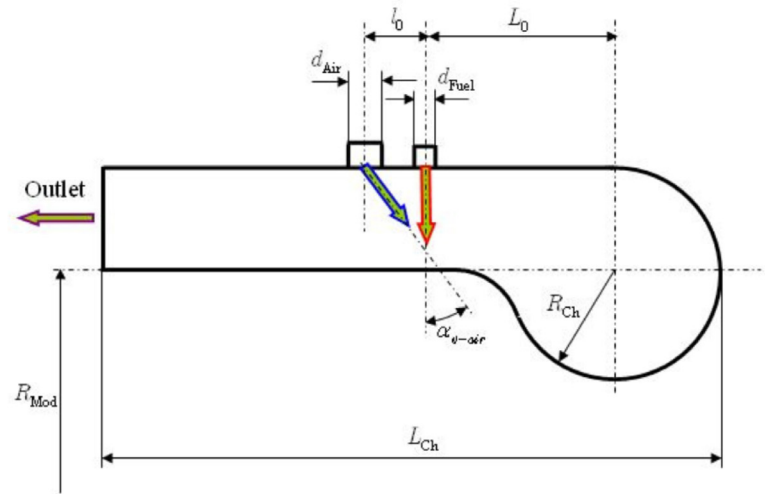
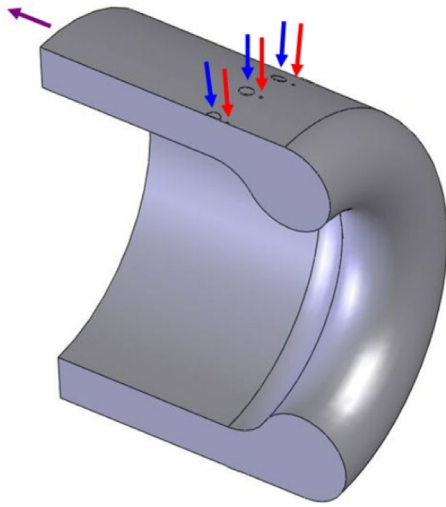


Fig. 31. The FOGT concept [184].

recirculation induced by geometry require more exploration, especially in relation to experiments. The design of experiments able to simplify the analyses while being representative of the phenomena involved should be pursued.

## 6. Conclusions, open challenges and recommendations

This paper reviewed several studies directly related to FC in gas turbines. The study of this subject has multiple levels, ranging from the definition of FC to canonical experiments and modelling to design attempts for gas turbine combustors.

The generalization of results or their classification is currently impaired by the different and uncomprehensive definitions of FC. The lack of a broadly accepted definition limits the effectiveness of research, as results cannot be easily correlated.

The conclusions and recommendations of this review are summarized below.

Concerning the definition of FC:

- Existing definitions of FC are based on global parameters. However, because the regime is a result of local conditions, it is difficult to qualify it solely based on global parameters.

far as the development of applications is concerned, pollutant emissions could be incorporated in the definition of the FC regime boundaries, as it is the reason to explore the FC regime. However, as mentioned in Section 2, a definition based on pollutant emissions would not be physically consistent.

Concerning basic experimental investigations:

- Most of the fundamental experiments have been dedicated to JHC. Although the configuration has several advantages and has evolved to provide comprehensive databases, different test cases have to be developed to support the developments for applications in gas turbines, especially for design concepts relying on large recirculation zones.
- Fundamental experiments should be developed to include pollutant formation diagnostics and high operating pressures.

Concerning computational modelling:

- DNS studies have shown that reaction zones in the FC regime consists of thin reaction zones, intensely interacting with each other, and are not completely homogeneous. Although some

•  
As

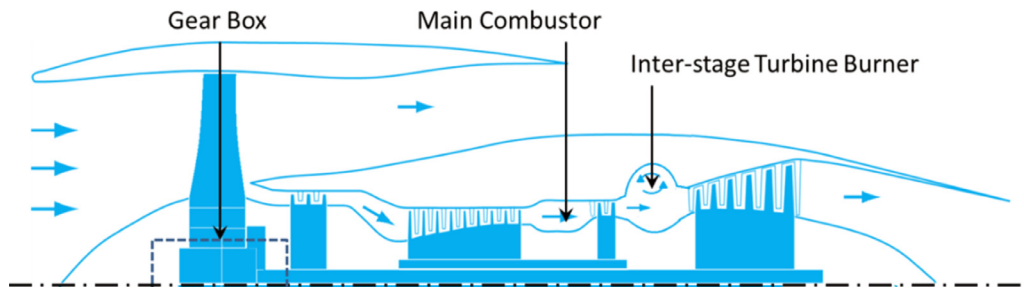


Fig. 32. The engine concept present along with the AHEAD project [186].

experiments have shown similar behaviour [75], it remains to be further explored experimentally as the scales investigated in DNS are considerably smaller than those of experimental investigations.

- Virtually every turbulence-chemistry and combustion modelling approach has been attempted for FC related problems. As far as JHC data is concerned, the best results were obtained using CMC and CSE. Recent adaptations and improvements in the EDC and flamelet-based models also show promising results.
- Even though computationally expensive, the evidenced importance of unsteady structures point to the an advantage of LES-based modelling to accurately capture the ignition and the extinction processes, resulting in better intermediate species predictions.
- The conclusions from JHC modelling should be extrapolated carefully as these experiments are not a good representation for all FC related applications.
- Modelling is still unreliable in terms of predicting emissions and intermediate species. This is one the main impediments of using numerical models in designing gas turbine combustors.

Concerning conceptual designs for gas turbines:

- The current concepts attempting to design a FC combustor for gas turbines rely on recirculation created either by jet entrainment, a large recirculation zone, or a combination of both. The former method might be limited in operating flexibility as the recirculation is directly proportional to the jets momenta.
- Data available from experiments performed on combustors operating in the FC regime is scarce. High pressure experiments and the use of advanced diagnostic techniques should be pursued to increase our understanding.
- Most designs failed mainly because of low combustion efficiency (high CO emissions), higher pressure loss, narrow operational range, higher complexity, or unfeasibility of integration in the engine.
- The full required operational envelope should be considered in the development of FC-based designs. The attainment of low emissions should be guaranteed also for part-load operation.
- The integration of combustor concepts within engines is usually neglected and should be considered in the early stages of the design in order to increase its feasibility.
- Systematic investigation regarding acoustic oscillations and stability should be performed in the framework of FC, as there is a lack of studies in this area, which prevents designers from taking advantage of the regime in that respect.
- The exploration of innovative engine architectures may pave the ground to the successful attainment of FC in gas turbines, as shown by the use of an inter-turbine burner.
- Staged combustion could be a possible way of reducing  $O_2$  concentration to facilitate FC in practical combustion systems.

- If the level of development for FC-based designs allows, comparisons with other approaches should be performed to either justify or disprove the design.

We can conclude that the designers of a gas turbine engine operating in the FC regime currently cannot rely on the full understanding of the phenomena involved. This fact does not mean that a design is not possible, since similar situations are common in engineering practices. Full understanding is not a requirement for an engineering product.

However, we understand that the current difficulties can be tackled by studying key features of the FC regime, namely reaction zone structures, influence of local Damköhler and Karlovitz numbers, role of heat transfer and higher pressures, and emissions formation. There is a lack of experiments combining pollutant related chemistry data and reaction zone structures. Progress in these areas will ultimately lead to more effective design strategies, that will remain effective also when transitions to power and propulsion technologies with lower  $CO_2$  footprint are made.

## Acknowledgements

The authors would like to thank CNPq (National Counsel of Technological and Scientific Development - Brazil) for the financial support. The authors are grateful to Xu Huang for providing his simulation results on the DJHC-I flame.

## References

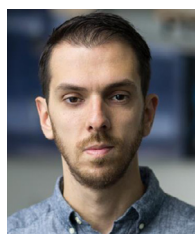
- [1] James SR. Hominid use of fire in the lower and middle Pleistocene: a review of the evidence. *Current Anthropol* 1989;30:1–26.
- [2] Gohardani AS, Douleris G, Singh R. Challenges of future aircraft propulsion: a review of distributed propulsion technology and its potential application for the all electric commercial aircraft. *Progr Aerosp Sci* 2011;47:369–91.
- [3] Yin F, Rao AG. Performance analysis of an aero engine with interstage turbine burner. In: *Proceedings of the 23rd ISABE conference*, Manchester, UK; 2017 Sep 3–8.
- [4] ICAO Engine Exhaust Emissions Databank, ICAO, Doc 9646- AN/943, Version 23, November 2016.
- [5] Flightpath ACARE. 2050-Europe's Vision for aviation. *Advisory Council for Aeronautics Research in Europe*; 2011.
- [6] Klein M. Overview of worldwide ground-based regulatory framework. In: Lieuwen TC, Yang V, eds. *Gas turbine emissions*. New York: Cambridge University Press; 2013. p. 95–120.
- [7] Nathan GJ, Jafarian M, Dally BB, Saw WL, Ashman PJ, Hu E, Steinfeld A. Solar thermal hybrids for combustion power plant: A growing opportunity. *Progr Energy Combust Sci* 2017;64:4–28.
- [8] Brouwer AS, van den Broek M, Seebregts A, Faaij A. Impacts of large-scale intermittent renewable energy sources on electricity systems, and how these can be modelled. *Renew Sustain Energy Rev* 2014;33:443–66.
- [9] Chen H, Cong TN, Yang W, Tan C, Li Y, Ding Y. Progress in electrical energy storage system: a critical review. *Progr Nat Sci* 2009;19:291–312.
- [10] Overman N, Cornwell M, Gutmark EJ. Application of Flameless Combustion in gas turbine engines. In: *Proceedings of the 42nd AIAA/ASME/SAE/ASEE joint propulsion conference & exhibit*, Sacramento, USA; 2006 Jul 9–12.
- [11] Pompei F, Heywood JB. The role of mixing in burner-generated carbon monoxide and nitric oxide. *Combust Flame* 1972;19:407–18.



- [12] Biagioli F, Güthe F. Effect of pressure and fuel–air unmixedness on NOx emissions from industrial gas turbine burners. *Combust Flame* 2007;151:274–88.
- [13] Dederichs S, Zarzal N, Habisreuther P, Beck C, Prade B, Krebs W. Assessment of a gas turbine NOx reduction potential based on a spatiotemporal unmixedness parameter. *J Eng Gas Turbines Power* 2013;135:1–8.
- [14] Plessing T, Peters N, Wünnig JG. Laseroptical investigation of highly preheated combustion with strong exhaust gas recirculation. *Symp (Int) Combust* 1998;27:3197–204.
- [15] Cavaliere A, de Joannon M. Mild combustion. *Prog Energy Combust Sci* 2004;30:329–66.
- [16] Li PF, Mi JC, Dally BB, Wang FF, Wang L, Liu ZH, Chen S, Zheng CG. Progress and recent trend in MILD combustion. *Sci China Technol Sci* 2011;54:255–69.
- [17] Wünnig JA, Wünnig JG. Flameless oxidation to reduce thermal NO-formation. *Prog Energy Combust Sci* 1997;23:81–4.
- [18] Evans MJ, Medwell PR, Wu H, Stagni A, Ihme M. Classification and lift-off height prediction of non-premixed MILD and autoignitive flames. *Proc Combust Inst* 2017;36:4297–304.
- [19] Rao AG, Levy Y. A new combustion methodology for low emission gas turbine engines. In: *Proceedings of the 8th international symposium on high temperature air combustion and gasification*, Pozan, Poland; 2010.
- [20] Oberlack M, Arlitt R, Peters N. On stochastic Damköhler number variations in a homogeneous flow reactor. *Combust Theory Model* 2000;4:495–509.
- [21] Goodwin G, Moffat HK, Speth RL. Cantera: an object-oriented software toolkit for chemical kinetics, thermodynamics, and transport processes Version 2.3.0. <http://www.cantera.org>; 2017. doi: 10.5281/zenodo.170284.
- [22] Smith GP, Frenklach M, Moriarty NW, Eiteneer B., Goldenberg M., Bowman C.T., Hanson R.K., Song S., Gardiner Jr. W.C., Lissianski V.V., Qin Z. [http://www.me.berkeley.edu/gri\\_mech/](http://www.me.berkeley.edu/gri_mech/).
- [23] Galletti C, Parente A, Tognotti L. Numerical and experimental investigation of a mild combustion burner. *Combust Flame* 2007;151:649–64.
- [24] Cabra R, Chen JY, Dibble RW, Karpets AN, Barlow RS. Lifted methane-air jet flames in a vitiated coflow. *Combust Flame* 2005;143:491–506.
- [25] Yoo CS, Sankaran R, Chen JH. Three-dimensional direct numerical simulation of a turbulent lifted hydrogen jet flame in heated coflow: flame stabilization and structure. *J Fluid Mech* 2009;640:453–81.
- [26] Borghi R. Turbulent combustion modelling. *Prog Energy Combust Sci* 1988;14:245–92.
- [27] Peters N. *Turbulent combustion*. Cambridge University Press; 2000.
- [28] Law CK. *Combustion physics*. Cambridge University Press; 2006.
- [29] Derudi M, Villani A, Rota R. Sustainability of mild combustion of hydrogen-containing hybrid fuels. *Proc Combust Inst* 2007;31:3393–400.
- [30] Tunçer O, Kaynaroglu B, Karakaya MC, Kahraman S, Çetiner-Yıldırım O, Baytaş C. Preliminary investigation of a swirl stabilized premixed combustor. *Fuel* 2014;114:870–4.
- [31] Li H, Elkady AM, Evulet AT. Effect of exhaust gas recirculation on NOx formation in premixed combustion system. In: *Proceedings of the 47th AIAA aerospace sciences meeting including the new horizons forum and aerospace exposition*, Orlando, USA; 2009.
- [32] Ravi S, Morones A, Petersen EL. Effects of hydrogen addition on the flame speeds of natural gas blends under uniform turbulent conditions. *ASME Turbo Expo* 2015. In: *Proceedings of the ASME turbo expo*, Montreal, Canada; 2015.
- [33] Isaac BJ, Parente A, Galletti C, Thornock JN, Smith PJ, Tognotti L. A novel methodology for chemical time scale evaluation with detailed chemical reaction kinetics. *Energy Fuels* 2013;27:2255–65.
- [34] Dally BB, Karpets AN, Barlow RS. Structure of turbulent non-premixed jet flames in a diluted hot coflow. *Proc Combust Inst* 2002;29:1147–54.
- [35] Li X, Dai Z, Wang F. Characteristic chemical time scale analysis of a partial oxidation flame in hot syngas coflow. *Energy Fuels* 2017;31:4382–90.
- [36] Christo FC, Dally BB. Modeling turbulent reacting jets issuing into a hot and diluted coflow. *Combust Flame* 2005;142:117–29.
- [37] Parente A, Sutherland JC, Dally BB, Tognotti L, Smith PJ. Investigation of the MILD combustion regime via principal component analysis. *Proc Combust Inst* 2011;33:333–41.
- [38] Medwell PR, Kalt PAM, Dally BB. Simultaneous imaging of OH, formaldehyde, and temperature of turbulent nonpremixed jet flames in a heated and diluted coflow. *Combust Flame* 2007;148:48–61.
- [39] Medwell PR, Kalt PAM, Dally BB. Imaging of diluted turbulent ethylene flames stabilized on a Jet in Hot Coflow (JHC) burner. *Combust Flame* 2008;152:100–13.
- [40] Medwell PR, Kalt PAM, Dally BB. Reaction zone weakening effects under hot and diluted oxidant stream conditions. *Combust Sci Technol* 2009;181:937–53.
- [41] Gordon RL, Masri AR, Mastorakos E. Heat release rate as represented by  $[OH] \times [CH_2O]$  and its role in autoignition. *Combust Theory Model* 2009;13:645–70.
- [42] McEnally CS, Pfefferle LD. Experimental study of nonfuel hydrocarbon concentrations in coflowing partially premixed methane/air flames. *Combust Flame* 1999;118:619–32.
- [43] Medwell PR, Blunck DL, Dally BB. The role of precursors on the stabilisation of jet flames issuing into a hot environment. *Combust Flame* 2014;161:465–74.
- [44] Cabra R, Myhrvold T, Chen JY, Dibble RW, Karpets AN, Barlow RS. Simultaneous laser Raman-Rayleigh-LIF measurements and numerical modeling results of a lifted turbulent  $H_2/N_2$  jet flame in a vitiated coflow. *Proc Combust Inst* 2002;29:1881–8.
- [45] Medwell PR, Dally BB. Effect of fuel composition on jet flames in a heated and diluted oxidant stream. *Combust Flame* 2012;159:3138–45.
- [46] Oldenhof E, Tummers MJ, van Veen EH, Roekaerts DJEM. Role of entrainment in the stabilisation of jet-in-hot-coflow flames. *Combust Flame* 2011;158:1553–63.
- [47] Arteaga Mendez LDA, Tummers MJ, van Veen EH, Roekaerts DJEM. Effect of hydrogen addition on the structure of natural-gas jet-in-hot-coflow flames. *Proc Combust Inst* 2015;35:3557–64.
- [48] Wu Z, Masri AR, Bilger RW. An experimental investigation of the turbulence structure of a lifted  $H_2/N_2$  jet flame in a vitiated co-flow. *Flow Turbul Combust* 2006;76:61–81.
- [49] Gordon RL, Masri AR, Mastorakos E. Simultaneous Rayleigh temperature, OH- and  $CH_2O$ -LIF imaging of methane jets in a vitiated coflow. *Combust Flame* 2008;155:181–95.
- [50] Najm HN, Paul PH, Mueller CJ, Wyckoff PS. On the adequacy of certain experimental observables as measurements of flame burning rate. *Combust Flame* 1998;113:312–32.
- [51] Dold JW. Flame propagation in a nonuniform mixture: analysis of a slowly varying triple flame. *Combust Flame* 1989;76:71–88.
- [52] Sidey JAM, Mastorakos E. Simulations of laminar non-premixed flames of methane with hot combustion products as oxidiser. *Combust Flame* 2016;163:1–11.
- [53] Oldenhof E, Tummers MJ, van Veen EH, Roekaerts DJEM. The turbulent flow-field of the Delft Jet-in-Hot-Coflow burner. In: *Proceedings of the 5th European thermal-sciences conference*, Eindhoven, The Netherlands; 2008.
- [54] Oldenhof E, Tummers MJ, van Veen EH, Roekaerts DJEM. Ignition kernel formation and lift-off behaviour of jet-in-hot-coflow flames. *Combust Flame* 2010;157:1167–78.
- [55] Oldenhof E, Tummers MJ, van Veen EH, Roekaerts DJEM. Conditional flow field statistics of jet-in-hot-coflow flames. *Combust Flame* 2013;160:1428–40.
- [56] Evans MJ, Chinnici A, Medwell PR, Ye J. Ignition features of methane and ethylene fuel-blends in hot and diluted coflows. *Fuel* 2017;203:279–89.
- [57] Oldenhof E, Tummers MJ, van Veen EH, Roekaerts DJEM. Transient response of the Delft jet-in-hot coflow flames. *Combust Flame* 2012;159:697–706.
- [58] Arndt CM, Gounder JD, Meier W, Aigner M. Auto-ignition and flame stabilization of pulsed methane jets in a hot vitiated coflow studied with high-speed laser and imaging techniques. *Appl Phys B* 2012;108:407–17.
- [59] Arndt CM, Schießel R, Gounder JD, Meier W, Aigner M. Flame stabilization and auto-ignition of pulsed methane jets in a hot coflow: influence of temperature. *Proc Combust Inst* 2013;34:1483–90.
- [60] Arndt CM, Papageorge MJ, Fuest F, Sutton JA, Meier W, Aigner M. The role of temperature, mixture fraction, and scalar dissipation rate on transient methane injection and auto-ignition in a jet in hot coflow burner. *Combust Flame* 2016;167:60–71.
- [61] Medwell PR, Dally BB. Experimental observation of lifted flames in a heated and diluted coflow. *Energy Fuels* 2012;26:5519–27.
- [62] Duwig C, Li B, Li ZS, Aldén M. High resolution imaging of flameless and distributed turbulent combustion. *Combust Flame* 2012;159:306–16.
- [63] Dunn MJ, Masri AR, Bilger RW. A new piloted premixed jet burner to study strong finite-rate chemistry effects. *Combust Flame* 2007;151:46–60.
- [64] Colonna P, van der Stelt TP. *FluidProp: a program for the estimation of thermo physical properties of fluids*. Delft, The Netherlands: Energy Technology Section, Delft University of Technology; 2004 <http://www.FluidProp.com>.
- [65] Ye J, Medwell PR, Dally BB, Evans MJ. The transition of ethanol flames from conventional to MILD combustion. *Combust Flame* 2016;171:173–84.
- [66] Ye J, Medwell PR, Evans MJ, Dally BB. Characteristics of turbulent n-heptane jet flames in a hot and diluted coflow. *Combust Flame* 2017;183:330–42.
- [67] Cabra R, Hamano Y, Chen JY, Dibble RW, Acosta F, Holve D. Ensemble diffraction measurements of spray combustion in a novel vitiated coflow turbulent jet flame burner. NASA Glenn Research Center; 2000 Report No.: 2000-210466. Grant No.: NAG3-2103.
- [68] Cabra R, Dibble RW, Chen JY. Characterization of liquid fuel evaporation of a lifted methanol spray flame in a vitiated coflow burner. NASA Glenn Research Center; 2002 Report No.: 2002-212083. Grant No.: NAG3-2103.
- [69] O'Loughlin W, Masri AR. A new burner for studying auto-ignition in turbulent dilute sprays. *Combust Flame* 2011;158:1577–90.
- [70] O'Loughlin W, Masri AR. The structure of the auto-ignition region of a turbulent dilute methanol sprays issuing in a vitiated co-flow. *Flow Turbul Combust* 2012;89:13–35.
- [71] Rodrigues HC, Tummers MJ, van Veen EH, Roekaerts DJEM. Spray flame structure in conventional and hot-diluted combustion regime. *Combust Flame* 2015;162:759–73.
- [72] Rodrigues HC, Tummers MJ, van Veen EH, Roekaerts DJEM. Effects of coflow temperature and composition on ethanol spray flames in hot-diluted coflow. *Int J Heat Fluid Flow* 2015;51:309–23.
- [73] Rebola A, Costa M, Coelho PJ. Experimental evaluation of the performance of a flameless combustor. *Appl Therm Eng* 2013;50:805–15.
- [74] Kruse S, Kerschgens B, Berger L, Varea E, Pitsch HG. Experimental and numerical study of MILD combustion for gas turbine applications. *Appl Energy* 2015;148:456–65.
- [75] Dally BB, Riesmeier E, Peters N. Effect of fuel mixture on moderate and intense low oxygen dilution combustion. *Combust Flame* 2004;137:418–31.
- [76] Ye J, Medwell PR, Varea E, Kruse S, Dally BB, Pitsch HG. An experimental study on MILD combustion of prevaporised liquid fuels. *Appl Energy* 2015;151:93–101.

- [77] Castela M, Verissimo AS, Rocha AMA, Costa M. Experimental study of the combustion regimes occurring in a laboratory combustor. *Combust Sci Technol* 2012;184:243–58.
- [78] Verissimo AS, Rocha AMA, Costa M. Operational, combustion, and emission characteristics of a small-scale combustor. *Energy Fuels* 2011;25:2469–80.
- [79] Verissimo AS, Rocha AMA, Costa M. Importance of the inlet air velocity on the establishment of flameless combustion in a laboratory combustor. *Exp Therm Fluid Sci* 2013;44:75–81.
- [80] Verissimo AS, Rocha AMA, Costa M. Experimental study on the influence of the thermal input on the reaction zone under flameless oxidation conditions. *Fuel Process Technol* 2013;106:423–8.
- [81] Verissimo AS, Rocha AMA, Coelho PJ, Costa M. Experimental and numerical investigation of the influence of the air preheating temperature on the performance of a small-scale mild combustion. *Combust Sci Technol* 2015;187:1724–41.
- [82] Zhou B, Costa M, Li Z, Aldén M, Bai XS. Characterization of the reaction zone structures in a laboratory combustor using optical diagnostics: from flame to flameless combustion. *Proc Combust Inst* 2017;36:4305–12.
- [83] Khalil AEE, Gupta AK. Thermal field investigation under distributed combustion conditions. *Appl Energy* 2015;160:477–88.
- [84] Khalil AEE, Gupta AK. Fuel property effects on distributed combustion. *Fuel* 2016;171:116–24.
- [85] Khalil AEE, Gupta AK. Fostering distributed combustion in a swirl burner using prevaporized liquid fuels. *Appl Energy* 2018;211:513–22.
- [86] Khalil AEE, Gupta AK. On the flame-flow interaction under distributed combustion conditions. *Fuel* 2016;183:17–26.
- [87] Khalil AEE, Gupta AK. The role of CO<sub>2</sub> on oxy-colorless distributed combustion. *Appl Energy* 2017;188:466–74.
- [88] Sidey JAM, Mastorakos E. Visualization of MILD combustion from jets in cross-flow. *Proc Combust Inst* 2015;35:3527–45.
- [89] Khalil AEE, Gupta AK. Mixture preparation effects on distributed combustion for gas turbine application. In: Agarwal AK, Pandey A, Gupta AK, Aggarwal SK, Kushari A, eds. *Novel combustion concepts for sustainable energy development*. New Delhi, India: Springer; 2014. p. 277–96.
- [90] Sorrentino G, Sabia P, de Joannon M, Ragucci R, Cavaliere A, Göktolga MU, et al. Development of a novel cyclonic flow combustion chamber for achieving MILD/Flameless combustion. *Energy Procedia* 2015;66:141–4.
- [91] Sorrentino G, Sabia P, de Joannon M, Cavaliere A, Ragucci R. The effect of diluent on the sustainability of MILD combustion in a cyclonic burner. *Flow Turbul Combust* 2016;96:449–68.
- [92] de Joannon M, Sabia P, Sorrentino G, Bozza P, Ragucci R. Small size burner combustion stabilization by means of strong cyclonic recirculation. *Proc Combust Inst* 2017;36:3361–9.
- [93] Bilger RW, Pope SB, Bray KNC, Driscoll JF. Paradigms in turbulent combustion research. *Proc Combust Inst* 2005;30:21–42.
- [94] van Oijen JA, de Goey PH. Modelling of premixed laminar flames using flamelet-generated manifolds. *Combust Sci Technol* 2000;161:113–37.
- [95] Pierce CD, Moin P. Progress-variable approach for large-eddy simulation of non-premixed turbulent combustion. *J Fluid Mech* 2004;504:73–97.
- [96] Abtahizadeh E, de Goey P, van Oijen J. LES of Delft Jet-in-Hot Coflow burner to investigate the effect of preferential diffusion on autoignition of CH<sub>4</sub>/H<sub>2</sub> flames. *Fuel* 2017;191:36–45.
- [97] Abtahizadeh E, de Goey P, van Oijen J. Development of a novel flamelet-based model to include preferential diffusion effects in autoignition of CH<sub>4</sub>/H<sub>2</sub> flames. *Combust Flame* 2015;162:4358–69.
- [98] Klimenko AY, Bilger RW. Conditional moment closure for turbulent combustion. *Prog Energy Combust Sci* 1999;25:595–687.
- [99] Labahn JW, Dovizio D, Devaud CB. Numerical simulation of the Delft-Jet-in-Hot-Coflow (DJHC) flame using conditional source-term estimation. *Proc Combust Inst* 2015;35:3547–55.
- [100] Haworth DC. Progress in probability density function methods for turbulent reacting flows. *Prog Energy Combust Sci* 2010;36:168–259.
- [101] Nicolle A, Dagaut P. Occurrence of NO-reburning in MILD combustion evidenced via chemical kinetic modeling. *Fuel* 2006;85:2469–78.
- [102] Mancini M, Schwöppe P, Weber R, Orsino S. On mathematical modelling of flameless combustion. *Combust Flame* 2007;150:54–9.
- [103] Li P, Wang F, Mi J, Dally BB, Mei Z, Zhang J, Parente A. Mechanisms of NO formation in MILD combustion of CH<sub>4</sub>/H<sub>2</sub> fuel blends. *Int J Hydrogen Energy* 2014;39:19187–203.
- [104] Galletti C, Ferrarotti M, Parente A, Tognotti L. Reduced NO formation models for CFD simulations of MILD combustion. *Int J Hydrogen Energy* 2015;40:4884–97.
- [105] Sepman AV, Abtahizadeh SE, Mokhov AV, van Oijen JA, Levinsky HB, de Goey LPH. Numerical and experimental studies of the NO formation in laminar coflow diffusion flames on their transition to MILD combustion regime. *Combust Flame* 2013;160:1364–72.
- [106] Bowman CT, Hanson RK, Davidson DF, Gardiner Jr. W.C., Lissianski V, Smith G.P., Golden D.M., Frenklach M., Goldenberg M. [http://www.me.berkeley.edu/gri\\_mech/](http://www.me.berkeley.edu/gri_mech/)
- [107] Smith G.P., Golden D.M., Frenklach M., Moriarty N.W., Eiteneer B., Goldenberg M., Bowman C.T., Hanson R.K., Song S., Gardiner Jr. W.C., Lissianski V., Qin Z. [http://www.me.berkeley.edu/gri\\_mech/](http://www.me.berkeley.edu/gri_mech/)
- [108] Yoo CS, Richardson ES, Sankaran R, Chen JH. A DNS study on the stabilization mechanism of a turbulent lifted ethylene jet flame in highly-heated coflow. *Proc Combust Inst* 2011;33:1619–27.
- [109] Lu TF, Yoo CS, Chen JH, Law CK. Three dimensional direct numerical simulation of a turbulent lifted hydrogen jet flame in heated coflow: a chemical explosive mode analysis. *J Fluid Mech* 2010;652:45–64.
- [110] Luo Z, Yoo CS, Richardson ES, Chen JH, Law CK, Lu T. Chemical explosive mode analysis for a turbulent lifted ethylene flame in highly-heated coflow. *Combust Flame* 2012;159:265–74.
- [111] van Oijen JA. Direct numerical simulation of autoigniting mixing layers in MILD combustion. *Proc Combust Inst* 2013;34:1163–71.
- [112] Göktolga MU, van Oijen JA, de Goey PH. 3D DNS of MILD combustion: A detailed analysis of heat loss effects, preferential diffusion, and flame formation mechanisms. *Fuel* 2015;159:784–95.
- [113] Minamoto Y, Dunstan TD, Swaminathan N, Cant RS. DNS of EGR-type turbulent flame in MILD condition. *Proc Combust Inst* 2013;34:3231–8.
- [114] Minamoto Y, Swaminathan N, Cant RS, Leung T. Reaction zones and their structure in MILD combustion. *Combust Sci Technol* 2014;186:1075–96.
- [115] Minamoto Y, Swaminathan N. Scalar gradient behaviour in MILD combustion. *Combust Flame* 2014;161:1063–75.
- [116] Minamoto Y, Swaminathan N, Cant RS, Leung T. Morphological and statistical analysis of reaction zones in MILD and premixed combustion. *Combust Flame* 2014;161:2801–14.
- [117] Minamoto Y, Swaminathan N. Subgrid scale modelling for MILD combustion. *Proc Combust Inst* 2015;35:3529–36.
- [118] Locci C, Colin O, Michel JB. Large Eddy Simulation of small-scale flameless combustor by means of diluted homogeneous reactors. *Flow Turbul Combust* 2014;93:305–47.
- [119] Colin O, Michel JB. A two-dimensional tabulated flamelet combustion model for furnace applications. *Flow Turbul Combust* 2016;97:631–62.
- [120] Lamouroux J, Ihme M, Fiorina B, Gicquel O. Tabulated chemistry approach for diluted combustion regimes with internal recirculation and heat loss. *Combust Flame* 2014;161:2120–36.
- [121] Huang X, Tummers MJ, Roekaerts DJEM. Experimental and numerical study of MILD combustion in a lab-scale furnace. *Energy Procedia* 2017;120:395–402.
- [122] Huang X. Measurements and model development for flameless combustion in a lab-scale furnace. PhD Thesis, Delft University of Technology, October 2018
- [123] Ihme M, See YC. LES flamelet modeling of a three-stream MILD combustor: analysis of flame sensitivity to scalar inflow conditions. *Proc Combust Inst* 2011;33:1309–17.
- [124] Ihme M, Zhang J, He G, Dally BB. Large-eddy simulation of a Jet-in-Hot-Coflow burner operation in the oxygen-diluted combustion regime. *Flow Turbul Combust* 2012;89:449–64.
- [125] Sarraes G, Mahmoudi Y, Arteaga Mendez LD, van Veen EH, Tummers MJ, Roekaerts DJEM. Modeling of turbulent natural gas and biogas flames of the Delft Jet-in-Hot-Coflow burner: effects of coflow temperature, fuel temperature and fuel composition on the flame lift-off height. *Flow Turbul Combust* 2014;93:607–35.
- [126] Domingo P, Vervisch L, Veynante D. Large-eddy simulation of a lifted methane jet flame in a vitiated coflow. *Combust Flame* 2008;152:415–32.
- [127] Göktolga MU, van Oijen JA, de Goey PH. Modeling MILD combustion using a novel multistage FGM method. *Proc Combust Inst* 2017;36:4269–77.
- [128] Masri AR, Cao RR, Pope SB, Goldin GM. PDF calculations of turbulent lifted flames of H<sub>2</sub>/N<sub>2</sub> fuel issuing into a vitiated co-flow. *Combust Theory Modelling* 2004;8:1–22.
- [129] Cao RR, Pope SB, Masri AR. Turbulent lifted flames in a vitiated coflow investigated using joint PDF calculations. *Combust Flame* 2005;142:438–53.
- [130] De A, Dongre A. Assessment of turbulence-chemistry interaction models in MILD combustion regime. *Flow Turbul Combust* 2015;94:439–78.
- [131] Myhrvold T, Ertesvåg IS, Gran IR, Cabra R, Chen JY. A numerical investigation of a lifted H<sub>2</sub>/N<sub>2</sub> turbulent jet flame in a vitiated coflow. *Combust Sci Technol* 2006;178:1001–30.
- [132] De A, Oldenhof E, Sathiah P, Roekaerts DJEM. Numerical simulation of Delft-Jet-in-Hot-Coflow (DJHC) flames using the Eddy Dissipation Concept model for turbulence-chemistry interaction. *Flow Turbul Combust* 2011;87:537–67.
- [133] Mardani A, Tabejamaat S, Mohammadi MB. Numerical study of the effect of turbulence on rate of reactions in the MILD combustion regime. *Combust Theory Modelling* 2011;15:753–72.
- [134] Aminian J, Galletti C, Shahhosseini S, Tognotti L. Numerical investigation of a MILD combustion burner: analysis of mixing field, chemical kinetics and turbulence-chemistry interaction. *Flow Turbul Combust* 2012;88:597–623.
- [135] Frassoldati A, Sharma P, Cuoci A, Faravelli T, Ranzi E. Kinetic and fluid dynamics modeling of methane/hydrogen jet flames in diluted coflow. *Appl Therm Eng* 2010;30:376–83.
- [136] Mardani A, Tabejamaat S, Ghamari M. Numerical study of influence of molecular diffusion in the Mild combustion regime. *Combust Theory Model* 2010;5:747–74.
- [137] Mardani A. Optimization of the Eddy Dissipation Concept (EDC) model for turbulence chemistry interactions under hot diluted combustion of CH<sub>4</sub>/H<sub>2</sub>. *Fuel* 2017;191:114–29.

- [138] Evans MJ, Medwell PR, Tian ZF. Modeling lifted jet flames in a heated coflow using an optimized eddy dissipation concept model. *Combust Sci Technol* 2015;187:1093–109.
- [139] Aminian J, Galletti C, Tognotti L. Extended EDC local extinction model accounting finite-rate chemistry for MILD combustion. *Fuel* 2016;165:123–33.
- [140] Parente A, Malik MR, Contino F, Cuoci A, Dally BB. Extension of the Eddy Dissipation Concept for turbulence/chemistry interactions to MILD combustion. *Fuel* 2016;163:98–111.
- [141] Li Z, Cuoci A, Sadiki A, Parente A. Comprehensive numerical study of the Adelaide Jet in Hot-Coflow burner by means of RANS and detailed chemistry. *Energy* 2017. doi: 10.1016/j.energy.2017.07.132.
- [142] Bao H. MSc Thesis. Delft University of Technology; 2017.
- [143] Kim SH, Huh KY, Dally BB. Conditional moment closure modeling of turbulent nonpremixed combustion in diluted hot coflow. *Proc Combust Inst* 2005;30:751–7.
- [144] Kronenburg A, Mastorakos E. The Conditional Moment Closure Model. In: Echekki T, Mastorakos E, eds. *Turbulent combustion modeling: advances, new trends and perspectives*. Dordrecht: Springer; 2011. p. 91–118.
- [145] Patwardhan SS, De S, Lakshmisha KN, Raghunandan BN. CMC simulations of a lifted turbulent jet flame in a vitiated coflow. *Proc Combust Inst* 2009;32:1705–12.
- [146] Labahn JW, Devaud CB. Large Eddy Simulations (LES) including Conditional Source-term Estimation (CSE) applied to two Delft-Jet-in-Hot-Coflow (DJHC) flames. *Combust Flame* 2016;164:68–84.
- [147] Kulkarni RM, Polifke W. LES of the Delft-Jet-In-Hot-Coflow (DJHC) with tabulated chemistry and stochastic fields combustion model. *Fuel Process Technol* 2013;107:138–46.
- [148] Bhaya R, De A, Yadav R. Large eddy simulation of MILD combustion using PDF-based turbulence-chemistry interaction models. *Combust Sci Technol* 2014;186:1138–65.
- [149] Cuoci A, Frassoldati A, Stagni A, Faravelli T, Ranzi E, Buzzi-Ferraris G. Numerical modeling of NO<sub>x</sub> formation in turbulent flames using a kinetic post-processing technique. *Energy Fuels* 2013;27:1104–22.
- [150] Kazakov A., Frenklach M. <http://www.me.berkeley.edu/drm/>
- [151] Duwig C, Stankovic D, Fuchs L, Li G, Gutmark E. Experimental and numerical study of flameless combustion in a model gas turbine combustor. *Combust Sci Technol* 2008;180:279–95.
- [152] Aminian J, Galletti C, Shahhosseini S, Tognotti L. Key modeling issues in prediction of minor species in diluted-preheated combustion conditions. *Appl Therm Eng* 2011;31:3287–300.
- [153] McDonell V, Klein M. Ground-based gas turbine combustion: metrics, constraints, and system interactions. In: Lieuwen TC, Yang V, eds. *Gas turbine emissions*. New York: Cambridge University Press; 2013. p. 24–80.
- [154] Lefebvre AH, Ballal DR. Gas turbine combustion: alternative fuels and emissions. Boca Raton: CRC press; 2010.
- [155] Correa SM. A review of NO<sub>x</sub> formation under gas-turbine combustion conditions. *Combust Sci Technol* 1992;87:329–62.
- [156] Vishwa Chandran NM. Combustion of hydrogen rich syngas fuels in gas turbines: an integrated modelling to address fuel flexibility issues, M.Sc. thesis. Delft University of Technology; 2012.
- [157] Rolls Royce plc. The jet engine. Chichester: John Wiley & Sons; 2015.
- [158] Farokhi S. Aircraft propulsion. Chichester: John Wiley & Sons; 2009.
- [159] Sander F, Caroni R, Rofka S, Benz E. Flue gas recirculation in a gas turbine: impact on performance and operational behavior. ASME Turbo Expo 2011. In: Proceedings of the ASME turbo expo, Vancouver, Canada; 2011. Jun 6–11.
- [160] American Society for Testing and Materials. Standard specification for diesel fuel oil, biodiesel blend (B6 to B20). Annual book of ASTM standards. West Conshohocken, PA: ASTM International; 2008. Method D7467.
- [161] International Civil Aviation Organization - Airport Air Quality Manual, ICAO, Doc 9889, First Edition, 2011. ISBN 978-92-9231-862-8.
- [162] Environmental Protection Agency. Standards of performance for stationary gas turbines. Federal Register 77, 2012.
- [163] Lückert R, Meier W, Aigner M. FLOX® combustion at high pressure with different fuel compositions. *J Eng Gas Turbines Power* 2008;130:1–7.
- [164] Lammel O, Schütz H, Schmitz G, Lückert R, Stöhr M, Noll B, et al. FLOX® combustion at high power density and high flame temperatures. *J Eng Gas Turbines Power* 2010;132:1–10.
- [165] Sadanandan R, Lückert R, Meier W, Wahl C. Flame characteristics and emissions in flameless combustion under gas turbine relevant conditions. *J Propul Power* 2011;27:970–80.
- [166] Schütz H, Lammel O, Schmitz G, Rödiger T, Aigner M. EZEE®: a high power density modulating FLOX® combustor. ASME Turbo Expo 2012. In: Proceedings of the ASME turbo expo, Copenhagen, Denmark; 2012. Jun 11–15.
- [167] Rödiger T, Lammel O, Aigner M, Beck C, Krebs W. Part-load operation of a piloted FLOX® combustion system. *J Eng Gas Turbines Power* 2013;135:1–9.
- [168] Zanger J, Monz T, Aigner M. Experimental investigation of the combustion characteristics of a double-staged FLOX®-based combustor on an atmospheric and a micro gas turbine test rig. ASME Turbo Expo 2015. In: Proceedings of the ASME turbo expo, Montreal, Canada; 2015. Jun 15–19.
- [169] Guillou E, Cornwell M, Gutmark E. Application of “flameless” combustion for gas turbine engines. In: Proceedings of the 47th AIAA aerospace sciences meeting including the new horizons forum and aerospace exposition, Orlando, USA; 2009. Jan 5–8.
- [170] Zizin A, Lammel O, Severin M, Ax H, Aigner M. Development of a jet-stabilized low-emission combustor for liquid fuels. ASME Turbo Expo 2015. In: Proceedings of the ASME turbo expo, Montreal, Canada; 2015. Jun 15–19.
- [171] Gounder JD, Zizin A, Lammel O, Aigner M. Spray characteristics measured in a new FLOX® based low emission combustor for liquid fuels using laser and optical diagnostics. ASME Turbo Expo 2016. In: Proceedings of the ASME turbo expo, Seoul, South Korea; 2016. Jun 13–17.
- [172] Gounder JD, Zizin A, Lammel O, Rachner M, Aigner M, Kulkarni SR. Experimental and numerical investigation in a new FLOX® based combustor for liquid fuels for Micro Gas Turbine Range Extender (MGT-REX). AIAA Propulsion and Energy Forum 2016. In: Proceedings of the 52nd AIAA/SAE/ASME joint propulsion conference, Salt Lake City, USA; 2016. Jul 25–27.
- [173] Arghode VK, Gupta AK. Role of thermal intensity on operational characteristics of ultra-low emission colorless distributed combustion. *Appl Energy* 2013;111:930–56.
- [174] Lammel O, Stöhr M, Kutne P, Dem C, Meier W, Aigner M. Experimental analysis of confined jet flames by laser measurement techniques. *J Eng Gas Turbines Power* 2012;134:1–9.
- [175] Yin Z, Boxx I, Stöhr M, Lammel O, Meier W. Confinement-induced instabilities in a jet-stabilized gas turbine model combustor. *Flow Turbul Combust* 2016;98:217–35.
- [176] Severin M, Lammel O, Meier W, Aigner M. Flame stabilization regimes of lean premixed confined jet flames at different Reynolds numbers. AIAA Propulsion and Energy Forum. In: Proceedings of the 53rd AIAA/SAE/ASME joint propulsion conference, Atlanta, USA; 2017. Jul 10–12.
- [177] Levy Y, Sherbaum V, Arfi P. Basic thermodynamics of FLOXCOM, the low-NO<sub>x</sub> gas turbines adiabatic combustor. *Appl Therm Eng* 2004;24:1593–605.
- [178] Levy Y, Sherbaum V, Erenburg V. Fundamentals of low-NO<sub>x</sub> gas turbine adiabatic combustor. In: Proceedings of the ASME turbo expo, USA; 2005. June 6–9th 2005.
- [179] Levy Y, Sherbaum V, Erenburg V. The role of the recirculating gases in the MILD combustion regime formation. ASME Turbo Expo 2007. In: Proceedings of the ASME turbo expo, Montreal, Canada; 2007. May 14–17.
- [180] Melo MJ, Sousa JMM, Costa M, Levy Y. Experimental investigation of a novel combustor model for gas turbines. *J Propul Power* 2009;25:609–17.
- [181] Melo MJ, Sousa JMM, Costa M, Levy Y. Flow and combustion characteristics of a low-NO<sub>x</sub> combustor model for gas turbines. *J Propul Power* 2011;27:1212–7.
- [182] Levy Y, Rao AG, Sherbaum V. Preliminary analysis of a new methodology for flameless combustion in gas turbine combustors. In: Proceedings of the ASME turbo expo, Montreal, Canada; 2007. May 14–17.
- [183] Levy Y, Rao AG, Sherbaum V. Chemical kinetic and thermodynamics of flameless combustion methodology for gas turbine combustors. In: Proceedings of the 43rd AIAA/ASME/SAE/ASME joint propulsion conference & exhibit, Cincinnati, USA; 2007. June 8–11.
- [184] Levy Y, Christo FC, Gaissinski I, Erenburg V, Sherbaum V. Design and performance analysis of a gas turbine flameless combustor using CFD simulations. ASME Turbo Expo 2012. In: Proceedings of the ASME Turbo Expo, Copenhagen, Denmark; 2012. Jun 11–15.
- [185] Joos F, Brunner P, Schulte-Werning B, Syed K. Development of the sequential combustion system for the ABB GT24/GT26 gas turbine family. In: Proceedings of the international gas turbine and aeroengine congress & exhibition, Birmingham, UK; 1996. Jun 11–15.
- [186] Rao AG, Yin F, van Buijtenen JP. A hybrid engine concept for multi-fuel blended wing body. *Aircr Eng Aerosp Technol Int J* 2014;86:483–93.
- [187] Yin F, Rao AG. Off-design performance of an interstage turbine burner turbofan engine. *J Eng Gas Turbines Power* 2017;139:1–8.
- [188] Levy Y, Erenburg V, Sherbaum V, Gaissinski I. Flameless oxidation combustor development for a sequential combustion hybrid turbofan engine. ASME Turbo Expo 2016. In: Proceedings of the ASME turbo expo, Seoul, South Korea; 2016. Jun 13–17.
- [189] Perpignan AAV, Talboom MG, Levy Y, Rao AG. Emission modelling of an inter-turbine burner based on Flameless combustion. *Energy Fuels* 2018;32:822–38.
- [190] Vaz DC, Borges ARJ, van Buijtenen JP, Spliethoff H. On the stability range of a cylindrical combustor for operation in the FLOX regime. ASME Turbo Expo 2004. In: Proceedings of the ASME turbo expo, Vienna, Austria; 2004. Jun 14–17.
- [191] Li G, Gutmark EJ, Overman N, Cornwell M, Stankovic D, Fuchs L, Vladimir M. Experimental study of a flameless gas turbine combustor. ASME Turbo Expo 2006. In: Proceedings of ASME turbo expo, Barcelona, Spain; 2006. May 8–11.
- [192] Vaz DC. Towards the application of flameless combustion to micro gas turbines, Ph.D. thesis. Universidade Nova de Lisboa; 2007.
- [193] Zhou Z, Xiong Y, Huang M, Zhang Z, Xiao Y. Experimental and numerical investigations of a MILD combustor applied for gas turbine. In: Proceedings of the ASME turbo expo, Seoul, South Korea; 2016. Jun 13–17.
- [194] Seliger H, Stöhr M, Yin Z, Huber A, Aigner M. Experimental and numerical analysis of a FLOX®-based combustor for a 3 kW micro gas turbine under atmospheric conditions. In: Proceedings of the ASME turbo expo, Charlotte, USA; 2017. Jun 26–30.



**André A. V. Perpignan** is a PhD candidate at the Faculty of Aerospace Engineering at the Delft University of Technology. He concluded his MSc on studying gas turbine engine



components at the University of São Paulo. After that, he worked for some time in industry, where he conducted simulations related to combustion processes. He has joined the TU Delft to conduct research in applicability of flameless combustion to gas turbine engines. His PhD is focused on computational fluid dynamics and chemistry analysis of pollutant emissions. He is an enthusiast of combustion studies and aims to develop an academic career in this field.



**Arvind Gangoli Rao**, is as an Associate Professor in the Faculty of Aerospace Engineering at TU Delft. Dr. Gangoli Rao is a specialist in aircraft propulsion and has worked on a variety of problems related to gas turbines and low NOx combustion techniques for aero engines. Has authored around 70 publications. Dr. Gangoli Rao has been involved in several EU projects and was also the coordinator of the EC funded AHEAD project (<http://www.ahead-euproject.eu/>). He is also a member of the ACARE (Advisory Committee for Research and innovation in Europe) working group on Energy and Environment and is a board member of the ISABE (International Society of Air Breathing Engine). He obtained his MSc and PhD from Indian Institute of Technology-Bombay, India. He carried out his post-doctoral research in Technion, Haifa-Israel. He has been working at TU Delft from 2008 onwards.



**Dirk Roekaerts** is a Full Professor in the Faculty of Mechanical, Maritime and Materials Engineering at Delft University of Technology (TU Delft) since 2005 and in the department of Mechanical Engineering at Eindhoven University of Technology (TU/e) since 2016. His research aims to develop and validate accurate computational models of combustion processes and more generally concerns reactive flows with

phase change and heat transfer as occurring in many energy applications. Prof. dr. Dirk Roekaerts obtained his PhD in Theoretical Physics from Katholieke Universiteit Leuven in Belgium in 1981. Next, during his civil service, he was responsible for organization of activities on 'Science, Technology and Society'. As a Postdoc Researcher at

the Universities of Essen, Germany, and Leuven, Belgium, he went on to investigate links between nonlinear phenomena, supersymmetry and stochastic processes. From 1987 to 2005 he was a Research Physicist at the Shell Research and Technology Centre in Amsterdam, investigating complex flows in industrial equipment such as furnaces, gasifiers and chemical reactors. From 1991 until 2005 he was part-time professor at TU Delft.